ISSN: 0128-7680

Pertanika Journal of

SCIENCE & TECHNOLOGY

VOLUME 8 NO.2
JULY 2000

A scientific journal published by Universiti Putra Malaysia Press

Pertanika Journal of Science & Technology

About the Journal

Pertanika, the poineer journal of UPM, began publication in 1978. Since then, it has established itself as one of the leading multidisciplinary journals in the tropics. In 1992, a decision was made to streamline Pertanika into three journals to meet the need for specialised journals in areas of study aligned with the strengths of the univeristy. These ara **(i) Pertanika Journal of Tropical Agricultural Science, (ii) Pertanika Journal of Science and Technology (iii) Pertanika Journal of Social Science and Humanities**.

Aims and Scope

Pertanika Journal of Science and Technology welcomes full papers and short communications in English or Bahasa Melayu in the fields of chemisty, physics, mathematics and statistics, engineering, environmental control and management, ecology and computer science. It is published twice a year in January and July.

Articles must be reports of research not previously or simultaneously published in other scientific or technical journals.

Communications are notes of a significant finding intended for rapid publication. It should not exceed five double-spaced typerwritten pages and must be accompanied by a letter from the author justifying its publication as a communication.

Reviews are critical appraisals of literature in areas that are of interest to a broad spectrum of scientists and researchers. Review papers will be published upon invitation.

Submission of Manuscript

Three complete clear copies of the manuscript are to be submitted to

The Chief Editor
Pertanika Journal of Science and Technology
Universiti Putra Malaysia
43400 UPM Serdang, Selangor Darul Ehsan
MALAYSIA
Tel: 89486101 Ext: 1326; Fax (603)89416172

Proofs and Offprints

Page proofs, illustration proofs, the copy-edited manuscript and an offprint order form will be sent to the author. Proofs must be checked very carefully within the specified time as they will not be proofread by the Press editors.

Authors will receive 20 offprints of each article. Additional copies can be ordered from the Secretary of the Editorial Board by filling out the offprint order form.

Published by Universiti Putra Malaysia Press
ISSN No.: 0128-7680

PERTANIKA EDITORIAL OFFICE
Research Management Centre (RMC)
1st Floor, IDEA Tower II
UPM-MTDC, Technology Centre
Universiti Putra Malaysia
43400 Serdang, Selangor, Malaysia
Tel: +603 8947 1622, 8947 1619, 8947 1616

Pertanika Journal of Science & Technology

Volume 8 No. 2, 2000

Contents

ISSN: 0128-7680
Pertanika J. Sci. & Technol. 8(2): 117-124 (2000)

Kesan Suhu dan Kadar Terikan ke atas Sifat Regangan Komposit Getah Asli Termoplastik (HDPE/NR) Berpenguat Gentian Karbon Pendek

Sahrim Hj. Ahmad dan Nor Hasimah Mohamed
Program Sains Bahan
Fakulti Sains Fizis dan Gunaan
Universiti Kebangsaan Malaysia
43600 Bangi, Selangor Darul Ehsan, Malaysia

Received: 19 Julai 1999

ABSTRAK

Komposit getah asli termoplastik (TPNR) berpenguat gentian karbon dengan arah orientasi rawak telah dihasilkan dengan kaedah pengadunan leburan menggunakan gentian yang dirawat dengan asid sulfurik dan gentian tanpa rawatan. Kesan rawatan permukaan gentian, kadar terikan dan suhu terhadap sifat mekanik komposit TPNR dikaji pada pelbagai komposisi gentian (10% - 40%). Keputusan menunjukkan kekuatan regangan meningkat dengan penambahan gentian. Didapati kekuatan regangan juga meningkat dengan kadar terikan dari 10^{-3} hingga 10^{-1} s^{-1} dan menurun dengan peningkatan suhu persekitaran. Keputusan juga menunjukkan bahawa sifat mekanik komposit TPNR dengan gentian yang dirawat meningkat dengan peningkatan komposisi gentian berbanding dengan gentian tanpa rawatan. Mikrograf Mikroskop Imbasan Elektron (SEM) pada permukaan patah pula jelas menunjukkan terdapatnya pelekatan yang baik antara gentian dan matrik pada komposit TPNR yang dirawat asid sulfurik.

Kata kunci: getah asli termoplastik, komposit TPNR, gentian karbon, rawatan permukaan

ABSTRACT

Thermoplastic natural rubber (TPNR) composite was prepared using melt blending method. The TPNR composites have been made with carbon fibers with random planar orientation both with treated and untreated with 1M sulfuric acid. The effect of surface treatment on the carbon fibre, strain rate and temperature on mechanical properties of the composites at various fibre loading (10%-40%) was investigated. It was found that the tensile properties of surface treated carbon fibre TPNR composite increased linearly with fiber concentration and decreased as temperature increased. The tensile stress also increased linearly with strain rate from 10^{-3} to 10^{-1} s^{-1}. SEM micrograph on the fractured surface has shown that the sulfuric treated fibre had improved the fiber-matrix adhesion of TPNR.

Keywords: Thermoplastic natural rubber, TPNR composites, carbon fibre, surface treatment

PENGENALAN

Sifat mekanik polimer dan komposit dipengaruhi oleh pelbagai faktor seperti kadar terikan dan suhu (Agbossu *et al.* 1994 & Hartingsveldt *et al.* 1991). Sifat komposit bergentian pendek dipengaruhi oleh antara muka gentian dan matrik. Big (1987) mendapati bahan penguat dalam bentuk gentian pendek dapat meningkat sifat mekanik sesuatu polimer kerana kebolehannya menahan beban tegasan yang dipindahkan daripada matrik polimer (Figueiredo *et al.* 1990). Kajian lepas (Krekel 1994) yang melibatkan rawatan asid-bes menunjukkan terhasilnya lekatan yang baik antara gentian dan matrik kerana ia dapat meningkatkan kekasaran gentian karbon dan seterusnya memperbaiki mod kegagalan (Donnet & Ehrburger 1977). Rawatan permukaan secara pengoksidaan akan menambahkan kumpulan berfungsi pada gentian dan seterusnya meningkatkan ketegaran di kawasan antara muka (Figueiredo *et al.* 1990). Kumpulan berfungsi seperti – COOH memberikan sumbangan pelekatan yang tertinggi pada permukaaan karbon (Krekel *et al.* 1993). Kekuatan lekatan melalui kumpulan berfungsi ini meningkat dengan peningkatan atom oksigen (Sawada *et al.* 1993).

Kajian tentang kesan suhu dan kadar terikan bagi kestabilan sifat mekanik adalah penting terutamanya untuk penggunaan dalam struktur komposit (Wu 1991). Gentian karbon tidak terjejas pada suhu kurang daripada 200°C. Sebaliknya kebanyakan bahan termoplastik akan mengalami perubahan rapuh-kenyal pada suhu yang agak tinggi yang dikenali sebagai suhu peralihan kaca, T_g (Cowley *et al.* 1997). Keadaan ini menjelaskan bahawa matrik polimer bergantung kepada suhu, dengan perubahan secara dramatik apabila menghampiri suhu peralihan kaca T_g. Modulus Young dan tegasan putus dalam kajian Nicolais *et al.* (1971) didapati berkurangan dengan peningkatan suhu. Pada kawasan suhu ini, sifat kelikatan bahan meningkat dan tindak balas mekanik polimer lebih bergantung pada kadar terikan (Detassis *et al.* 1995). Dengan demikian modulus Young dan kekuatan alah secara umumnya bergantung kepada kadar ujian yang digunakan (Hartingsveldt *et al.* 1991).

Kertas ini membincangkan kesan rawatan asid, kadar terikan dan suhu ke atas komposit bergentian karbon pendek yang dirawat dengan asid sulfurik.

KAEDAH

Bahan-bahan

Getah asli (NR) jenis SMR-L dibekalkan oleh Guthrie (M) Bhd.; Cecair getah asli (LNR) disediakan secara fotooksidaan oleh Jabatan Kimia, UKM; Polietilena berketumpatan tinggi (HDPE) jenis HMA-016 berketumpatan 0.956 gcm^{-3} dikeluarkan oleh Mobil (M) Sdn. Bhd; Gentian karbon daripada jenis PAN dibekalkan oleh Toray, dengan ± 6 mm panjang; Asid sulfurik berkepekatan 95-97% dibekalkan oleh Merck; Asid nitrik berkepekatan 69-71% dibekalkan oleh Fischer Inorganic, dan natrium hidroksida dibekalkan oleh Hamburg Chemicals dalam bentuk hablur.

Rawatan Gentian Karbon

Gentian dibasuh menggunakan air suling dan dikeringkan pada suhu 110°C selama dua jam. Asid sulfurik (1M) dipanaskan sebanyak 300 ml sehingga suhu mencapai 100°C. Selepas itu gentian seberat 30g direndam ke dalam asid sulfurik selama 1 jam. Gentian tersebut kemudiannya dibasuh dengan menggunakan 1M NaOH dan direflukskan dengan 1M NaOH selama 1 jam. Gentian dikeluarkan dan diekstrakkan dengan air suling dalam kelalang isipadu selama 5 hari. Gentian yang telah bersih dikeringkan pada suhu ambien (27°C) selama 2 hari sebelum digunakan.

Penyediaan Matrik TPNR

NR/HDPE diadun menggunakan Brabender PL 2000 dengan komposisi 60/40 menggunakan 10% LNR sebagai pengserasi. Adunan ini dilakukan pada suhu 135°C dengan kadar putaran 30 rpm selama 15 minit. Matriks TPNR kemudian dikisar dengan Refec Granulator PL 300S menjadi butiran halus.

Penyediaan Komposit TPNR

Gentian karbon terawat dan matrik TPNR dimasukkan ke dalam mesin pemutar Brabender dengan komposisi gentian (10%-40%) pada suhu 135°C dan kelajuan 11 rpm selama 11 minit.

Pencirian Bahan

Kekuatan regangan diukur dengan menggunakan alat Universal jenis Llyod PL 2000 buatan Sintech mengikut prosedur piawai ASTM D412 pada kelajuan 50 mm/min, 100mm/min, 500mm/min dan 900mm/min bagi sampel berbentuk "dumbell". Kekuatan hentaman diukur dengan menggunakan mesin bandul digital Universal Fractoscope berjenama Ceast 6545/000 mengikut prosedur piawai ASTM D256-88. Morfologi permukaan patah dikaji menggunakan Mikroskop Imbasan Elektron model XL 30 berjenama Philips.

KEPUTUSAN DAN PERBINCANGAN

Rajah 1 menunjukkan penambahan komposisi gentian sehingga 20% meningkatkan nilai tegasan maksimum komposit TPNR dan mengalami penurunan pada komposisi 30% dan 40%. Nilai tegasan adalah lebih tinggi pada komposit dengan gentian yang dirawat dengan asid sulfurik berbanding komposit dengan gentian tanpa rawatan. Keadaan ini terjadi kerana terdapat lekatan yang baik antara matrik TPNR dan gentian yang disebabkan wujudnya mekanisme ikatan kimia dan daya-daya tarikan (Figueiredo *et al.* 1990) oleh kumpulan berfungsi. Kumpulan berfungsi -OH pada permukaan gentian karbon terjana akibat rawatan asid sulfurik (Nakanishi *et al.* 1994). Pada komposisi yang lebih tinggi pula padatan gentian yang rapat menyebabkan matrik tidak dapat meresap di antara gentian dan seterusnya mengakibatkan kurang keberkesanannya terhadap bebanan (Karan 1991).

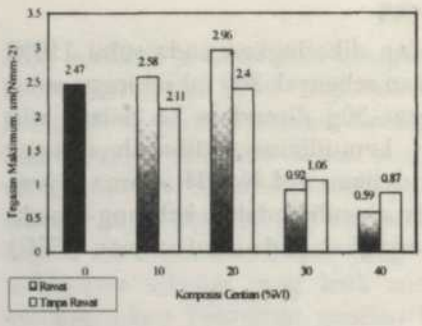

Rajah 1 : Histogram tegasan maksimum melawan komposisi gentian

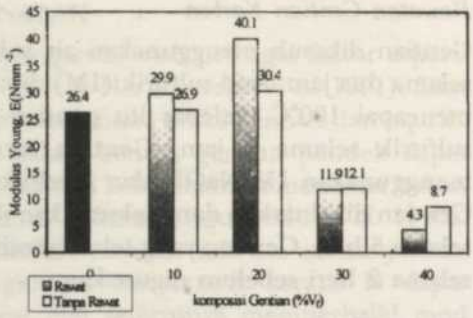

Rajah 2 : Histogram modulus Young melawan komposisi gentian

Daripada pemerhatian pada Rajah 2 didapati penambahan gentian meningkatkan modulus Young. Peningkatan modulus Young ini adalah menepati teori penguat yang dicadangkan oleh Kerner (Nicolais *et al.* 1971). Nilai modulus Young komposit didapati meningkat dengan peratus gentian sehingga 20%. Peningkatan ini adalah didapati lebih tinggi pada komposit dengan gentian yang dirawat. Tetapi apabila nilai peratus gentian melebihi 20%, modulus Young komposit jatuh dengan ketara terutamanya bagi komposit dengan gentian yang dirawat. Keadaan ini berlaku kerana kekuatan regangan gentian berkurang apabila rawatan dilakukan ke atasnya (Wu *et al.* 1995). Oleh itu penambahan gentian yang dirawat melebihi 20% menyebabkan komposit mudah mengalami kegagalan apabila bebanan dikenakan kerana kecacatan permukaan yang dihasilkan.

Rajah 3 menunjukkan plot tegasan alah melawan kadar terikan. Daripada rajah tersebut didapati tegasan alah meningkat hampir linear dengan kadar terikan. Ini adalah sesuai dengan teori Eyring.

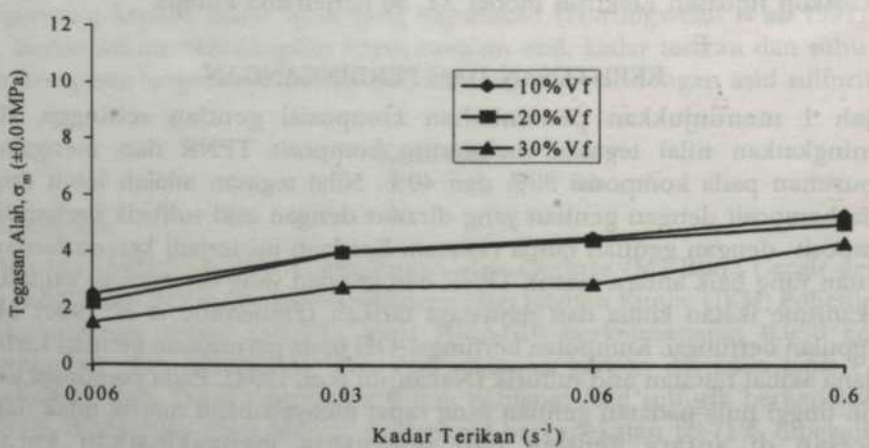

Rajah 3: Graf tegasan maksimum melawan kadar terikan pada suhu bilik

Rajah 4 menunjukkan tegasan maksimum juga meningkat dengan peningkatan kadar terikan yang dikenakan ke atas semua komposisi gentian. Pada kadar terikan yang rendah berlaku mekanisma canggaan yang disebabkan oleh proses terma. Mekanisma ini adalah dikawal oleh canggaan pada matrik dan tegasan akibat kehadiran gentian dan kumin hablur di dalam matrik (Agbossou *et al.*, 1994). Oleh itu kegagalan berlaku dengan mudah pada kadar terikan yang rendah. Menurut Abbossou *et al.* (1994), kadar terikan yang tinggi dikaitkan melalui model mekanik spring yang mengikuti hukum kelikatan Newton. Oleh itu mekanisma canggaan pada kadar terikan yang tinggi adalah berbeza daripada proses terma teraktif. Kajian yang dilakukan oleh Briscoe *et al.* (1985) menunjukkan tiada peningkatan di dalam aliran tegasan pada kadar terikan yang tinggi.

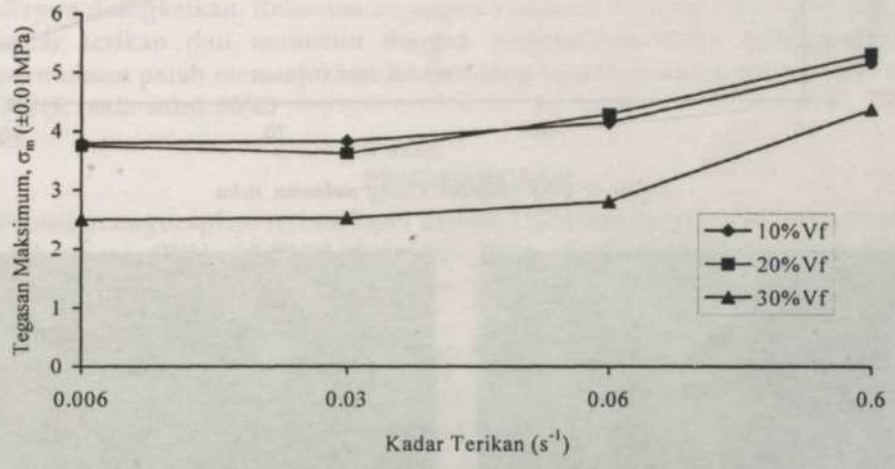

Rajah 4: Graf modulus Young melawan kadar terikan pada suhu bilik

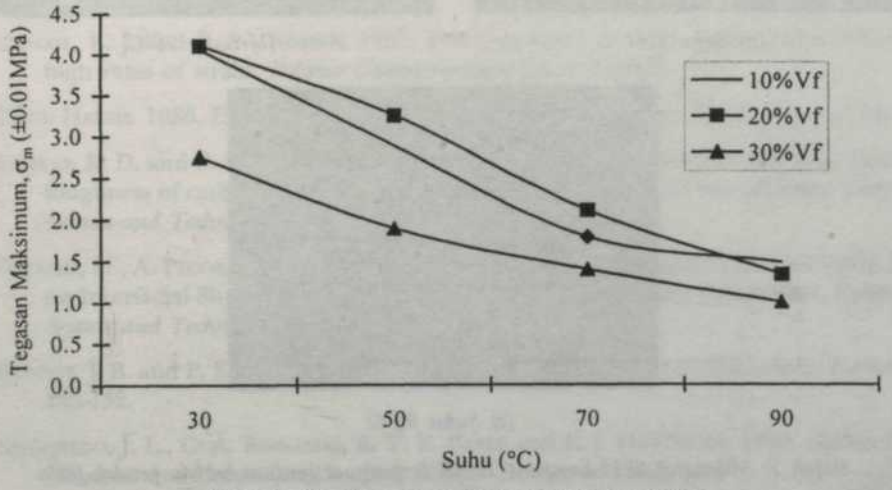

Rajah 5: Graf tegasan maksimum melawan suhu

Rajah 5 menunjukkan tegasan maksimum menurun apabila suhu persekitaran ditingkatkan daripada 30°C ke 90°C. Nilai tegasan ini didapati lebih tinggi pada komposisi dengan gentian 20%. Disebabkan matrik TPNR mengalami canggaan apabila menghampiri suhu lebur T_m, iaitu pada suhu yang

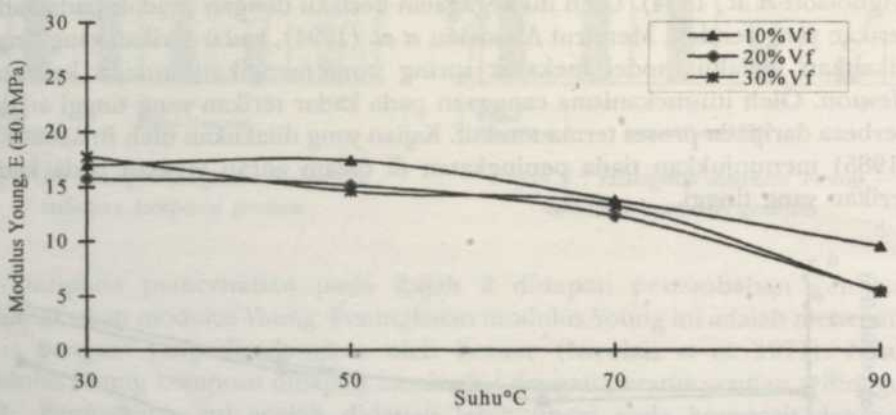

Rajah 6: Graf modulus Young melawan suhu

(a) Suhu 50°C

(b) Suhu 70°C

(c) Suhu 90°C

Rajah 7: Mikrograf SEM komposit TPNR berpenguat gentian karbon pendek pada komposisi gentian 20% pada pembesaran 500 X

lebih tinggi terutamanya pada suhu 90°C, maka ini mengakibatkan lekatan antara gentian dan matrik menjadi lemah. Pada ketika ini daya penarikan keluar gentian daripada matrik dikurangkan (Cowley *et al.* 1997). Oleh yang demikian, didapati modulus Young komposit jatuh dengan ketara pada 90°C kerana kegagalan pada antara muka yang serius (Rajah 6). Corak penurunan nilai ini dapat diterangkan dengan mikrograf mikroskop imbasan elektron (SEM) pada Rajah 7 yang diperolehi dari komposit bergentian 20%. Rajah 7 menunjukkan gentian adalah melekat dengan kuat pada suhu 50°C.

KESIMPULAN

Kajian menunjukkan sifat mekanik komposit TPNR menggunakan rawatan pengoksidaan secara pembasahan asid sulfurik ke atas gentian karbon pendek berjaya ditingkatkan. Kekuatan regangan komposit didapati meningkat dengan kadar terikan dan menurun dengan peningkatan suhu. Mikrograf SEM permukaan patah menunjukkan lekatan yang kuat di antara gentian dan matrik TPNR pada suhu 50°C.

PENGHARGAAN

Penulis mengucapkan terima kasih kepada UKM dan kerajaan Malaysia melalui mekanisme IRPA 03-02-02-0007 dan IRPA 09-02-02-0074 kerana bantuan kewangan dan Che Moh Wan bagi menjayakan penyelidikan ini.

RUJUKAN

Agbossou, A., P. Mele and N. Alberola. 1994. Strain Rate and Coupling Agent Effect in Discontinuous Glass Fiber Reinforced Polypropylene Matrix. *Journal of Composite Materials* **28**(9): 821-836.

Big, D.M. 1987. Mechanical properties of particulate filled polymers. *Polymer Composites,* **8**: 115-122.

Briscoe, B. J. and R. W. Nosker. 1985. The flow stress of high density polyethylene at high rates of strain. *Polymer Communications* **26**: 307-308.

Bryan Harris. 1986. *Engineering Composite Material* vd. 1. London: The Institute of Metals.

Cowley, K. D. and P. W. R. Beaumont. 1997. The interlaminar and intralaminar fracture toughness of carbon fibre/ polymer composites: The effect of temperature. *Composite Science and Technology* **57**: 1433-1444.

Detassis, M., A. Pegoretti and C. Migliaresi. 1995. Effect of Temperature and Strain Rate on Interfacial Shear Stress Transfer I Carbon / Epoxy Model Composites. *Composites Science and Technology* **53**: 39-46.

Donnet, J. B. and P. Ehrburger. 1977. Carbon fibre in polymer reinforcement. *Carbon* **15**: 143-152.

Figueiredo, J. L., C. A. Bernardo, R. T. K. Baker and K. J. Hüttinger. 1990. *Carbon Fibres Filaments and Composites.* London: Kluwer Academic Publishers.

HARTINGSVELDT, E. A. A. V. and J. J. V. AARTSEN. 1991. Strain-rate dependence of interfacial adhesion in particle-reinforced polymers. *Polymer* **32**(8) : 1482-1487.

KARAN, G. N. 1991. Effect of fibre volume on tensile properties of real unidirectional fibre-reinforced composites. *Composites* **22**(2): 84-88.

KREKEL, G., K. J. HÜTTINGER and W. P. HOFFMAN. 1994. The relevance of the surface structure and surface chemistry of carbon fibers in their adhesion to high temperature thermoplastics: Part II Surface chemistry. *Journal of Materials Science* **29**: 3461-3468.

MÄDER, E. 1997. Study of fibre surface treatments for control of interphase properties in composites. *Composites Science and Technology* **57**: 1077-1088.

MOHD ISHAK, Z. A. and J. P. BERRY. 1993. Impact properties of short carbon fiber reinforced nylon 6.6. *Polymer Engineering and Science* **33**: 1483-1487.

NAKAO, F., Y. TANAKA and H. ASAI. 1992. Surface characterization of carbon fibres and interfacial properties of carbon fibre composites. *Composites* **23**: 365-372.

NICOLAIS, L. and M. NARKIS. 1971. Stress-strain behavior of styrene-acrylonitrile/glass bead composites in the glassy region. *Polymer Engineering and Science* **11**(3): 194-199.

SAWADA, Y., Y. NAKANISHI and T. FUKUDA. 1993. Effect of carbon fibre surface on interfacial adhesive strength in CFRP. *Composites* **24**: 573-579.

THOMASON, J. L. and M. A. VLUG. 1996. Influence of fibre length and concentration on the properties of glass fibre-reinforced polyethylene: 1. Tensile and flexural modulus. *Composites* **27A**: 477-484.

WU, H. F. 1991. Effect of temperature and strain rate on tensile mechanical properties of ARALL-1laminates. *Journal of Material Science* **26**:3721-3729.

ZIELKE, U., K. J. HÜTTINGER and W. P. HOFFMAN. 1996. Surface-oxidized carbon fibers: II. chemical modification. *Carbon* **34**: 999-1005.

ISSN: 0128-7680
Pertanika J. Sci. & Technol. 8(2): 125-135 (2000)

Rainfall in Sarawak

Alejandro Livio Camerlengo, Mohd. Azmi Ambak and Mohd. Nasir Saadon
Faculty of Applied Sciences and Technology
University Putra Malaysia Terengganu
21030 Kuala Terengganu, Malaysia

Received: 11 May 1999

ABSTRACT

The main objective of this study is to help understand, on a monthly basis, both the rainfall intensity and the distribution of rainy days in the state of Sarawak. Our results show that: (a) no direct correlation between the number of rainy days (the rainfall intensity) and the total amount of rainfall has been encountered, and (b) the rainfall intensity field is de-coupled from the number of rainy days distribution.

ABSTRAK

Objektif utama manuskrip ini adalah untuk memahami, dalam konteks bulanan, keamatan taburan hujan dan taburan hari hujan di negeri Sarawak. Keputusan kami menunjukkan bahawa: (a) tiada korolasi jelas antara jumlah hari hujan (keamatan taburan hujan) dengan jumlah keseluruhan taburan hujan yang dicatatkan, dan (b) keputusan keamatan taburan hujan adalah tidak berpasangan dengan keputusan untuk jumlah hari hujan.

Keywords: Sarawak, rainfall, inter-monsoon period, direct correlation

INTRODUCTION

Briefly, rainfall intensity is defined as the ratio between the total amount of monthly rainfall and the number of rainy days for that particular month. A rainy day may be defined as a specific day that rains more than 0.1 mm.

The aim of this study is to gain some understanding of Sarawak's rainfall distribution. To the authors' knowledge no previous undertaking of Sarawak' s rainfall has been done before. Therefore, our study represents the first of such an attempt.

Unfortunately, as of to-date, the only available rainfall data of Sarawak pertain to its west coast. That is to say, there are no rainfall data at further inland and its mountains. Therefore, our results are rather preliminary and should be viewed in that context. A clearer picture of Sarawak's rainfall distribution will emerge in the near future whenever more rainfall stations are installed and in doing so, a better and more accurate data set becomes available.

We have previously investigated both the monthly distribution of the number of rainy days and rainfall intensity in Peninsular Malaysia. In order to

make comparisons, the reader is addressed to that particular manuscript (Camerlengo & Somchit, 1998).

DATA

As in the Camerlengo and Somchit (1998) study, the rainfall data were obtained from the "Monthly Summary of Meteorological Observations" published by the Malaysian Meteorological Service (1982-96). In exactly the same way as in that particular study, the location of the stations as well as the name of each station is depicted in *Fig. 1* and Table 1, respectively.

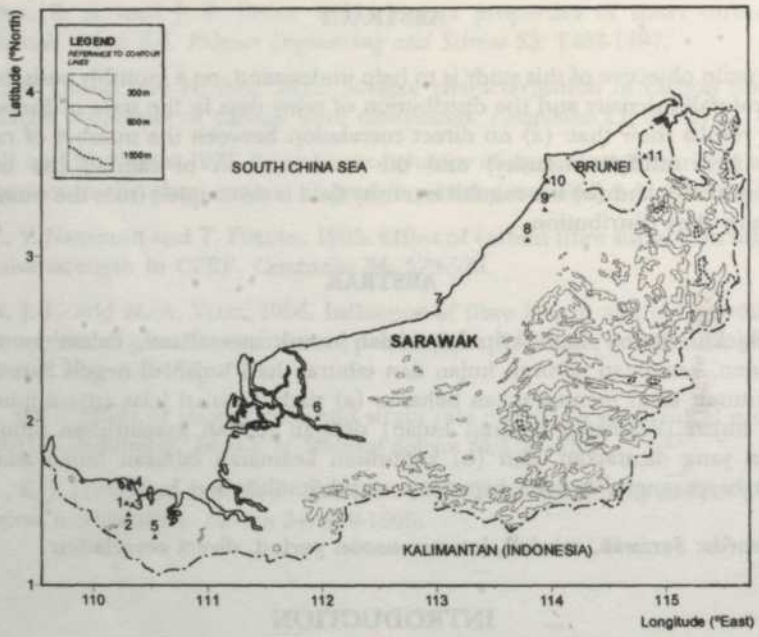

Fig 1. Location of the stations

Table 1
Name of the stations used in this study

Number	STATION	Longitude °E	Latitude °N	Elevation (m)
1	STAPOK	110° 17'	01° 30'	13
2	ARC SEMOGOK	110° 18'	01° 24'	62
3	KUCHING	110° 20'	01° 29'	22
4	RAMPANGI	110° 20'	01° 41'	2
5	TARAT	110° 32'	01° 12'	12
6	SIBU	111° 58'	02° 15'	31
7	BINTULU	113° 02'	03° 12'	3
8	KARABUNGAN	113° 49'	03° 49'	12
9	KABULOH	113° 58'	04° 05'	48
10	MIRI	113° 59'	04° 20'	17
11	UKONG	114° 51'	04° 33'	26

DISCUSSION AND RESULTS

Monthly Pattern of Rainy Days

An important gradient of rainy days between Karabungan and Bintulu and a somewhat gentler gradient from Karabungan towards Ukong (the northernmost station) are recorded during the first month of the year. Furthermore, a larger number of rainy days is encountered at the southernmost part of Sarawak (*Fig. 2*). It may be stated that the January distribution of rainy days follows the same pattern as the January monthly rainfall (Camerlengo *et al.* 1999).

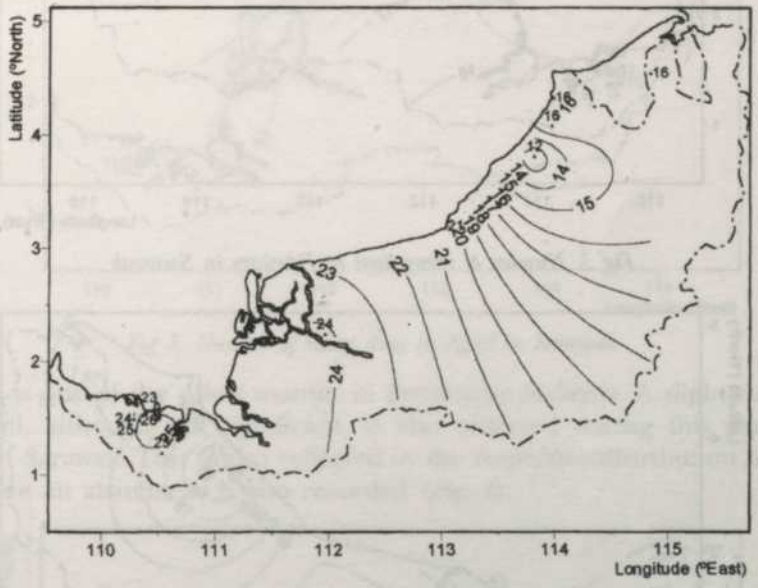

Fig 2. Number of rainy days in January in Sarawak

The retreat (southbound) of the NE monsoon may be attributable to the decrease of the number of rainy days recorded both in February and in March, where a milder gradient (compared to the antecedent month) between Karabungan and Bintulu still persists (*Figs. 3 & 4*). The same pattern as in the precedent month, larger (lesser) number of rainy days in the southern (northern) half, is observed.

As in the two precedent months, minimum number of rainy days is noticed in Karabungan in March. On the other hand, the largest number of rainy days is observed in Sibu during this particular month.

The end of the NE monsoon season makes the April distribution of rainy days to be somewhat more homogeneous than the one of the three previous months (*Fig. 5*). In particular, similar number of rainy days is observed at Ukong and south of Bintulu.

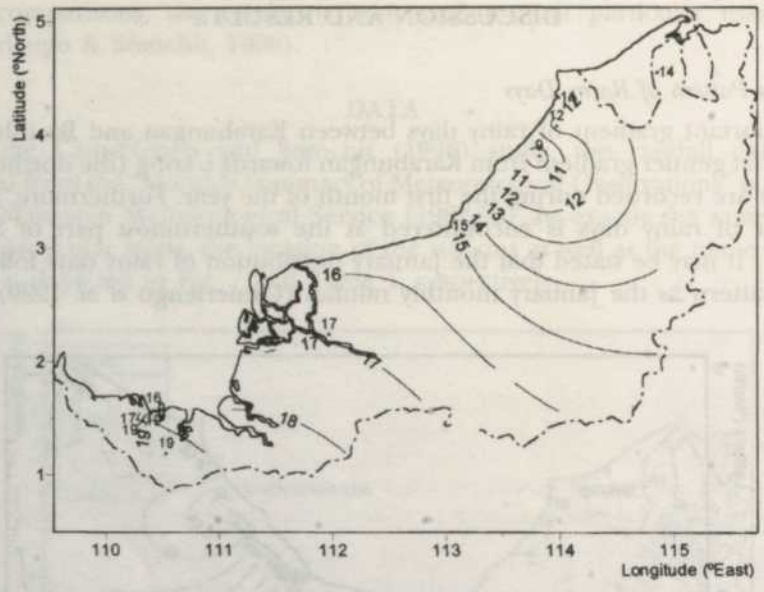

Fig 3. Number of rainy days in February in Sarawak

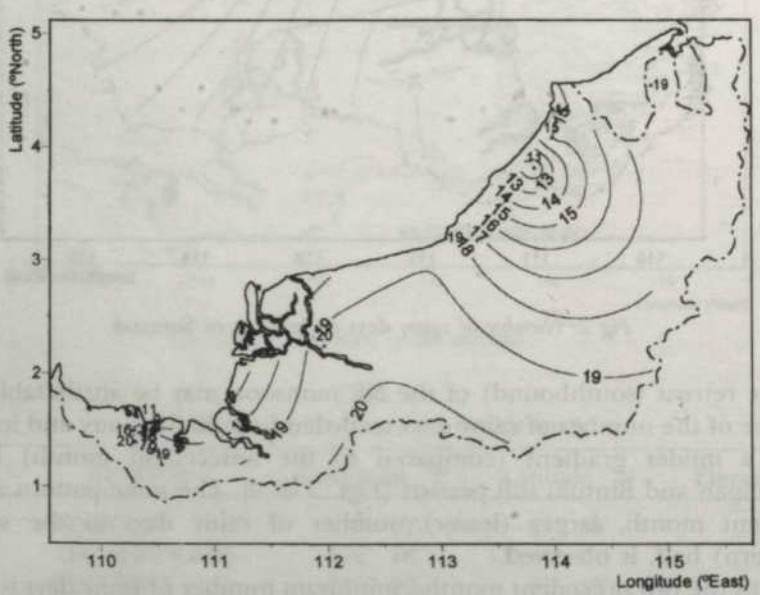

Fig 4. Number of rainy days in March in Sarawak

The first inter-monsoon period, represented by the poleward migration of the area of convergence ahead of the SE monsoon, is in May. In such instances, larger values of total rainfall are observed both in Peninsular Malaysia and in Sabah during this particular month (Dale 1959; Nieuwolt 1981). However, this feature is not noticed in Sarawak where there is no significant difference between both the April and the May total amount rainfall (Camerlengo *et al.*,

1999). This same situation prevails in the number of rainy days pattern of these two months.

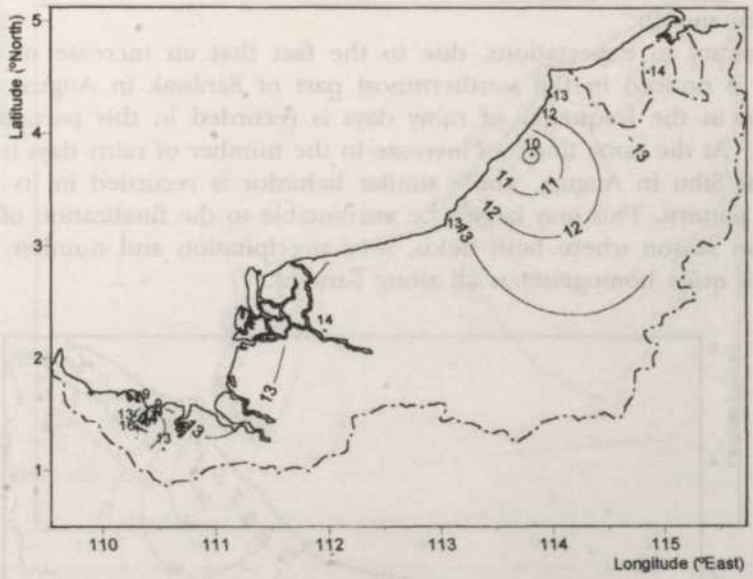

Fig 5. Number of rainy days in April in Sarawak

June is one of the driest months in Peninsular Malaysia. A slight decrease of rainfall, although not significant, is also observed during this particular month in Sarawak. This is also reflected in the respective distribution of rainy days where an abatement is also recorded (*Fig. 6*).

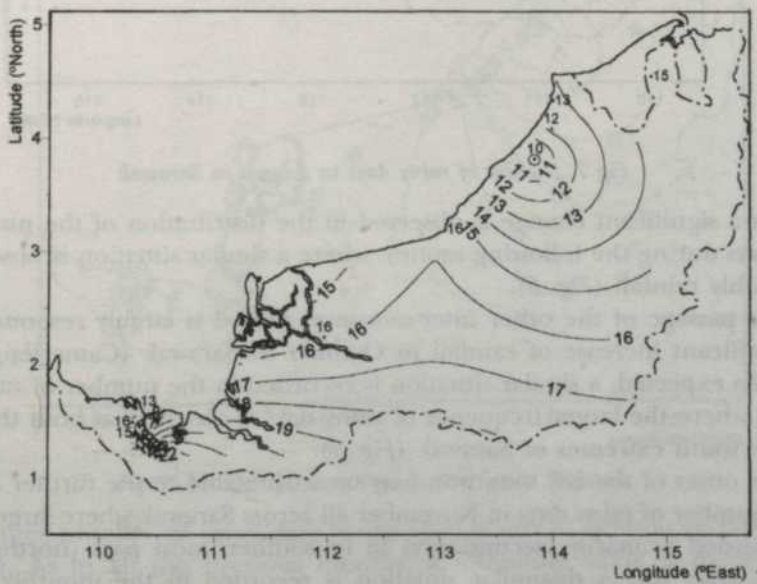

Fig 6. Number of rainy days in June in Sarawak

In spite of the fact that the July total amount of rainfall in both Rampangi and Tarat is somewhat similar, a significant gradient of the frequency (percentage) of rainy days is recorded between these two stations during this particular month.

Contrary to expectations, due to the fact that an increase of monthly rainfall is noticed in the southernmost part of Sarawak in August, a slight decrease in the frequency of rainy days is recorded in this particular area (*Fig. 7*). At the same time, an increase in the number of rainy days is noticed north of Sibu in August, where similar behavior is recorded in its monthly rainfall pattern. This may largely be attributable to the finalization of the SW monsoon season where both fields, total precipitation and number of rainy days, are quite homogeneous all along Sarawak.

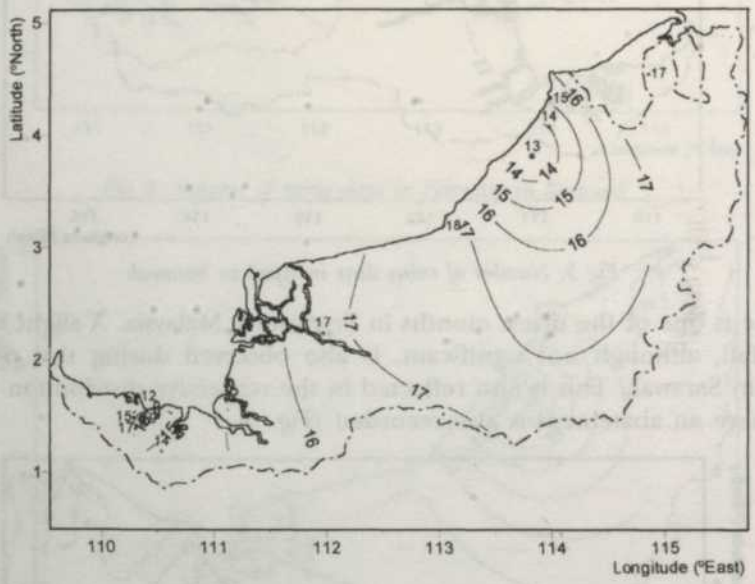

Fig 7. Number of rainy days in August in Sarawak

Not a significant change is observed in the distribution of the number of rainy days during the following month, where a similar situation is observed in its monthly rainfall (*Fig. 8*).

The passage of the other inter-monsoon period is largely responsible for the significant increase of rainfall in October in Sarawak (Camerlengo *et al.* 1999). As expected, a similar situation is recorded in the number of rainy days pattern where the larger frequency of rainy days is observed at both the north and the south extremes of Sarawak (*Fig. 9*).

The onset of the NE monsoon may be attributable to the further increase of the number of rainy days in November all across Sarawak where larger values are recorded primarily (secondarily) in its southernmost part (northernmost station) (*Fig. 10*). A dissimilar situation is recorded in the monthly rainfall distribution where a maximum value is observed at Ukong and somewhat lesser

values at the southern part of Sarawak. However, in both fields, a minimum value is perceived at Karabungan.

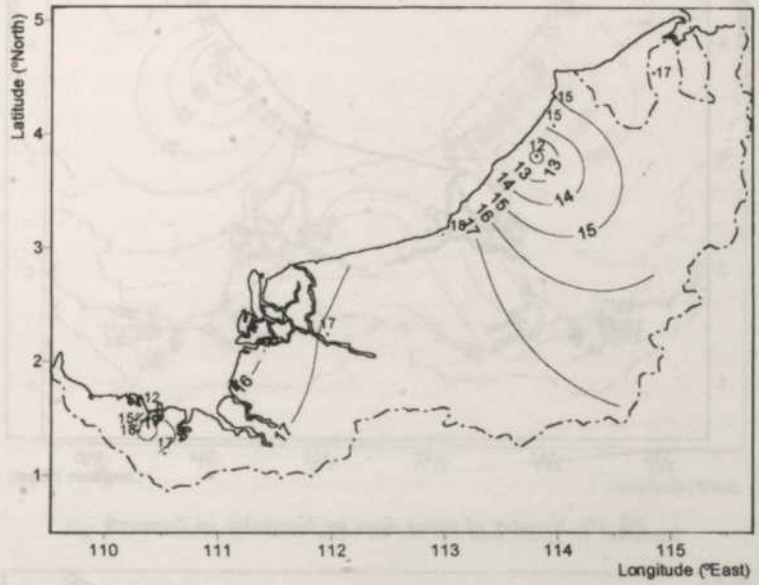

Fig 8. Number of rainy days in September in Sarawak

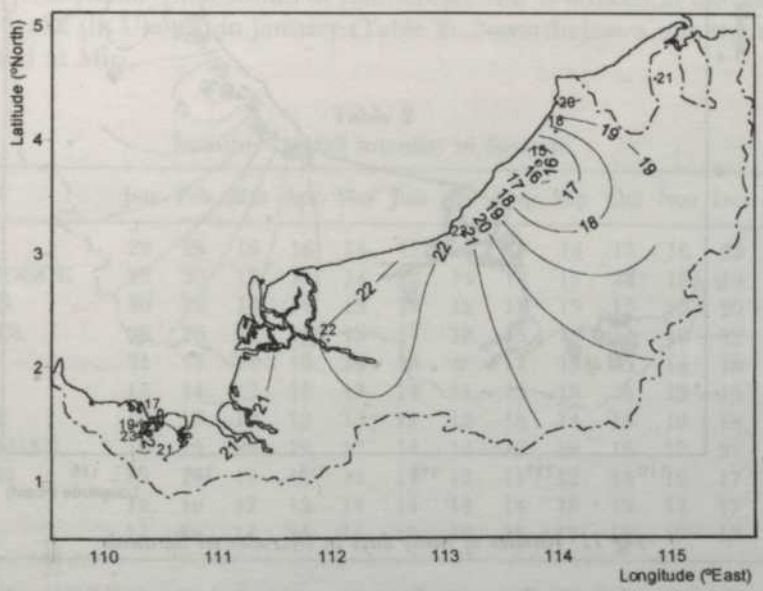

Fig 9. Number of rainy days in October in Sarawak

A larger number of rainy days is observed south of Bintulu in December (*Fig. 11*). As in all the previous months, a minimum value is perceived at Karabungan.

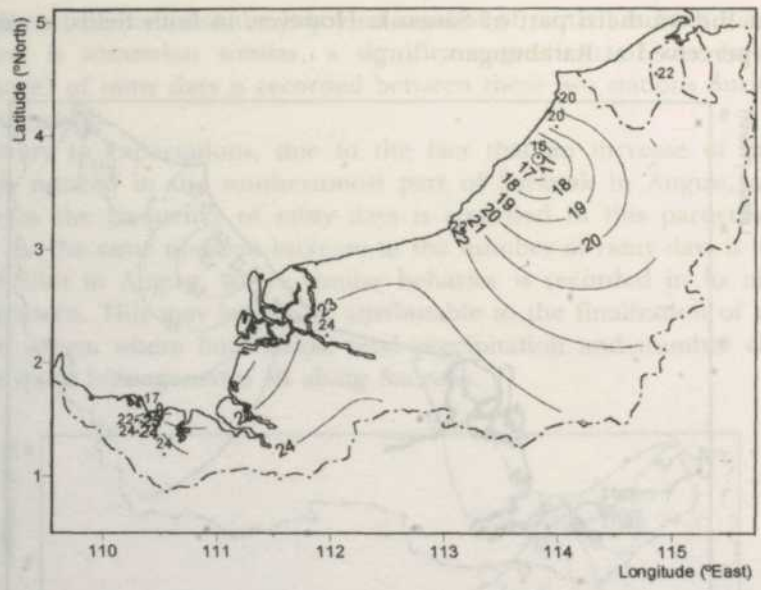

Fig 10. Number of rainy days in November in Sarawak

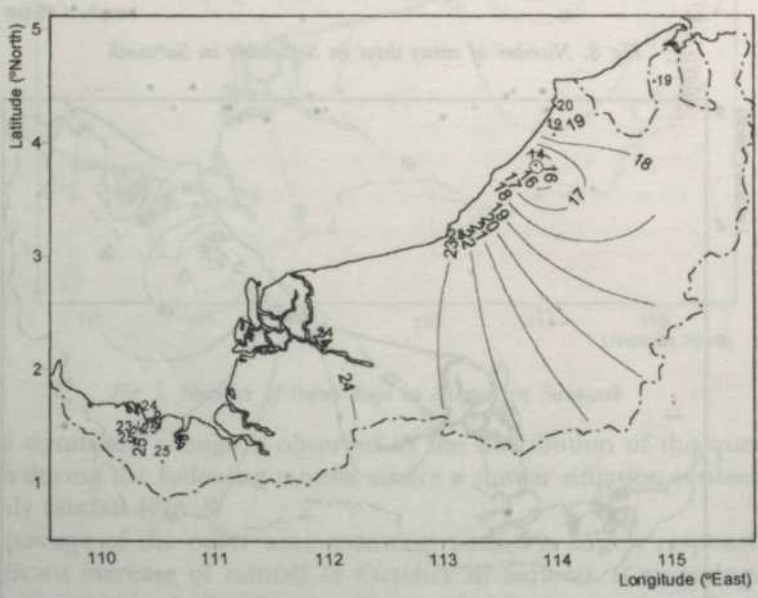

Fig 11. Number of rainy days in December in Sarawak

On an annual basis, larger values are recorded south of Bintulu and a significant minimum value is reported at Karabungan where the number of rainy days are approximately 60 % of the ones observed at Tarat (*Fig. 12*). The number of rainy days increases significantly from Karabungan towards Ukong.

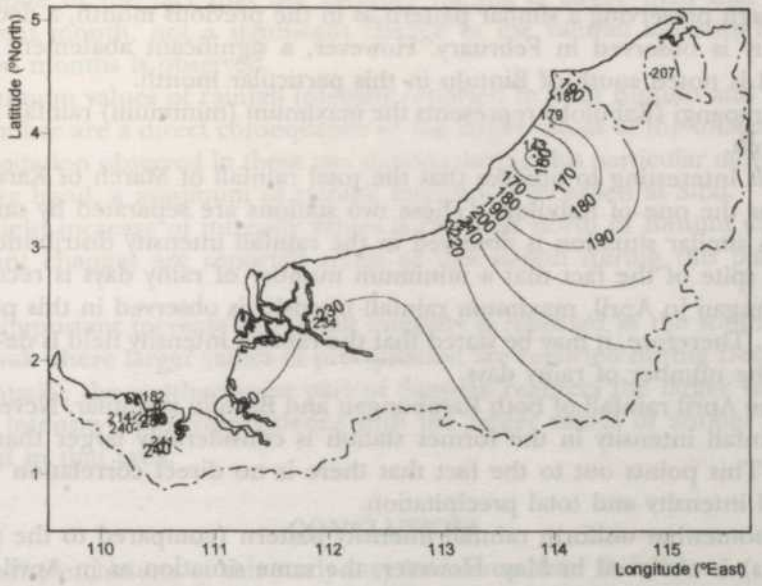

Fig 12. Number of rainy days on an annual basis in Sarawak

Distribution of Rainfall Intensity

A primary (secondary) maximum of rainfall intensity is noticed at the southern tip of Sarawak (in Ukong) in January (Table 2). Nevertheless, a minimum value is reported at Miri.

Table 2
Monthly rainfall intensity in Sarawak

STATION	Jan	Feb	Mar	Apr	May	Jun	Jul	Aug	Sep	Oct	Nov	Dec	Annual
STAPOK	29	25	19	16	14	17	13	18	14	17	16	22	19
ARC SEMOGOK	22	20	18	15	14	12	14	14	15	14	15	19	16
KUCHING	26	22	18	14	13	14	12	15	13	15	15	20	17
RAMPANGI	38	26	24	13	13	17	18	15	16	14	16	32	22
TARAT	21	17	21	16	14	13	9	17	15	15	18	18	16
SIBU	15	14	17	14	13	14	11	13	13	14	13	15	14
BINTULU	18	16	17	12	13	17	15	18	14	15	19	18	16
KARABUNGAN	16	15	25	19	17	14	14	15	19	16	17	21	17
KABULOH	13	10	10	15	14	14	12	11	12	13	16	17	13
MIRI	12	10	12	12	14	14	14	14	18	15	14	17	14
UKONG	17	18	14	14	16	15	16	15	17	17	19	17	16

It is interesting to notice that the rainfall intensity at Karabungan is identical to the one of Bintulu. This, in spite of the fact that that the total amount of rainfall in the latter station almost doubles the one of the former station for this particular month.

Although preserving a similar pattern as in the previous month, a decrease of intensity is observed in February. However, a significant abatement of total rainfall is noted south of Bintulu in this particular month.

Rampangi (Kabuloh) represents the maximum (minimum) rainfall intensity in March.

It is interesting to observe that the total rainfall of March of Karabungan doubles the one of Kabuloh. (These two stations are separated by only a few km.) A similar situation is observed in the rainfall intensity distribution.

In spite of the fact that a minimum number of rainy days is recorded at Karabungan in April, maximum rainfall intensity is observed in this particular month. Therefore, it may be stated that the rainfall intensity field is de-coupled from the number of rainy days.

The April rainfall of both Karabungan and Bintulu is similar. Nevertheless, the rainfall intensity in the former station is considerably larger than in the latter. This points out to the fact that there is no direct correlation between rainfall intensity and total precipitation.

A somewhat uniform rainfall intensity pattern (compared to the previous months) is observed in May. However, the same situation as in April prevails where a maximum value is recorded at Karabungan. Furthermore, a secondary maximum is also perceived at Ukong.

With the exception of the southern tip of Sarawak where a large disparity of intensity values is reported, not a significant change in the intensity field is observed in June.

It is interesting to observe that the June rainfall intensity field is rather more homogeneous than both the total rainfall and the number of rainy day fields for this particular month.

A considerable decrease of rainfall intensity is noticed at the southern tip of Sarawak in July, where a minimum value is reported at Tarat. On the other hand, a maximum value is observed at Ukong, the northernmost station of Sarawak.

The July rainfall of Bintulu is 80 % higher than that of Karabungan (Camerlengo *et al.*, 1999). However, the rainfall intensity at both stations is practically similar for this particular month.

While the rainfall intensity increases in August in the southern tip of Sarawak, maximum values are observed at Bintulu and Stapok.

A large gradient of rainfall intensity is recorded between two neighboring stations, Karabungan and Kabuloh, where both extremes - maximum and minimum - are recorded in September.

It is also interesting to notice that in spite of the fact that the monthly rainfall in Ukong (293 mm), is considerably larger than in Karabungan (223 mm), rainfall intensity in the latter station is somewhat larger than in the former. Again, no direct correlation between rainfall intensity and total monthly precipitation may be established.

October's as well as September's rainfall intensity is confined to a very limited range of values.

In spite of the fact that the October rainfall is larger than that in the antecedent month, not a significant change in the rainfall intensity field of these two months is observed.

Maximum values of rainfall intensity reported in both Bintulu and Ukong in November are a direct consequence of the larger values of the total amount of precipitation observed in these two stations during this particular month. On the other hand, a minimum of rainfall intensity is recorded at Sibu.

A slight increase of intensity values is reported north of Bintulu while no significant changes are reported south of this station during this particular month.

An important increase in rainfall intensity is reported in the southern tip of Sarawak where larger values of precipitation are reported during December.

Annually, the southernmost part of Sarawak registers the larger values of rainfall intensity in correspondence with the larger values of annual rainfall observed in that area.

CONCLUSION

The main conclusions of this study may be summarized as follows:

1. There is no significant direct correlation between the number of rainy days and the total amount of rainfall for a given month.
2. The rainfall intensity field is de-coupled from the number of rainy days distribution, and
3. No significant direct correlation between rainfall intensity and total amount of precipitation for a given month has been encountered.

ACKNOWLEDGMENTS

This study was supported by an IRPA grant. Our thanks are also extended to the Malaysian Meteorological Service for providing us the necessary data to carry out this investigation.

REFERENCES

Camerlengo, A. L and N. Somchit. 1998. Monthly and rainfall variability in Peninsular Malaysia. *Pertanika J. of Sci. & Technol.* 8(1). 73-83.

Camerlengo, A. L., M. Nasir S., M. Azmi Ambak. and N. Somchit. 1999: On the monthly distribution of precipitation in Sarawak. *Pertanika J. of Sci & Technol.* in press.

Dale, W. L. 1959. The rainfall in Malaya, Part I. *J. Trop. Geogr.* **13:** 23-37.

Malaysian Meteorological Service: Monthly Summary of Meteorological Observations (1982-96) issued under the authority of the Director General, Malaysian Meteorological Service, Petaling Jaya, Malaysia.

Nieuwolt, S. 1981. The climates of the Continental Southeast Asia, Chapter 1. In *World Survey of Climatology* eds. Takahasi and Arakawa, p. 1-37. Elsevier Scientific Publishing Co.

ISSN: 0128-7680
Pertanika J. Sci. & Technol. 8(2): 137-147 (2000)

Sifat Mekanik Berkas Vaskular Batang Kelapa Sawit

Asmaliah Saroji dan K.O. Lim
Pusat Pengajian Sains Fizik, Universiti Sains Malaysia
11800 Pulau Pinang, Malaysia

Received: 12 Mei 1999

ABSTRAK

Penyelidikan dijalankan untuk mengkaji kaitan antara sifat tegasan-terikan berkas vaskular batang kelapa sawit dengan peratus kelembapannya dan juga kaitan antara sifat mekanik tersebut dengan mikrostruktur berkas vaskular berdasarkan ciri graf tegasan-terikan yang diperolehi. Hasil menunjukkan bahawa semua berkas vaskular yang diuji menghasilkan 3 zon canggaan iaitu zon lengkuk hampir linear, zon plato dan akhirnya zon garis linear. Kewujudan zon plato itu kemudiannya diterangkan dengan merujuk kepada mikrostruktur berkas vaskular yang dikaji. Dengan kewujudan zon plato itu, lengkuk tegasan-terikan dapat dicirikan dengan 2 modulus elastik iaitu modulus awal dan modulus akhir. Modulus akhir didapati lebih tinggi berbanding dengan modulus awal dan ini menunjukkan bahawa berkas vaskular telah menjadi lebih tegar selepas zon plato terbentuk. Didapati juga sifat tegasan maksimum dan modulus akhir meningkat apabila kelembapan berkas vaskular berkurang.

ABSTRACT

The objective of the project is to investigate the relationship between the stress-strain characteristics of oil palm trunk vascular bundles and its moisture content. Based on the stress-strain graphs, the mechanical characteristics are then related to the microstructure of the vascular bundles. The results show that for all samples tested, 3 zones of deformation are found i.e an initial zone that is slightly curving, a plateau zone and finally a linear zone. The existence of the plateau zone is then explained in terms of the vascular bundle microstructure. As a result of the presence of the plateau zone, the stress-strain curve is then described by 2 modulus of elasticity i.e the initial modulus and final modulus. The final modulus was found to be higher than the initial modulus thus indicating that the vascular bundles become stiffer after encountering the plateau zone. The maximum stress and final modulus of the vascular bundles were found to increase when the moisture content of the vascular bundles decreased.

Kata kunci: sifat mekanik, berkas vaskular, batang kelapa sawit

PENGENALAN

Kajian ke atas sifat batang kelapa sawit termasuk sifat mekanik telah mula dijalankan semenjak ladang kelapa sawit perlu melalui proses penanaman semula. Ini adalah kerana jumlah penghasilan batang dan pelepah pokok kelapa sawit meningkat dari setahun ke setahun. Oleh itu, kajian-kajian ke atas

sifat bahan buangan ini giat dijalankan seperti mengkaji sifat fizikal, sifat kimia, dan juga sifat mekanik. Kajian ke atas sifat mekanik batang kelapa sawit telah mula dijalankan seawal tahun 1985.

Jadual 1 menunjukkan perbandingan beberapa sifat mekanik batang kelapa sawit dengan beberapa spesis batang pokok. Killmann & Lim (1985) mendapati kekuatan lentur batang pokok kelapa sawit secara amnya rendah berbanding dengan spesis lain tetapi setanding dengan batang pokok kelapa. Nilai tertinggi dicapai pada kawasan periferal bahagian bawah batang manakala kawasan pusat bahagian atas batang menunjukkan nilai kekuatan yang paling rendah.

Corak yang sama juga diperhatikan pada sifat kekuatan kemampatan. Nilai bagi batang kelapa sawit sangat rendah berbanding spesis lain tetapi setanding dengan batang pokok getah (Killmann & Lim 1985).

Walau bagaimanapun, nilai kekerasan bagi batang kelapa sawit adalah rendah berbanding dengan semua spesis kayu yang diuji, termasuklah batang pokok getah dan pokok kelapa tetapi ia agak setanding dengan 'Norway spruce' dan kayu poplar (Killmann & Lim 1985).

Pada masa ini, telah ada beberapa produk yang dihasilkan daripada batang kelapa sawit seperti *medium density fibreboard (MDF), mineral-bonded particleboard, blockboard, plywood* dan perabot (Chew *et al.* 1991), namun banyak yang masih berada di tahap kurang memuaskan kerana terdapat pelbagai masalah untuk menghasilkan produk-produk tersebut. Oleh itu, satu penyelidikan telah dimulakan untuk mengkaji sifat mekanik berkas vaskular batang kelapa sawit dengan harapan bahawa sifat tersebut akan dapat menyumbang kepada pemahaman tentang prestasi produk yang dihasilkan daripada batang kelapa sawit.

JADUAL 1
Perbandingan ciri-ciri *Elaeis guineensis* dengan beberapa spesis

Spesis	Ketumpatan (kering ketuhar) (kg/m^3)	Modulus elastik (Mpa)	Modulus patah (Mpa)	Kekerasan (N)
Kelapa sawit (30 tahun)	220-550	800-8000	8-45	350-2450
kelapa (60 tahun)	250-850	3100-11400	26-105	520-4400
pokok tamar	410	1719-2745	11-23	2000
Norway spruce	300-640	11000	66	2140
Beech	490-880	16000	105	5650
Poplar	360-560	8300	76	2500
Cengal	820	19600	149	9480
Kapur	690	13200	73	5560
D.R. Meranti	540	12700	71	3960
Kayu getah	530	8800	58	4230

Sumber: Killmann & Lim (1985)

BAHAN DAN KAEDAH

Untuk melaksanakan projek ini, berkas vaskular batang kelapa sawit yang telah tua dan yang baru ditebang digunakan. Berkas vaskular diambil secepat mungkin dari 3 segmen mengikut ketinggian (kawasan pucuk, tengah, dan pangkal) dan mengikut kedalaman batang iaitu luaran dan dalaman.

Oleh itu, projek ini mempunyai 6 segmen yang diuji. Bagi setiap segmen, sekurang-kurangnya 4 set berkas vaskular diambil untuk dikaji sama ada sifat mekaniknya berubah berbanding nilai kelembapan. Nilai kelembapan diambil dengan cara membiarkan berkas vaskular kering pada suhu bilik selama beberapa hari. Untuk setiap set, berkas vaskular dikeringkan dengan jumlah hari yang berlainan supaya setiap set mempunyai nilai kelembapan yang berlainan. Nilai kelembapan ditentukan dengan cara mengeringkan sampel di dalam alat analisis kelembapan sehingga berat sampel tidak lagi berubah. Perbezaan berat sampel sebelum dan selepas pengeringan diambil sebagai nilai kelembapan sampel.

Ujikaji dijalankan dengan menggunakan mesin ujian tegangan model LR5K dari LLOYD Instruments Ltd. Daripada ujian ini, data daya maksimum dan pemanjangan maksimum yang sepadan dihasilkan. Untuk mengira tegasan, luas keratan rentas berkas vaskular yang telah dicangga hingga putus perlu dicari. Ini dilakukan dengan memotong berkas vaskular sedekat mungkin dengan kawasan yang patah untuk mendapatkan keratan rentasnya. Kemudian kepingan berkas vaskular tersebut diletakkan di atas kaca slaid dan dibalut dengan loytape. Imej keratan rentas berkas vaskular diperbesarkan dahulu dengan menggunakan mikroskop sebelum gambarnya dirakamkan dengan menggunakan kamera. Selepas itu, luas keratan rentas dicari dengan teknik surihan iaitu dengan menggunakan kertas surih dan menyurih luas ke atas gambar keratan rentas berkas vaskular yang telah diperbesarkan itu. Teknik ini digunakan kerana bentuk keratan rentas berkas vaskular tidak simetri. Kemudian tegasan dan terikan boleh ditentukan dan hubungan di antara parameter tersebut dapat diplotkan supaya modulus elastik berkas vaskular dapat ditentukan.

Mikrostruktur berkas vaskular pula dikaji dengan menggunakan mikroskop pengimbas elektron (SEM) mengikut peringkat-peringkat yang terbentuk dalam graf tegasan-terikan. Peringkat-peringkat tersebut ialah: (1) berkas vaskular mentah (kawalan), (2) ketika di zon plato, (3) selepas zon plato dan (4) selepas sampel putus. Kajian ini bertujuan untuk melihat sebarang perubahan yang berlaku ke atas mikrostruktur berkas vaskular apabila ujian tegangan dikenakan ke atasnya. Penyediaan sampel untuk kajian mikrostruktur ini dilakukan dengan cara mengoyak secara membujur berkas-berkas vaskular yang telah dikenakan ujian mengikut peringkat di atas tanpa menggunakan sebarang alat untuk mengelakkan kerosakan pada mikrostrukturnya. Kemudian sampel dilapisi dengan emas mengikut prosedur piawai sebelum diimbas di bawah mikroskop elektron.

Keputusan eksperimen ditunjukkan di dalam Jadual 2 dan 3. Takrifan untuk keputusan yang ditunjukkan dalam jadual-jadual tersebut adalah seperti berikut:

JADUAL 2

Modulus awal, modulus akhir, terikan maksimum, dan panjang zon plato bagi segmen-segmen terpilih dengan peratus kelembapan awal yang berlainan

segmen / % kelembapan	mod.awal (x 10^9 Nm^{-2})	mod.akhir (x 10^9 Nm^{-2})	terikan maks (%)	panjang zon. plato (%)
2O(2) / 21.22	0.73 ±0.07	1.04 ±0.23	7.43 ±0.42	8.52 ±0.84
2O(1) / 11.20	0.87 ±0.11	1.54 ±0.21	6.44 ±0.27	10.21 ±0.73
2O(3) / 9.08	0.95 ±0.04	1.66 ±0.06	6.65 ±0.35	9.44 ±1.21
2O(4) / 8.71	1.26 ±0.14	2.24 ±0.20	5.54 ±0.25	10.65 ±0.57
2O(5) / 8.42	1.32 ±0.22	2.45 ±0.30	6.17 ±0.53	9.15 ±0.60
2I(1) / 40.29	1.15 ±0.07	1.35 ±0.06	7.18 ±0.43	10.18 ±0.99
2I(3) / 38.85	1.21 ±0.12	1.55 ±0.16	6.45 ±0.40	12.56 ±0.33
2I(2) / 16.71	1.08 ±0.09	1.24 ±0.10	7.05 ±0.32	11.01 ±0.96
2I(4) / 10.24	1.18 ±0.12	1.50 ±0.19	8.22 ±0.54	9.22 ±0.43
7O(1) / 61.79	0.55 ±0.03	1.17 ±0.11	6.87 ±0.35	11.09 ±0.57
7O(2) / 54.87	1.17 ±0.07	1.92 ±0.12	5.28 ±0.20	11.87 ±0.58
7O(3) / 44.64	0.82 ±0.08	1.40 ±0.14	6.52 ±0.21	10.17 ±1.03
7O(4) / 8.16	1.00 ±0.09	1.96 ±0.17	6.46 ±0.33	9.61 ±0.56
7I(2) / 45.40	0.95 ±0.10	1.11 ±0.15	8.21 ±0.27	8.35 ±0.23
7I(1) / 44.64	0.78 ±0.11	0.86 ±0.13	7.46 ±0.45	11.56 ±1.22
7I(3) / 29.57	1.10 ±0.07	1.13 ±0.07	6.94 ±0.16	10.72 ±0.44
7I(4) / 7.71	0.93 ±0.08	1.43 ±0.15	6.32 ±0.36	9.73 ±1.64
13O(1) / 36.2	0.80 ±0.02	3.39 ±0.25	6.33 ±0.34	9.34 ±0.33
13O(3) / 24.7	0.76 ±0.08	2.87 ±0.34	7.14 ±0.38	8.98 ±0.35
13O(2) / 10.0	0.96 ±0.08	4.09 ±0.35	7.20 ±0.36	8.32 ±0.79
13O(4) / 8.32	1.18 ±0.11	4.65 ±0.25	6.66 ±0.44	8.58 ±0.56
13I(1) / 52.95	0.87 ±0.08	1.29 ±0.10	7.13 ±0.17	9.17 ±0.37
13I(2) / 40.43	0.94 ±0.09	1.36 ±0.15	6.67 ±0.42	9.19 ±1.22
13I(3) / 38.96	1.11 ±0.07	1.82 ±0.18	6.24 ±0.47	11.01 ±1.12
13I(4) / 9.85	1.21 ±0.15	2.29 ±0.45	7.35 ±0.23	8.16 ±0.57
13I(5) / 9.75	1.63 ±0.17	2.02 ±0.22	5.56 ±0.43	11.36 ±0.80

Keterangan simbol segmen:
contoh :- 13I(5) : 13 - bahagian batang (13-pangkal, 7-tengah, 2-pucuk)
I - zon batang (O-luaran, I-dalaman)
(5) - set kelima berkas vaskular dengan kelembapan awal tertentu

- Modulus awal: modulus awal dikira daripada kecerunan pada titik asalan graf tegasan lawan terikan
- Modulus akhir: modulus akhir dikira daripada kecerunan pada titik kepatahan berlaku graf tegasan lawan terikan
- % terikan maksimum, E_{max} = pemanjangan maksimum / panjang asal
  $= (\Delta l_{max} / l_0) \times 100$
  dengan l_0 = panjang asal dan Δl_{max} = pemanjangan maksimum

- % panjang zon plato = (terikan zon plato/terikan maksimum) x 100
  = panjang zon plato sebagai peratus pemanjangan maksimum
- Tegasan ketika plato, tegasan maksimum, dan daya maksimum diambil terus dari graf yang terhasil. Tegasan, σ dianggap sebagai tegasan sebenar kerana luas keratan rentas sampel dikira selepas canggaan dikenakan.
- Luas dikira dengan teknik yang telah disebut dalam bahagian kaedah.
- Setiap data yang ditunjukkan adalah data purata dari 5 sampel yang diuji.

JADUAL 3

Tegasan, σ ketika plato, luas keratan rentas purata, tegasan maksimum, dan daya maksimum bagi segmen-segmen terpilih dengan peratus kelembapan yang berlainan

segmen / % kelembapan	σ (ketika datar) (x 10^6 Nm^{-2})	tegasan maks (x 10^6 Nm^{-2})	luas A, (x 10^{-7} m^2)	Daya maksimum F, (N)
2O(2) /21.22	29.20 ±2.31	56.17 ± 2.78	7.60 ±0.10	42.62 ±1.12
2O(1) /11.20	31.20 ±3.27	67.02 ±12.07	6.57 ±0.46	41.93 ±4.65
2O(3) / 9.08	35.20 ±2.82	75.42 ± 6.18	6.20 ±0.09	46.83 ±4.04
2O(4) / 8.71	37.60 ±1.94	81.16 ±16.03	5.56 ±0.28	43.66 ±5.98
2O(5) / 8.42	40.80 ±6.17	94.73 ± 3.72	5.66 ±0.54	52.89 ±3.59
2I(1) / 40.29	38.00 ±1.7	81.55 ± 6.71	5.20 ±0.30	42.59 ±4.78
2I(3) / 38.85	49.20 ±5.12	73.72 ± 8.99	4.45 ±0.28	31.99 ±2.35
2I(2) / 16.71	43.20 ±1.77	71.99 ± 3.72	4.95 ±0.23	35.36 ±1.79
2I(4) / 10.24	44.20 ±6.05	102.57 ± 6.45	5.53 ±0.54	55.64 ±3.17
7O(1)/ 61.79	22.50 ±1.88	51.95 ± 4.04	8.99 ±0.52	46.09 ±2.55
7O(2)/ 54.87	36.00 ±2.17	67.71 ± 3.70	6.15 ±0.43	41.32 ±2.84
7O(3)/ 44.64	25.20 ±2.35	64.31 ± 4.93	8.21 ±0.43	52.06 ±2.87
7O(4)/ 8.16	28.20 ±3.71	81.70 ±11.03	6.86 ±0.51	53.89 ±4.02
7I(2) / 45.40	33.40 ±2.71	80.85 ± 7.00	6.10 ±0.78	47.26 ±2.38
7I(1) / 44.64	30.90 ±3.63	55.96 ± 9.00	6.89 ±0.91	35.63 ±3.42
7I(3) / 29.57	35.00 ±1.34	74.48 ± 3.81	5.93 ±0.22	43.98 ±1.95
7I(4) / 7.71	33.40 ±1.6	62.97 ± 6.96	5.50 ±0.34	34.87 ±4.68
13O(1)/ 36.2	23.40 ±1.99	106.69 ± 7.49	9.41 ±0.60	99.24 ±5.54
13O(3)/ 24.7	24.80 ±2.57	105.64 ±10.3	10.20 ±0.86	104.27 ±2.43
13O(2)/ 10.0	28.00 ±1.73	147.81 ±11.4	8.16 ±0.17	120.00 ±7.48
13O(4)/ 8.32	33.00 ±2.09	153.90 ±15.4	6.97 ±0.28	106.67 ±10.49
13I(1)/ 52.95	26.80 ±3.28	71.60 ± 6.37	7.59 ±0.81	53.09 ±4.05
13I(2)/ 40.43	30.60 ±3.09	72.21 ± 3.82	7.58 ±0.33	54.39 ±2.94
13I(3)/ 38.96	33.40 ±1.78	85.06 ± 8.81	6.52 ±0.38	54.61 ±4.33
13I(4)/ 9.85	35.00 ±3.55	113.01 ±10.9	5.83 ±0.24	65.60 ±5.82
13I(5)/ 9.75	34.40 ±5.33	83.98 ±14.25	6.91 ±0.51	55.87 ±7.37

Daripada Jadual 2 dan 3, hubungan antara tegasan dan terikan dapat dibuat seperti ditunjukkan dalam Rajah 1. Didapati bahawa lengkuk tegasan-terikan tidak mematuhi Hukum Hooke tetapi secara umumnya ia boleh dibahagi kepada 3 zon seperti berikut:

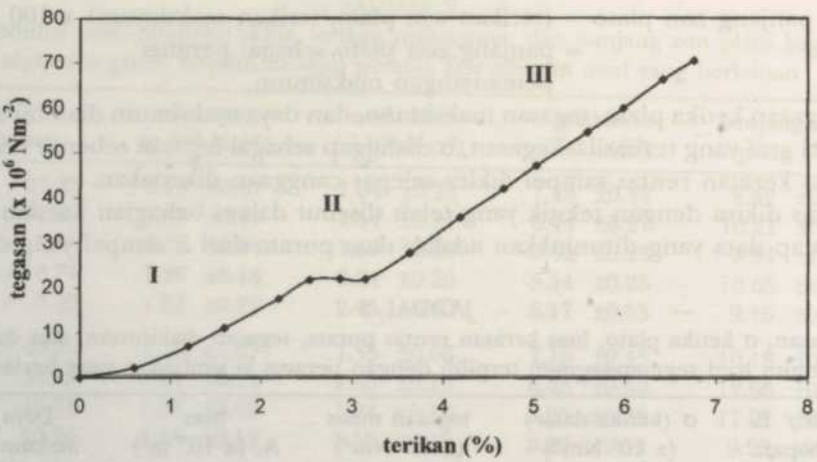

Rajah 1: Graf tegasan lawan terikan bagi sampel 13I 1(3).

Terdapat tiga zon yang nyata iaitu zon I, zon II, dan zon III.

a) Zon lengkuk hampir linear (zon I)
Secara keseluruhan, garis graf di kawasan ini kecuali di bahagian awalan, pemanjangan berlaku lebih cepat apabila berkas vaskular dicangga. Ini menunjukkan pemanjangan mudah berlaku tanpa mengenakan daya yang besar.

b) Zon plato (zon II)
Zon plato ditakrifkan sebagai kawasan tegasan malar terhadap terikan. Keadaan ini wujud bagi semua sampel yang diuji tetapi tidak semua plato mempunyai bentuk yang lurus mengufuk. Kebanyakan plato berbentuk mendatar tetapi ada juga sebahagian kecil yang melengkuk sedikit ke atas atau ke bawah terutamanya di hujung zon plato. Walau bagaimanapun, peratus panjang plato tidak menunjukkan sebarang corak peningkatan atau penurunan. Nilainya berbeza-beza dan mempunyai julat dari 8.16% hingga 12.56% sahaja.

c) Zon garis linear (zon III)
Pada kawasan ini, hampir semua sampel menunjukkan kelinearan antara tegasan dan terikan. Ia seolah-olah mematuhi Hukum Hooke yang mana tegasan berkadar terus dengan terikan. Tegasan bertambah selari dengan terikan sehingga kepatahan berlaku.

Penyelidikan mikrostruktur berkas vaskular dijalankan mengikut peringkat-peringkat seperti yang telah disebut dalam bahagian kaedah. Imej yang telah dirakamkan dari mikroskop pengimbas elektron ditunjukkan dalam Rajah 2(a-e).

Daripada imej yang telah dirakamkan, mikrostruktur dalaman berkas vaskular batang kelapa sawit tidak menunjukkan sebarang perubahan yang ketara tetapi pemerhatian dapat ditumpukan pada keadaan xilem kerana hanya struktur xilem sahaja yang menunjukkan sedikit perubahan. Walau bagaimanapun, rupa bentuk xilem tidak seiras antara satu sama lain kerana ujian dilakukan ke atas berkas vaskular yang berbeza.

Rajah 2a menunjukkan struktur xilem bagi berkas vaskular yang tidak dikenakan sebarang ujian. Ia berfungsi sebagai kawalan iaitu untuk dibandingkan dengan mikrostruktur berkas vaskular yang lain. Rajah itu menunjukkan struktur xilem yang tersusun rapi kerana tiada canggaan dibuat ke atasnya.

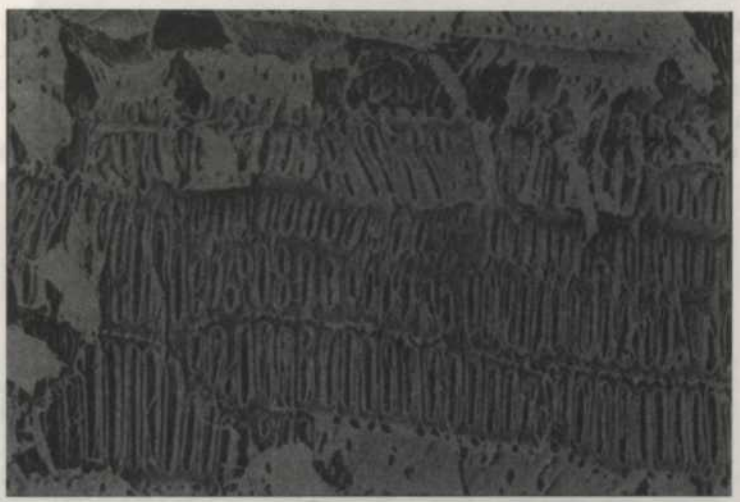

Rajah 2a: Mikrostruktur berkas vaskular kawalan
Skala: 2.2 cm = 50 μm

Rajah 2b menunjukkan xilem kelihatan seperti meregang sedikit. Sungguhpun demikian, wujudnya ketidakpastian di sini kerana sampel dicerap selepas ujian dihentikan secara tiba-tiba. Sebaliknya apa yang dilihat mungkin memang merupakan apa yang berlaku di zon plato.

Rajah 2b: Mikrostruktur berkas vaskular ketika di zon plato
Skala: 2.2 cm = 50 μm

Rajah 2c menunjukkan struktur xilem yang telah mengalami kerosakan yang mana ia telah terkoyak pada satu bahagian. Di sini juga terdapat kemusykilan iaitu sama ada ia terkoyak kerana canggaan atau terkoyak semasa pengoyakan keratan membujur. Walau bagaimanapun, didapati hanya xilem sahaja yang terusik sedangkan jiran-jirannya tidak mengalami sebarang perubahan.

Rajah 2d menunjukkan kawasan berkas vaskular yang telah putus. Didapati permukaannya tidak rata sama sekali dan terdapat kesan-kesan gentian halus mengalami canggaan. Di sini, xilem tidak dapat diperhatikan manakala Rajah 2e menunjukkan keratan rentas berkas vaskular pada pembesaran 130 kali. Berkas vaskular tersebut mengandungi satu vessel besar, floem dan gentian.

Rajah 2c: Mikrostruktur berkas vaskular sebelum putus
Skala: 2.2 cm = 50 μm

Rajah 2d: Mikrostruktur berkas vaskular selepas putus
Skala: 2.2 cm = 50 μm

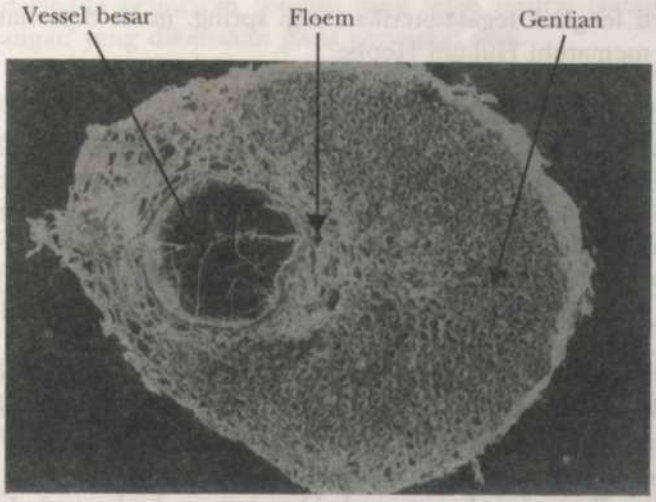

Rajah 2e: Keratan rentas berkas vaskular
Skala: 2.3 cm = 200 μm

PERBINCANGAN

Graf Tegasan-Terikan

Daripada penyelidikan mikrostruktur berkas vaskular dengan menggunakan SEM, sungguhpun tidak begitu ketara tetapi masih dapat diperhatikan adanya sedikit perubahan pada struktur dalaman. Oleh itu, dapat dikatakan bahawa lengkuk graf tegasan-terikan yang terbahagi kepada 3 zon itu adalah disebabkan oleh mikrostruktur berkas vaskular itu sendiri.

Berkas vaskular terdiri daripada pelbagai jenis sel dan tisu. Apabila daya dikenakan terhadapnya, komponen-komponen ini terutamanya gentian dan dinding sel akan melawan daya yang dikenakan sehingga mengakibatkan ketegangan pada gentian dan dinding sel. Oleh kerana berkas vaskular adalah komposit kompleks, sifat tegasan-terikan boleh menjadi melengkuk sedikit, yang mana kadar terikan setiap komposit adalah tidak sama apabila daya tegangan dikenakan. Pada ketika satu komposit sedang mengalami terikan, mungkin satu komposit yang lain belum mengalaminya (seperti yang diperhatikan pada zon I dalam Rajah 1).

Apabila daya terus dikenakan, kemungkinan gentian dan dinding sel yang telah meregang itu akan patah dan gelinciran tisu berlaku dalam struktur kompleks ini. Apabila ini terjadi, sifat tegasan-terikan akan menghasilkan pemanjangan berkas vaskular tanpa ada perubahan daya. Ini menerangkan keadaan yang berlaku pada lengkuk tegasan-terikan zon II. Selain daripada itu, sel berhampiran spiral/heliks dinding sekunder xilem juga telah mula memisah kerana dinding sel primer telah pecah dalam zon I.

Apabila daya yang lebih besar dikenakan, struktur spiral/heliks dinding sekunder xilem yang bertindak seolah-olah seperti spring akan diregangkan dan mengakibatkan pertambahan dalam tegasan. Ini dapat diperhatikan dalam zon III lengkuk tegasan-terikan. Oleh kerana struktur spiral/heliks bertindak

balas seperti lengkuk tegasan-terikan bagi spring, maka diperhatikan bahawa zon III ini mematuhi Hukum Hooke.

Pengaruh Kelembapan Terhadap Data Ujikaji

Bagi nilai tegasan maksimum, kebanyakan sampel kecuali sampel 7I, didapati nilainya berkadar songsang dengan peratus kelembapan. Semakin kurang kandungan air di dalam berkas vaskular, semakin tinggi nilai tegasan maksimum. Begitu juga dengan kebanyakan nilai modulus elastik akhir. Nilai yang tertinggi bagi kedua-dua sifat tersebut ialah dari segmen 13O (pangkal pokok) yang mana nilai modulus akhir mencapai 4.65 x 10^9 Nm^{-2} manakala nilai bagi tegasan maksimum mencapai 153.9 x 10^6 Nm^{-2} (rujuk Jadual 1 dan 2). Keadaan ini boleh diterangkan dengan fakta bahawa dinding sel tumbuhan adalah sangat higroskopik kerana selulosa (kandungan utama dinding sel) mengandungi banyak kumpulan hidroksil yang sangat hidrofilik. Apabila ia didedahkan kepada kelembapan, dinding sel akan menyerap sebahagian besar air dan akan mengembang. Proses ini akan menyebabkan tegasan berkas vaskular berkurang. Kesan penyerapan molekul air adalah seperti 'plasticizer' iaitu untuk meneutralkan daya intermolekul antara makromolekul selulosa lalu meningkatkan ciri plastik dan mengurangkan kekuatannya. Ini bermakna berkas vaskular yang rendah kandungan kelembapannya mempunyai kekuatan yang lebih tinggi (Jastrzebski, 1959).

Daripada Jadual 1, diperhatikan bahawa nilai bagi terikan maksimum tidak mempunyai corak tertentu tidak kira sama ada mengikut peratus kelembapan mahupun mengikut kedudukan berkas vaskular. Ia berbeza-beza dari satu segmen ke satu segmen yang lain menyebabkan kesukaran untuk menyimpulkannya menjadi satu aturan umum. Walau bagaimanapun, nilai peratus terikan maksimum bagi batang kelapa sawit ini hanya mempunyai julat dari 5.28% (segmen 7O(2)) hingga 8.22% (segmen 2I(4)). Begitu juga dengan panjang zon plato di mana tiada corak spesifik untuk mengaitkannya dengan peratus kelembapan dan kedudukan berkas vaskular. Nilai bagi peratus panjang zon plato mempunyai julat dari 8.16% hingga 12.56%. Jika dilihat pada data bagi tegasan ketika zon plato terbentuk (Jadual 2), didapati nilai tegasan tersebut meningkat mengikut ketinggian pohon dan mengikut kedalaman batang. Semakin tinggi nilai tegasan ini bermakna semakin besar tenaga diperlukan untuk menyebabkan spesimen bahan mengalami peleheran. Ini menunjukkan bahawa berkas vaskular bahagian atas pokok adalah yang paling kuat berbanding berkas vaskular bahagian bawah pokok. Oleh itu, lebih tenaga diperlukan untuk mencapai titik alah. Walau bagaimanapun nilai tegasan zon plato ini berjulat antara 22.5 x 10^6 Nm^{-2} hingga 49.2 x 10^6 Nm^{-2}, dengan segmen 2I(3) merupakan segmen yang mempunyai nilai tertinggi.

KESIMPULAN

Hasil daripada projek ini, satu fenomena yang tidak dijangkakan berlaku telah ditemui iaitu terbentuknya zon plato dalam graf tegasan-terikan. Kesemua sampel yang diuji menghasilkan fenomena ini. Keadaan plato itu telah dikenal

pasti akibat daripada gelinciran tisu-tisu yang telah terurai ikatannya akibat daripada tegangan yang dikenakan pada peringkat awal.

Daripada data yang telah dikumpulkan dan dipuratakan, didapati bahawa terdapat dua kecerunan pada graf tegasan-terikan yang boleh menghasilkan dua nilai modulus elastik iaitu modulus awal dan modulus akhir. Walau bagaimanapun, nilai modulus elastik bagi berkas vaskular kelapa sawit hanya berjulat antara 0.55 x 10^9 Nm^{-2} hingga 1.63 x 10^9 Nm^{-2} bagi modulus awal dan berjulat antara 0.86 x 10^9 Nm^{-2} hingga 4.65 x 10^9 Nm^{-2} bagi modulus akhir. Ini membuktikan berkas vaskular menjadi bertambah kuat selepas peleheran berlaku. Bagi panjang zon plato pula, tiada corak spesifik yang dapat dikatakan tetapi peratus pemanjangan zon plato ini mempunyai julat antara 8.16% hingga 12.56% sahaja dan tertabur secara rawak tanpa mengira kedudukan berkas vaskular tersebut. Ujikaji ini menunjukkan bahawa bahagian yang paling tegar adalah bahagian bawah-luar batang terutama bagi segmen dengan peratus kelembapan yang rendah.

PENGHARGAAN

Projek ini telah dijalankan dengan bantuan Geran IRPA (No. 190/9605/2802).

RUJUKAN

CHEW, L.T., KHOO, K.C., RAHIM SUDIN & KHOZIRAH SHAARI. 1991. In *Oil Palm Stem Utilisation - Review of Research*, Research pamphlet No. 107. ed. Khozirah Shaari, Choon, K.K. & Abdul Razak Mohd Ali, p 35-50. Kuala Lumpur : Forest Research Institute Malaysia.

KILLMAN, W. & LIM, S.C. (1985). Anatomy and properties of oil palm stem. *Proceedings of the National Symposium of Oil Palm By-products for Agro-based Industries*, Kuala Lumpur. PORIM Buletin No. 11: 18-42. Kuala Lumpur: Palm Oil Research Institute Malaysia.

JASTRZEBSKI, Z.D. 1959. *The Nature and Properties of Engineering Materials.* 2nd ed. New York: John Wiley & Sons, Inc.

LAPORAN TAHUNAN 1997. Majlis Penanam-penanam Kelapa Sawit Malaysia.

Pertanika J. Sci. & Technol. 8(2): 149-159 (2000)
ISSN: 0128-7680

On the Monthly Distribution of Precipitation in Sarawak

Alejandro Livio Camerlengo, Mohd. Nasir Saadon, Mohd. Azmi Ambak and Lim You Rang
Faculty of Applied Sciences and Technology
University Putra Malaysia Terengganu
21030 Kuala Terengganu, Malaysia

Received: 11 May 1999

ABSTRAK

Didalam kertas ini, kajian mengenai taburan hujan bulanan dan variasi taburan hujan di Sarawak dijalankan. Keputusan utama kajian ini boleh di ringkaskan seperti berikut; (i) jumlah keseluruhan hujan bagi setiap stesen tidak berubah sewaktu musim monsun baratdaya , (ii) tiada korolasi salingan diantara variasi taburan hujan dengan taburan hujan, dan (iii) nilai variasi taburan hujan berkurangan di selatan Sibu sewaktu enam bulan pertama didalam setahun.

ABSTRACT

In this investigation the study of the monthly distribution of precipitation and the rainfall variability of Sarawak is addressed. The principal results of this manuscript may be summarized as follows; (i) the total amount rainfall of each station remains unchanged during the months of the southwest monsoon season, (ii) no definite inverse correlation between rainfall variability and precipitation has been established, and (iii) lesser values of rainfall variability are reported south of Sibu during the first six months of the year.

Keywords: northeast monsoon, Sarawak, southwest monsoon, rainfall, ENSO, inverse correlation

INTRODUCTION

The objective of this manuscript is to gain a better understanding of the total monthly rainfall in Sarawak. To the authors' knowledge, only a single study has been conducted in this regard (Camerlengo et al. 1997). However, in that particular study, a considerably smaller number of stations, as compared with our investigation, was considered. Furthermore, the analyzed stations (in the previous investigation) had a dissimilar number of years. It has been established that inter-annual variability, primarily due to ENSO events, plays a significant role in the precipitation field. Therefore, a better and more exhaustive analysis of monthly rainfall in Sarawak is mandatory.

Our methodology is different from the previous study as we have arbitrarily chosen to consider rainfall data for the same period of time i.e. fifteen years (from 1982 to 1996).

Dale (1959) and Camerlengo and Somchit (2000) studied the rainfall variability of Peninsular Malaysia. No similar attempt has been made for Sarawak. Therefore, this study represents the first such attempt. In doing so, and in order to be able to make reliable comparisons, we have chosen to follow Dale' s (1959) method of computation of rainfall variability.

Due to the fact that all our stations are affected by similar inter-annual variability we strongly feel that this manuscript is timely and opportune.

DATA

Rainfall data of 11 stations were obtained from the Monthly Summary of Meteorological Observations published by the Malaysian Meteorological Service (1982-96). For this purpose, the monthly average of rainfall of each station is calculated.

The standard deviation of rainfall is relatively high, ranging between 50 % and 100 %. The standard deviation gives good perception of the dispersion coefficient.

The location of the stations as well as the name of each station are indicated in *Fig. 1* and Table 1, respectively.

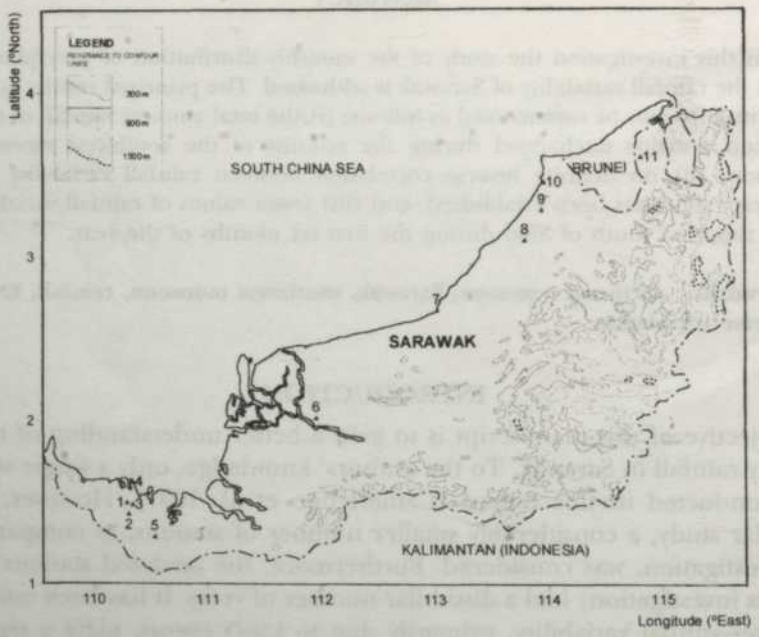

Fig 1. Location of the stations

DISCUSSION AND RESULTS

The retreat of the northeast (NE) monsoon season is mostly responsible for the larger rainfall values recorded in the southernmost part of Sarawak in January

TABLE 1
Name of the stations used in this study

Number	STATION	Longitude °E	Latitude °N	Elevation (m)
1	STAPOK	110° 17'	01° 30'	13
2	ARC SEMOGOK	110° 18'	01° 24'	62
3	KUCHING	110° 20'	01° 29'	22
4	RAMPANGI	110° 20'	01° 41'	2
5	TARAT	110° 32'	01° 12'	12
6	SIBU	111° 58'	02° 15'	31
7	BINTULU	113° 02'	03° 12'	3
8	KARABUNGAN	113° 49'	04° 05'	12
9	KABULOH	113° 58'	04° 05'	48
10	MIRI	113° 59'	04° 20'	17
11	UKONG	114° 51'	04° 33'	26

(*Fig. 2*). Indeed, the most salient feature during the first month of the year is the important gradient of precipitation in that particular area, where a decrease of 350 mm of rainfall is recorded between Rampangi and Tarat. (These two stations are approximately 60 km apart.)

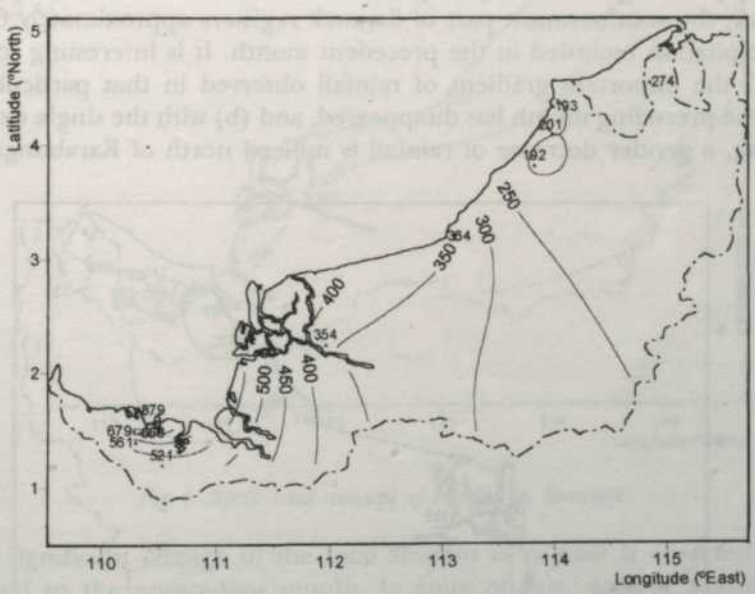

Fig 2. January: total amount of rainfall in Sarawak

A somewhat moderate decrease of rainfall is observed from Rampangi towards northern Sarawak. As a consequence of this, Sibu (roughly 200 km away from Rampangi) registers 354 mm of rainfall, and Miri (located at approximately 400 km from Rampangi) registers 193 mm.

An inverse correlation between total precipitation and rainfall variability is noticed in January (Table 2). As a consequence of this, lesser variability is recorded in areas with larger amount of precipitation, and vice-versa.

TABLE 2
Monthly rainfall variability of the stations used in this study

STATION	Jan	Feb	Mar	Apr	May	Jun	Jul	Aug	Sep	Oct	Nov	Dec	Annual
STAPOK	32	55	58	32	27	58	47	45	47	47	29	24	22
ARC SEMOGOK	32	59	39	39	29	21	48	45	31	28	22	15	10
KUCHING	26	57	52	38	27	50	45	52	38	34	29	21	12
RAMPANGI	32	67	50	42	33	61	70	62	68	55	74	43	18
TARAT	36	70	31	27	32	33	56	52	41	34	31	17	13
SIBU	40	58	30	38	39	53	51	70	38	28	18	34	15
BINTULU	61	63	59	55	37	52	37	59	35	23	28	24	16
KARABUNGAN	60	50	74	49	60	53	28	54	33	50	48	55	21
KABULOH	83	68	59	58	47	63	53	43	49	51	40	66	17
MIRI	64	64	65	42	39	49	54	42	48	54	42	48	17
UKONG	64	66	57	41	53	68	49	70	44	42	38	55	15

An important decrease of precipitation is recorded in February (*Fig. 3*). In particular, the southernmost part of Sarawak registers approximately 60 % of the precipitation recorded in the precedent month. It is interesting to notice that: (a) the important gradient of rainfall observed in that particular area during the preceding month has disappeared, and (b) with the single exception of Ukong, a gentler decrease of rainfall is noticed north of Karabungan.

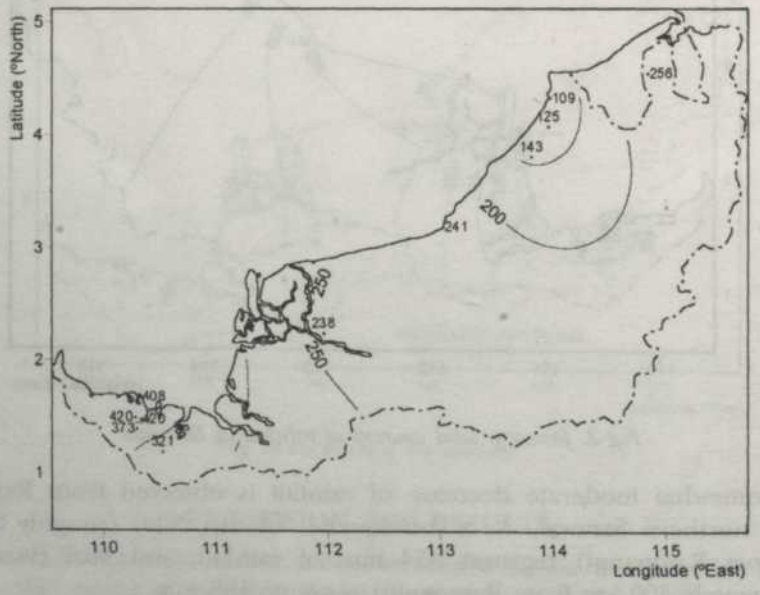

Fig 3. February: total amount of rainfall in Sarawak

A significant increase of rainfall variability is noticed in the southern part while similar values are observed in the northern half of Sarawak compared to the antecedent month (Table 2). Therefore, the inverse correlation between total precipitation and rainfall variability holds true for the southern half of Sarawak while for the northern half it becomes rather questionable.

No significant changes in both the total amount of rainfall and rainfall variability, except for the increase of total precipitation both in Sibu and in Tarat, are observed in March compared to the precedent month (Table 2). As a consequence of this, the above mentioned stations register a significant decrease in rainfall variability in March.

A decrease (increase) of precipitation is noted south (north) of Karabungan in April (*Fig. 4*). However, a decrease of rainfall variability is recorded at all stations during this particular month (Table 2). Therefore, the inverse correlation between total precipitation and rainfall variability does not hold true in this case.

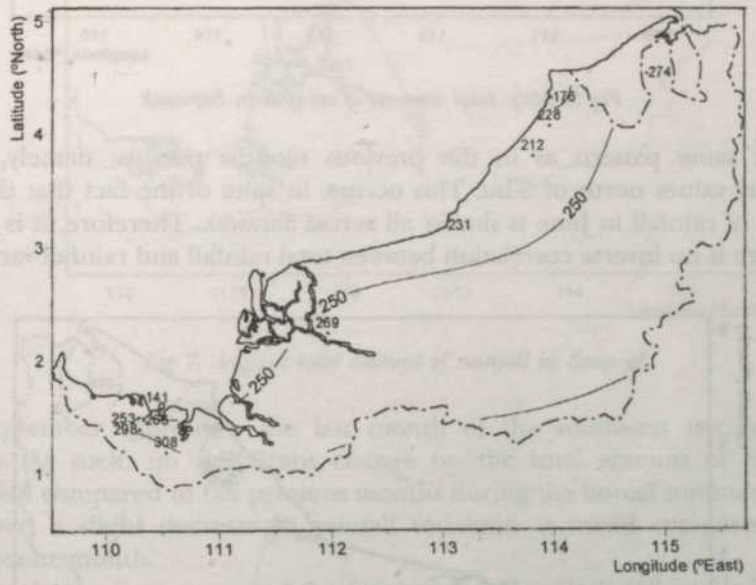

Fig 4. April: total amount of rainfall in Sarawak

No significant change in the total amount of rainfall is observed in May compared to the antecedent month. In spite of this, a slight abatement of rainfall variability is noticed in the southernmost part of our area of interest (Table 2). Again, the rule of thumb that states that there is an inverse correlation between total rainfall and rainfall variability becomes rather questionable (in Sarawak).

A further decrease of rainfall is observed in June compared to the previous month (*Fig. 5*). As a consequence of this, in general, a relative increase of rainfall variability is recorded (Table 2).

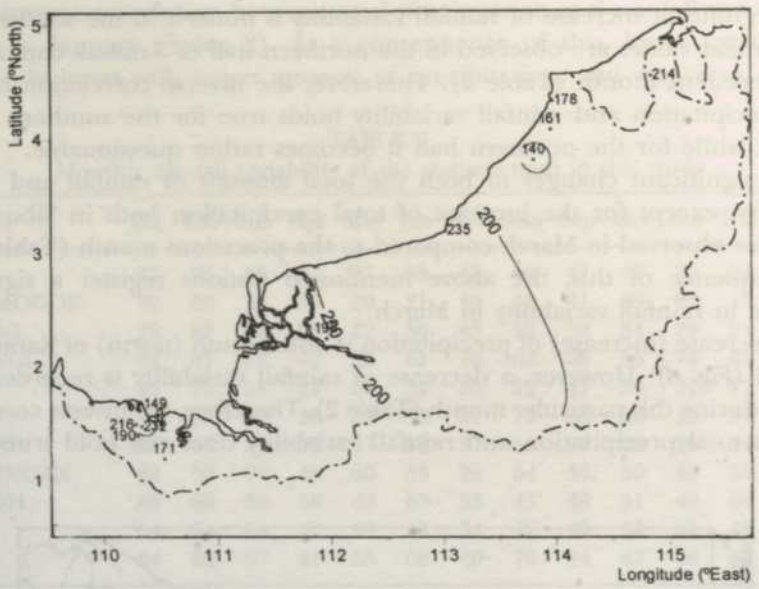

Fig 5. May: total amount of rainfall in Sarawak

The same pattern as in the previous months persists; namely, larger variability values north of Sibu. This occurs, in spite of the fact that the total amount of rainfall in June is similar all across Sarawak. Therefore, it is proven that there is no inverse correlation between total rainfall and rainfall variability.

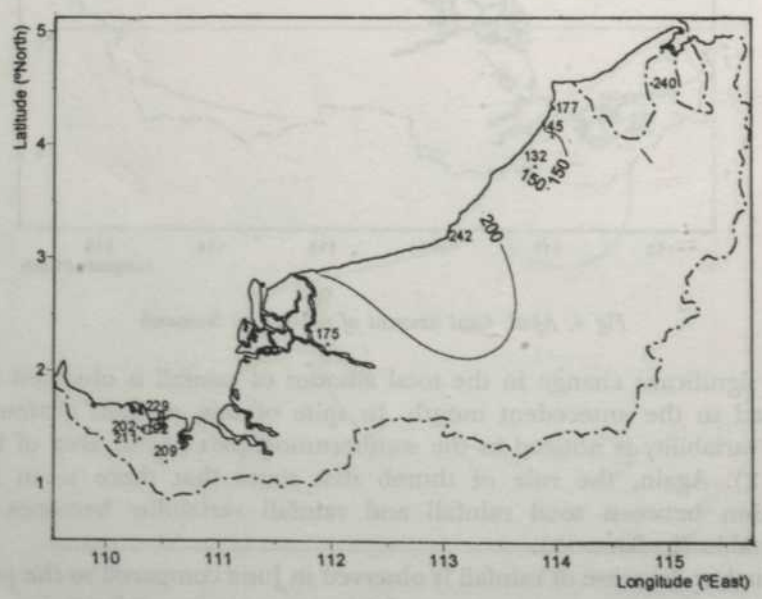

Fig 6. July: total amount of rainfall in Sarawak

No significant changes in the total amount of rainfall are observed in the following two months compared to June (*Figs. 5, 6 & 7*). In spite of this, a general decrease of rainfall variability is observed north of Sibu in July compared to the antecedent month (Table 2).

It is interesting to notice that the largest values of rainfall variability are recorded both in Sibu and Ukong during August. This, in spite of their high amount of rainfall, is recorded during this particular month at both stations.

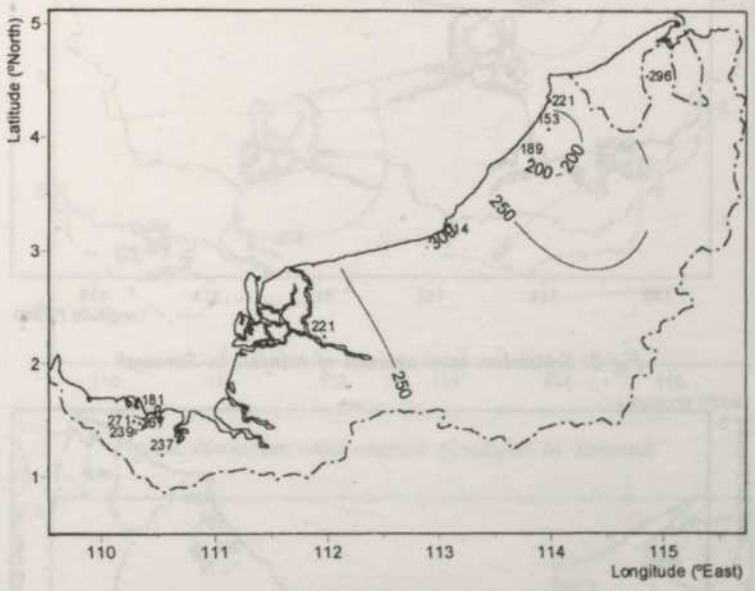

Fig 7. August: total amount of rainfall in Sarawak

September represents the last month of the southwest (SW) monsoon season. As such, no significant change on the total amount of rainfall is recorded compared to the previous months during the boreal summer (*Fig. 8*). However, a slight decrease in rainfall variability is noted compared to the antecedent month.

October represents one of the inter-monsoon periods (Nieuwolt 1981). As such, both the retreating SW monsoon and the advancing NE monsoon cause the formation of a broad area of convergence that favours uplifting with the consequent convective activity. This may help to explain the augmentation of rainfall in this particular month as compared with the previous one (*Fig. 9*).

It is also interesting to notice that the total amount of rainfall is larger in October than in the other inter-monsoon period, May. Nieuwolt (1981) attributes this to the fact that the degree of convergence in May is less strong than in October. On the other hand, no significant change in the rainfall variability is observed in this particular month compared to September.

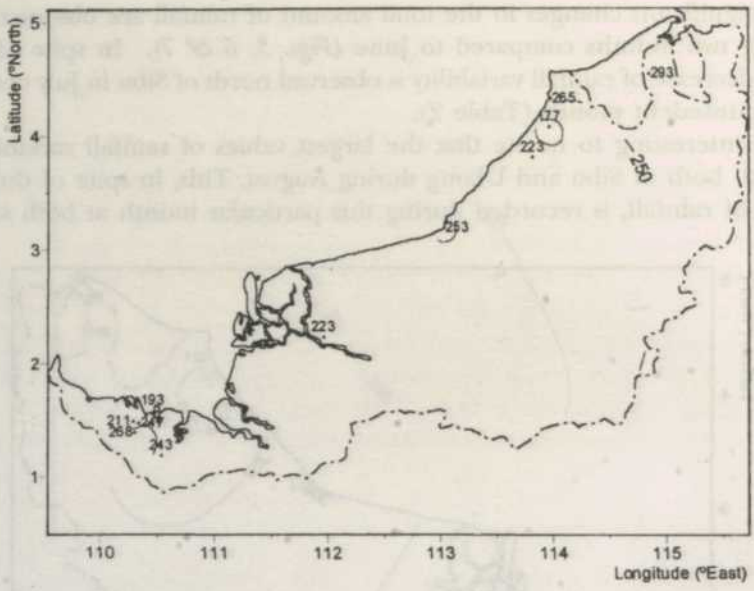

Fig 8. September: total amount of rainfall in Sarawak

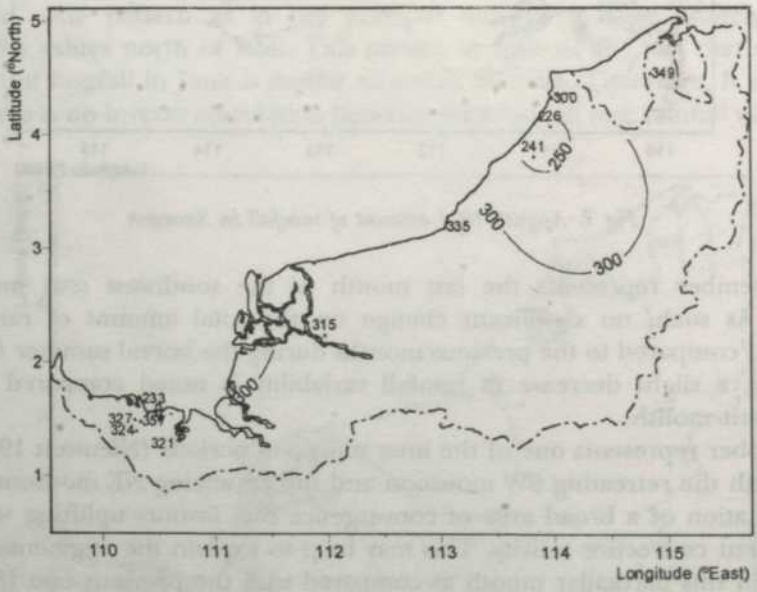

Fig 9. October: total amount of rainfall in Sarawak

The onset of the NE monsoon shows a slight increase of rainfall in November (*Fig. 10*). This is supported by a decrease of rainfall variability which is more significant south of Sibu.

The equatorward migration of the NE monsoon is largely responsible for the significant increase of rainfall in the southernmost part of Sarawak, where

a correspondent decrease of rainfall variability (in that particular area) is also noticed during the last month of the year (*Fig. 11*).

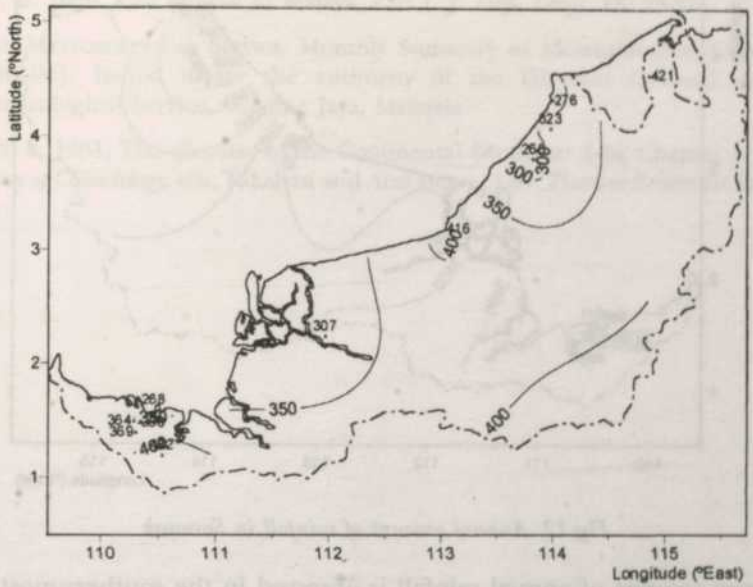

Fig 10. November: total amount of rainfall in Sarawak

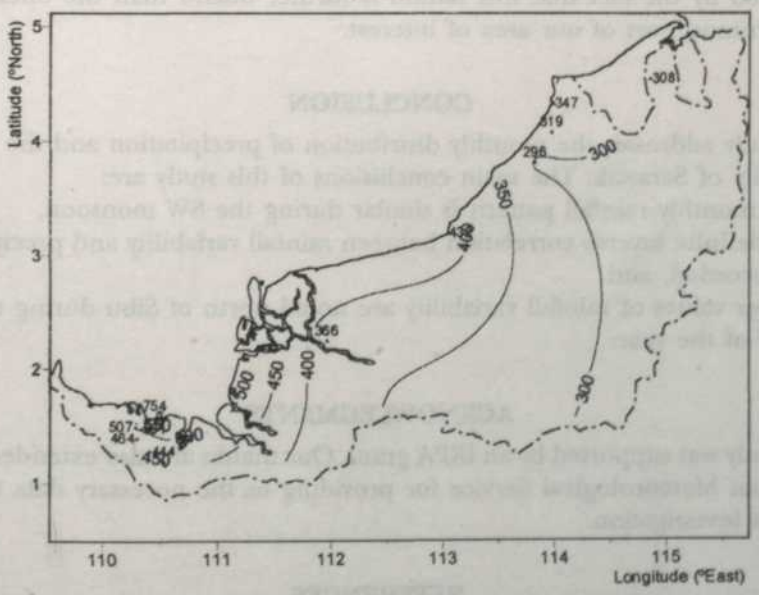

Fig 11. December: total amount of rainfall in Sarawak

On the other hand, no significant change in the total amount of rainfall is recorded, north of Sibu, in December. However, an increase of rainfall variability is noticed north of Sibu.

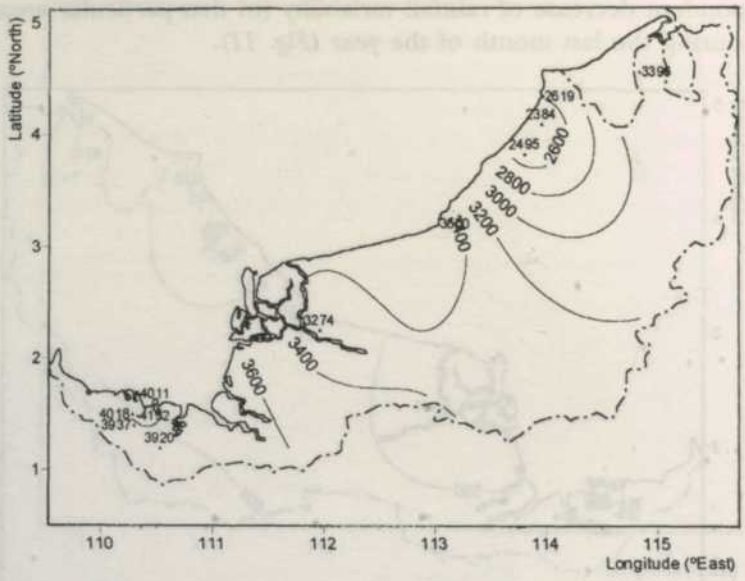

Fig 12. Annual amount of rainfall in Sarawak

Larger amount of annual rainfall is observed in the southernmost part of Sarawak (*Fig. 12*). Lesser amount of precipitation recorded at Sibu may be explained by the fact that this station is further inland than the ones in the southernmost part of our area of interest.

CONCLUSION

This study addresses the monthly distribution of precipitation and the rainfall variability of Sarawak. The main conclusions of this study are:

i the monthly rainfall pattern is similar during the SW monsoon,
ii no definite inverse correlation between rainfall variability and precipitation is recorded, and
iii larger values of rainfall variability are noted north of Sibu during the first half of the year.

ACKNOWLEGMENTS

This study was supported by an IRPA grant. Our thanks are also extended to the Malaysian Meteorological Service for providing us the necessary data to carry out this investigation.

REFERENCES

CAMERLENGO, A. L. M. NASIR S. and M. H. RUBANI. 1997. Monthly distribution of precipitation in Sabah and Sarawak., *J. of Phys. Sci.* 8: 57-63.

CAMERLENGO, A. L and N. SOMCHIT. 2000, Monthly and rainfall variability in Peninsular Malaysia. *Pertanika J. of Sci. & Technol.* 8 (1): 73-83

DALE, W. L. 1959. The rainfall in Malaya, Part I. *J. Trop. Geogr.* 13: 23-37.

MALAYSIAN METEOROLOGICAL SERVICE. Monthly Summary of Meteorological Observations (1982-96). Issued under the authority of the Director General, Malaysian Meteorological Service, Petaling Jaya, Malaysia.

NIEUWOLT, S. 1981. The climates of the Continental Southeast Asia, Chapter 1. In *World Survey of Climatology*, eds. Takahasi and Arakawa, p. 1-37. Elsevier Scientific Publishing Co.

Pertanika J. Sci. & Technol. 8(2):161-174 (2000)
ISSN: 0128-7680

An Efficient Parallel Quarter-sweep Point Iterative Algorithm for Solving Poisson Equation on SMP Parallel Computer

Othman M.[a] and Abdullah A. R.[b]

[a]Department of Communication Technology and Network
Faculty of Computer Science and Information Technology
University Putra Malaysia
43400 UPM Serdang, Selangor Darul Ehsan, Malaysia
E-mail: mothman @fsktm.upm.edu.my
[b]Department of Industrial Computing, University Kebangsaan Malaysia
43600 UKM Bangi Selangor Darul Ehsan, Malaysia

Received: 13 October 1998

ABSTRAK

Satu algoritma lelaran titik terbaru yang menggunakan pendekatan suku-sapuan telah menunjukkan masa pelaksanaan yang lebih cepat jika dibandingkan dengan algoritma lelaran titik penuh- dan separuh- sapuan untuk menyelesaikan persamaan Poisson dua dimensi (Othman *et al.* (1998)). Walau bagaimanapun, dua algoritma terakhir sesuai diimplementasikan secara selari (Evans (1984) dan Ali *et al.* (1997)). Dalam makalah ini, pengimplementasian algoritma selari yang terbaru dengan menggunakan strategi papan catur pada komputer selari multipemproses simetri akan diterangkan. Keputusan eksperimen daripada satu masalah kajian dibandingkan dengan keputusan dua algoritma selari terakhir.

ABSTRACT

A new point iterative algorithm which uses the quarter-sweep approach was shown to be much faster than the full-and half- sweep point iterative algorithms for solving two dimensional Poison equation (Othman *et al.* 1998)). However, the last two algorithms were found to be suitable for parallel implementation (Evans 1984) and Ali *et al.* (1997)). In this paper, the parallel implementation of the new algorithm with the chessboard (CB) strategy on Symmetry Multi Processors (SMP) parallel computer was presented. The experimental results of a test problem were compared with the later two parallel algorithms.

Keywords : Poisson equation, Parallel algorithms, Chessboard strategy, Full-, half- and quarter-sweep approaches, Performance evaluation

INTRODUCTION

The parallel point iterative algorithm which incorporates the full-sweep approach for solving a large and sparse linear system has been implemented successfully by Barlow and Evans (1982), and Evans(1984) while the half-sweep approach was introduced by Abdullah (1991) for the derivation of the four points *EDG*

method. Since the *EDG* method is explicit, it is suitable to be implemented in parallel on any parallel computer. Yousif and Evans (1995) implemented the parallel four, six and nine points *EDG* methods for solving the two dimensional Poisson equation, while Ali and Abdullah (1997) implemented the parallel point iterative algorithms which use the full- and half-sweep approaches for solving the two dimensional diffusion-convection equation. All the parallel point and block iterative algorithms were implemented on MIMD Sequent B8000 computer system at Parallel Algorithm Research Center (PARC), Loughborouh University of Technology, United Kingdom. In the case of point iterative algorithm, the results obtained shown that the parallel point iterative algorithm which uses the half-sweep approach is relatively faster than the parallel full-sweep point iterative algorithm. This is due to the lower total computational operations in the algorithm since only half of the total points are involved in the iterations.

In a more recent development, Othman *et al.* (1998) introduced a new point iterative algorithm which uses the quater-sweep approach for solving the two dimensional Poisson equation on MIMD computer system, the Sequent S27. The experimental and analytical results obtained have shown that the algorithm is superior than the point iterative algorithms which use the full- and half-sweep approaches. As we know, the iterative algorithm requires a tremendous amount of computer time for solving a large and sparse linear system With the advent of new emerging parallel computers, the parallel implementation of the new algorithm when incorporated with the CB strategy will improve the performance of the algorithm.

THE POINT ITERATIVE ALGORITHMS

The solution of two dimensional Poisson equation

$$\frac{\partial^2 u}{\partial x^2} + \frac{\partial^2 u}{\partial y^2} = f(x,y), \quad (x,y) \in \Omega^h, \tag{1}$$

in a unit square Ω^h with Dirichlet boundary condition using the finite difference methods, resulted in a large system of equations which is usually solved iteratively.

Assume equation (1) as our model problem defined in a unit square Ω^h with spacings $\Delta x = \Delta y = \frac{1}{n} = h$ in both x and y directions with $x_i = x_0 + ih$ and $y_j = y_0 + jh$ for all i, j = 0,1,2,...., n. when equation (1) is discretized using finite difference scheme , the most commonly used approximations is the standard five-points stencil given by

$$v_{i+1,j} + v_{i-1,j} + v_{i,j+1} + v_{i,j-1} - 4v_{i,j} = h^2 f_{i,j}. \tag{2}$$

where $v_{i,j}$ is an approximation to the exact solution $u(x_i,y_j)$ at the point (x_i, y_j) = (ih, jh). Equation (1) can also be discretized using similar scheme with a width of 2h and leads to the following stencil,

$$v_{i+2,j} + v_{i-2,j} + v_{i,j+2} + v_{i,j-2} - 4v_{i,j} = 4h^2 f_{i,j}. \quad (3)$$

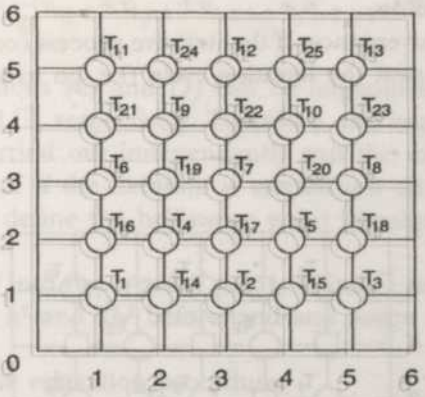

Fig 1. The solution domain Ω^h with the chessboard (CB) ordering strategy for o type of points

Another type of approximation derived from the rotated finite difference approximation can be obtained by rotating the x – y axis clockwise by 45°. Thus, the rotated difference approximation for equation (1) become (Abdullah (1991)),

$$v_{i+1,j+1} + v_{i-1,j-1} + v_{i+1,j-1} + v_{i-1,j+1} - 4v_{i,j} = 2h^2 f_{i,j}. \quad (4)$$

Equations (2), (3) and (4) have been used in the derivation of the new point iterative algorithm. A brief description of the full- and half-sweep points iterative algorithms are given below.

FULL-SWEEP POINT ITERATIVE ALGORITHM

Let us consider the solution at any point Ω^h may be obtained using the stencil five points finite difference approximation (equation (2)). The SOR algorithm involves may be described as follows

1. Define all the points in Ω^h, see Figure 1. Compute the value of h^2 beforehand and assign to a variable H.
2. Implement the relaxation procedure,

$$v_{i,j}^{(k+1)} = \omega\left(\tilde{v}_{i,j}^{(k+1)} - v_{i,j}^{(k)}\right) + v_{i,j}^{(k)}$$

where the $\tilde{v}_{i,j}^{(k+1)}$ are the intermediate solutions of the (k + 1) th Gauβ-Seidel iteration defined by

$$\tilde{v}_{i,j}^{(k+1)} = 0.25 * (v_{i,j+1}^{(k)} + v_{i-1,j}^{(k+1)} + v_{i+1,j}^{(k)} + v_{i,j-1}^{(k+1)} - H * f_{i,j}),$$

for all the points.

3. Check for convergence. If the iterative process converges, go to step (4), otherwise, repeat the iteration cycle (i.e. go to step (2)).
4. Stop.

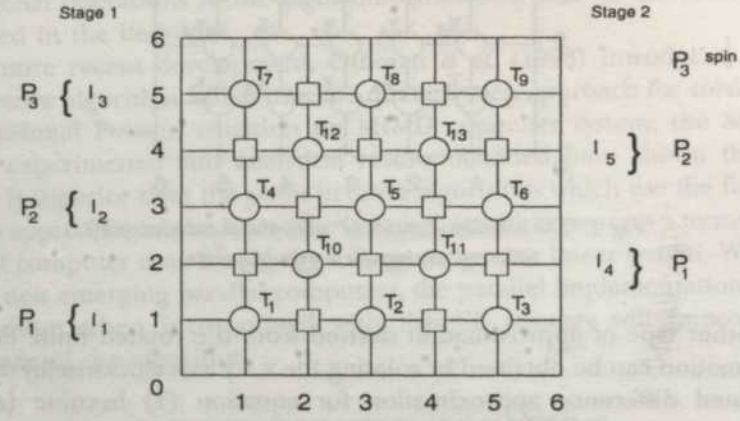

Fig 2. The solution domain Ω^h with the horizontal zebra line (HZL) ordering strategy for o type of points

HALF-SWEEP POINT ITERATIVE ALGORITHM

In this algorithm, the Ω^h is labelled into two types of points; ○ and □ as shown in Figure 2. The solution of any point either ○ or □ can be implemented by only involving the same type of point.

Using equation (4) and taking any group of two points (i.e. ○ and □) in Ω^h leads to the (2 x 2) system of equation,

$$\begin{bmatrix} 4 & 0 \\ 0 & 4 \end{bmatrix} \begin{bmatrix} v_{i,j} \\ v_{i+1,j} \end{bmatrix} = \begin{bmatrix} v_{i-1,j-1} + v_{i+1,j-1} + v_{i-1,j+1} + v_{i+1,j+1} - 2h^2 f_{i,j} \\ v_{i,j-1} + v_{i,j+1} + v_{i+2,j-1} + v_{i+2,j+1} - 2h^2 f_{i+1,j} \end{bmatrix} \quad (5)$$

Splitting equation (5) leads to a decoupled group of (1 x 1) equations in explicit form as,

$$\left[v_{i,j}\right] = \frac{1}{4}\left[v_{i-1,j-1} + v_{i+1,j-1} + v_{i-1,j+1} + v_{i+1,j+1} - 2h^2 f_{i,j}\right] \quad (6)$$

and

$$\left[v_{i+1,j}\right] = \frac{1}{4}\left[v_{i,j-1} + v_{i,j+1} + v_{i+2,j-1} + v_{i+2,j+1} - 2h^2 f_{i+1,j}\right]. \quad (7)$$

It is clear that equations (6) and (7) can be implemented by only involving points of type ○ and □, respectively. Therefore, the implementation of these equations can be carried out independently and the execution time can be reduced to nearly half if the iteration is carried out on either type of point. Hence, we may now define the half-sweep point iterative algorithm as,

1. Divide the Ω^h into two types of point; ○ and □, see Figure 2. Compute the values of h^2 and $2h^2$ beforehand and assign to variables H and I, respectively.
2. Implement the relaxation procedure,

   $$v_{i,j}^{(k+1)} = \omega\left(\tilde{v}_{i,j}^{(k+1)} - v_{i,j}^{(k)}\right) + v_{i,j}^{(k)}$$

   where the $\tilde{v}_{i,j}^{(k+1)}$ are the intermediate solutions of the (k + 1) th Gauβ-Seidel iteration defined by

   $$\tilde{v}_{i,j}^{(k+1)} = 0.25 * (v_{i-1,j+1}^{(k)} + v_{i-1,j-1}^{(k+1)} + v_{i+1,j+1}^{(k)} + v_{i+1,j-1}^{(k+1)} - I * f_{i,j}),$$

   for all the ○ points.
3. Check for convergence. If the iterative process converges, evaluate the solutions at the other half of points (i.e. □) using equation,

   $$v_{i,j} = 0.25 * (v_{i+1,j} + v_{i-1,j} + v_{i,j-1} + v_{i,j+1} - H * f_{i,j}),$$

   otherwise, repeat the iteration cycle (i. e. go to step (2)).
4. Stop.

QUARTER - SWEEP POINT ITERATIVE ALGORITHM

The Ω^h is labelled in three different types of points; ●, □ and ○ as shown in Figure 3. A group of ● points which involved in the iterative evaluations is about a quarter of the total point for a large size of points. The solution of any ● point can be computed by only involving points of type ●. Therefore, this computation can be carried out independently from the other two types of points; □ and ○.

Due to this independency, we can theoretically save the execution time by approximately a quarter if the iteration over the Ω^h is carried out only on the ● type of points. After the convergence criteria is achieved, the solutions of the remaining two types of points are executed directly at once starting from point type ○ and followed by □ using the equations (4) and (2), respectively. Hence , we may define the quarter-sweep point iterative algorithm as follows:

1. Divide the Ω^h into three types of point; ●, ○ and □, see Figure 3. Compute the values of h^2, $2h^2$ and $4h^2$ beforehand and assign to variables H, I and J, respectively.
2. Implement the relaxation procedure,

$$v_{i,j}^{(k+1)} = \omega\left(\tilde{v}_{i,j}^{(k+1)} - v_{i,j}^{(k)}\right) + v_{i,j}^{(k)}$$

where the $\tilde{v}_{i,j}^{(k+1)}$ are the intermediate solution of the (k + 1) th Gauβ-Seidel iteration defined by

$$\tilde{v}_{i,j}^{(k+1)} = 0.25 * (v_{i+2,j}^{(k)} + v_{i-2,j}^{(k+1)} + v_{i,j+2}^{(k)} + v_{i,j-2}^{(k+1)} - J * f_{i,j}),$$

for all the ● points.

3. Check for convergence. If the iterative process converges, evaluate the solutions at the other two points starting from point type ○ and followed by □ using the following

3.1. $v_{i,j} = 0.25 * (v_{i+1,j+1} + v_{i-1,j-1} + v_{i+1,j-1} + v_{i-1,j+1} - I * f_{i,j})$, and

3.2. $v_{i,j} = 0.25 * (v_{i+1,j} + v_{i-1,j} + v_{i,j+1} + v_{i,j-1} - H * f_{i,j})$,

respectively. Otherwise, repeat the iteration cycle (i. e. go to step (2)).

4. Stop.

The details of the algorithm can be found in Othman *et al.* (1998).

PARALLEL IMPLEMENTATION AND STRATEGIES

Assume the Ω^h is large with even size of points n. The optimal parallel strategy of parallelizing the full-, half- and quarter- sweep point iterative algorithms have been investigated and can be outlined as follows:

For Quarter-sweep Point Iterative Algorithm: From Figure 3, each ● point or task T_i for all i = 1, 2,..., N with $N = \frac{1}{4}(n-2)^2$ is assigned to available processor one at a time in CB strategy. The static schedulling is employed in this

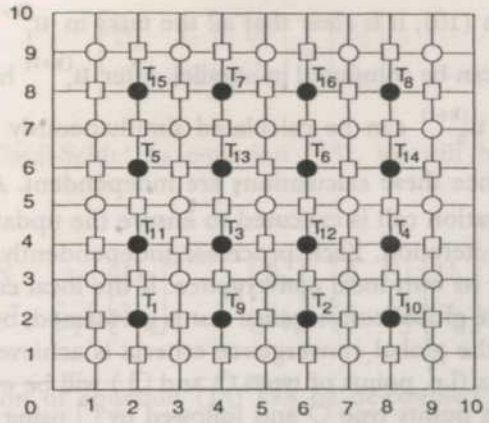

Fig 3. The solution domain Ω^h with the CB ordering strategy for ● type of points

implementation. By applying equation (3) in turn with such strategy to each task T_i in Ω^h will leads to a linear system as

$$\begin{bmatrix} D_r & U \\ U^T & D_b \end{bmatrix} \begin{bmatrix} u_r \\ u_b \end{bmatrix} = \begin{bmatrix} f_r \\ f_b \end{bmatrix} \tag{8}$$

with the diagonal sub matrices D_r and D_b of size $\left(\frac{N}{2} \times \frac{N}{2}\right)$ and each diagonal element is equivalent to -4. Applying the Gauβ-Seidel to equation (8), we will have

$$\begin{bmatrix} D_r & U \\ U^T & D_b \end{bmatrix} \begin{bmatrix} u_r \\ u_b \end{bmatrix}^{(k+1)} = \begin{bmatrix} f_r \\ f_b \end{bmatrix} - \begin{bmatrix} 0 & U \\ 0 & 0 \end{bmatrix} \begin{bmatrix} u_r \\ u_b \end{bmatrix}^{(k)}. \tag{9}$$

If the diagonal sub matrices D_r^{-1} and D_b^{-1} exist, we can evaluate equation (9) by first calculating

$$u_r^{(k+1)} = (1-\omega_e)u_r^{(k)} + \omega_e D_r^{-1}\left[f_r - U u_b^{(k)}\right] \tag{10}$$

followed by

$$u_b^{(k+1)} = (1-\omega_e)u_b^{(k)} + \omega_e D_b^{-1}\left[f_r - U^T u_r^{(k+1)}\right] \tag{11}$$

with the relaxation factor, ω_e.

From equation (10), it is clear that all the tasks in $u_r^{(k+1)}$ are independent of each other and can be computed in parallel. After $u_r^{(k+1)}$ has been completed, equation (11) or $u_b^{(k+1)}$ can be calculated simultaneously using the updated values of $u_r^{(k+1)}$ since these calculations are independent. At the end of each stage, a synchronization call is executed to ensure the updated values are used in the subsequent iteration. Each processor independently iterate on its own task and check for its own local convergence. If the local convergence criteria is achieved then the global convergence test is performed; otherwise repeat the iteration cycle. If the global convergence criteria is achieved, the solutions at the remaining tasks (i.e. points of types ○ and □) will be evaluated directly at once, starting from points type ○ and followed by □ using equations (4) and (2), respectively. These direct evaluations can be executed in parallel by assigning each remaining task in natural strategy to available processor one at a time. Otherwise increase the number of iteration and repeat the iteration cycle.

For Half-sweep Point Iterative Algorithm: The algorithm uses the horizontal zebra line (HZL) strategy which consists of two stages of calculation upon each iteration, see Figure 2. At the first stage, three rows of the ○ points or tasks T_i are assigned to each processor in alternate order and the same happen in stage two. Lines l_1, l_2 and l_3 are assigned to P_1, P_2 and P_3, respectively. After calculating all values at the half of the tasks in given lines in parallel, a synchronization call takes place which marks the end of the first stage. In the second stages, lines l_4 and l_5 are assigned to P_1 and P_2 respectively while P_3 is keep on spinning. In other words, a group of lines l_1, l_2, l_3 is updated at stage 1 and then followed by a second group of lines l_4, l_5 which is updated in stage 2. By applying equation (4) in turn to each group with such strategy, we will have a large linear system

$$\begin{bmatrix} D_{l_1} & & & U & & \\ & D_{l_2} & & U & U & \\ & & D_{l_3} & & U & \\ U^T & U^T & & D_{l_4} & & \\ & U^T & U^T & & D_{l_5} & \end{bmatrix} \begin{bmatrix} u_{l_1} \\ u_{l_2} \\ u_{l_3} \\ u_{l_4} \\ u_{l_5} \end{bmatrix} = \begin{bmatrix} f_{l_1} \\ f_{l_2} \\ f_{l_3} \\ f_{l_4} \\ f_{l_5} \end{bmatrix} \qquad (12)$$

where the diagonal sub matrices D_{l_1}, D_{l_2}, D_{l_3} and D_{l_4}, D_{l_5} of size $\left(\left\lceil\frac{N}{2}\right\rceil \times \left\lceil\frac{N}{2}\right\rceil\right)$ and $\left(\left\lfloor\frac{N}{2}\right\rfloor \times \left\lfloor\frac{N}{2}\right\rfloor\right)$, respectively with N = (n - 1) and the diagonal element is equivalent to –4. Since there are two stages, equation (12) can be rewrite as the following form

$$\begin{bmatrix} \hat{D}_1 & C \\ C^T & \hat{D}_2 \end{bmatrix} \begin{bmatrix} U_1 \\ U_2 \end{bmatrix} = \begin{bmatrix} B_1 \\ B_2 \end{bmatrix} \tag{13}$$

By applying the Gauβ-Seidel to equation (13), we will have the following equation

$$\begin{bmatrix} \hat{D}_1 & 0 \\ C^T & \hat{D}_2 \end{bmatrix} \begin{bmatrix} U_1 \\ U_2 \end{bmatrix}^{(k+1)} = \begin{bmatrix} B_1 \\ B_2 \end{bmatrix} - \begin{bmatrix} 0 & C \\ 0 & 0 \end{bmatrix} \begin{bmatrix} U_1 \\ U_2 \end{bmatrix}^{(k)}. \tag{14}$$

The explicit solution of equation (14) can be de-coupled into the following system of equations

$$U_1^{(k+1)} = (1-\omega_e)U_1^{(k)} + \omega_e \hat{D}_1^{-1}\left[B_1 - CU_2^{(k)}\right] \tag{15}$$

and

$$U_2^{(k+1)} = (1-\omega_e)U_2^{(k)} + \omega_e \hat{D}_2^{-1}\left[B_2 - C^T U_1^{(k+1)}\right] \tag{14}$$

with the diagonal sub matrices $\hat{D}_1$ and $\hat{D}_2$ exist.

Clearly, we can see that all the tasks in $U_1^{(k+1)}$ are independent of each other and can be computed in parallel. Each processor is assigned an approximately equal number of tasks to work on. After $U_1^{(k+1)}$ has been calculated, $U_2^{(k+1)}$ can be calculated simultaneously using the updated values of $U_1^{(k+1)}$ since this calculation is independent. However, since the most recent values of $U_1^{(k+1)}$ are to be used in equation (16), a synchronizing call has to be made before the calculation of $U_2^{(k+1)}$ strats. Each processor then checks for its local and global convergence criteria the same way as described in the previous method. Once the global convergence is achieved, the solution at the remaining tasks (i. e. points of type □) will be evaluated directly in parallel at once using equation (4) by assigning tasks of each row to different processor.

For Full-sweep Point Iterative Algorithm: All ○ points or tasks T_i for all i = 1, 2, ..., N with $N = (n-1)^2$ which involve in the process of iterative evaluation are assigned to available processor one at a time in the CB strategy, see Figure 1. This strategy is the same as mentioned in the quarter-sweep point iterative algorithm. If the local and global convergence criteria are achieved, the

TABLE 1
Relaxation factor ω_e, no. of iteration, strategies and max. error for all the parallel algorithms

h^{-1}	Method	ω_e	No. iteration	Strategies	Max. error
24	Full-	1.77	96	CB	5.42×10^{-6}
	Half-	1.70	69	HZL	2.88×10^{-4}
	Quarter-	1.59-1.60	49	CB	2.64×10^{-5}
36	Full-	1.84	145	CB	2.42×10^{-6}
	Half-	1.76	103	HZL	1.28×10^{-4}
	Quarter-	1.71	73	CB	1.06×10^{-5}
50	Full-	1.89	203	CB	1.25×10^{-6}
	Half-	1.84	141	HZL	6.64×10^{-4}
	Quarter-	1.78	98	CB	5.28×10^{-6}
70	Full-	1.92	281	CB	6.24×10^{-7}
	Half-	1.89	205	HZL	3.38×10^{-5}
	Quarter-	1.84	136	CB	2.63×10^{-6}
100	Full-	1.94	380	CB	3.15×10^{-7}
	Half-	1.92	289	HZL	1.66×10^{-5}
	Quarter-	1.89	203	CB	1.27×10^{-6}

iterative evaluation is stopped; otherwise repeat the iteration cycle.

PERFORMANCE EVALUATION

In order to confirm that the parallel quarter-sweep point iterative algorithm is better than the other parallel algorithms, the following experiments were carried out on the SMP parallel computer, the Sequent S27. All algorithms were applied to the following test problem,

$$\frac{\partial^2 u}{\partial x^2} + \frac{\partial^2 u}{\partial y^2} = (x^2 + y^2)e^{xy}, \quad (x,y) \in \Omega^h = [0,1] \times [0,1], \tag{17}$$

subject to the Dirichlet conditions and satisfying the exact solution $u(x,y) = e^{xy}$ for $(x,y) \in \partial\Omega^h$.

Throughout the experiments, the local convergence test was the maximum absolute error with the error tolerance $\varepsilon = 10^{-10}$. The experiments were performed on various sizes of n such as 24, 36, 50, 70, 100 and number of processors ranging from 1 to 5. For each n, the experimental value of ω_e was obtained to within ±0.01 by solving the problem for a range of values of ω_e and choosing those which give the minimum number of iterations. Table 1 lists the optimum value of ω_e number of iterations, strategies and maximum error for all the parallel algorithms and the timing results and speedup are presented in Table 2. For n = 100, the graphs of execution time, speedup and efficiency

TABLE 2
Execution time and speedup for all the parallel algorithms

h^{-1}	No. processors	Full-		Half-		Quarter-	
		Time	Speedup	Time	Speedup	Time	Speedup
24	1	4.8519	1.0000	1.8878	1.0000	0.6441	1.0000
	2	2.6289	1.8456	1.0521	1.7943	0.3739	1.7225
	3	1.8714	2.5926	0.8021	2.3533	0.2828	2.2770
	4	1.4975	3.2400	0.6100	3.0947	0.2211	2.9131
	5	1.3322	3.6420	0.5623	3.3572	0.2002	3.2164
36	1	16.6563	1.0000	6.3132	1.0000	2.1570	1.0000
	2	8.8748	1.8768	3.3785	1.8686	1.1685	1.8465
	3	6.4233	2.5931	2.5405	2.4850	0.8974	2.4036
	4	5.0936	3.2681	2.0121	3.1376	0.6905	3.1237
	5	4.2167	3.9500	1.6748	3.7695	0.5970	3.6125
50	1	45.5404	1.0000	16.6219	1.0000	5.5789	1.0000
	2	24.0318	1.8950	8.8426	1.8797	3.0786	1.8121
	3	16.8674	2.6999	6.4321	2.5842	2.2586	2.4700
	4	13.6692	3.3316	5.0450	3.2947	1.7155	3.2520
	5	10.9319	4.1658	4.1124	4.0418	1.4101	3.9562
70	1	125.8978	1.0000	48.3252	1.0000	15.3360	1.0000
	2	67.8831	1.9000	25.5685	1.8900	8.3356	1.8398
	3	46.2469	2.7889	17.7666	2.7200	5.8891	2.6041
	4	34.6940	3.6288	13.7592	3.5122	4.5747	3.3523
	5	28.6456	4.3950	11.4713	4.2127	3.8009	4.0348
100	1	353.5294	1.0000	146.2460	1.0000	48.1291	1.0000
	2	179.8033	1.9662	76.9520	1.9004	25.3738	1.8968
	3	127.3153	2.7768	52.8097	2.7693	17.6200	2.7315
	4	96.1932	3.6752	41.4294	3.5300	13.7472	3.5010
	5	79.1159	4.4685	33.8454	4.3210	11.5533	4.1658

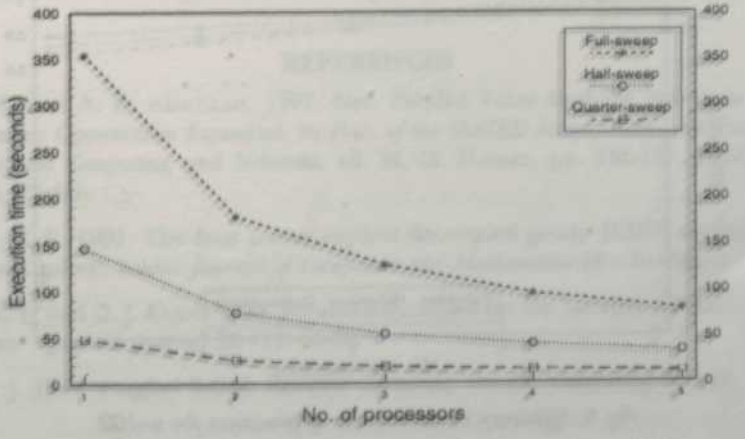

Fig 4. Execution time versus number of processors for n=100

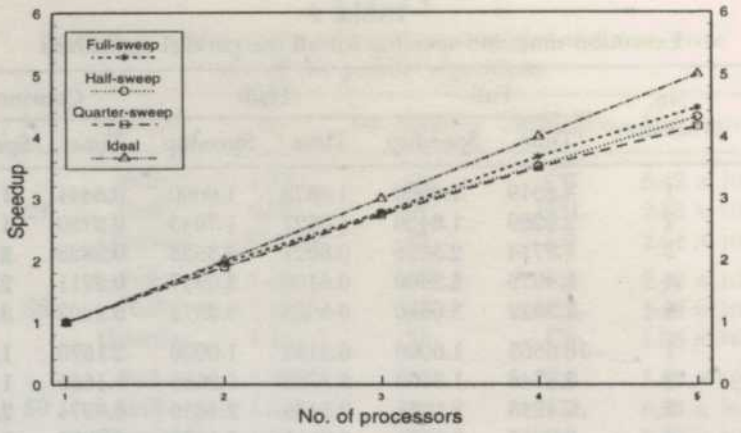

Fig 5. Speedup versus number of processors for n=100

versus number of processors are shown in *Figures 4, 5* and *6*, respectively.

The temporal performance parameter is usually used to compare the performance of different algorithms for solving the similar problem. It is defined as the inverse of the execution time where the unit is work done per second. The algorithm with the highest performance executes in the least time and therefore is the better algorithm. The graph of temporal performance versus number of processors of all the parallel algorithms is plotted and shown in Figure 7.

CONCLUSION

In Table 2, the timing results obtained have shown that the parallel quarter-

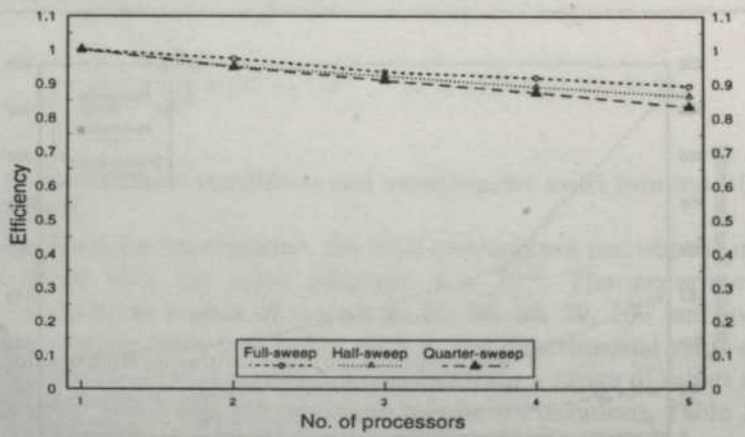

Fig 6. Efficiency versus number of processors for n=100

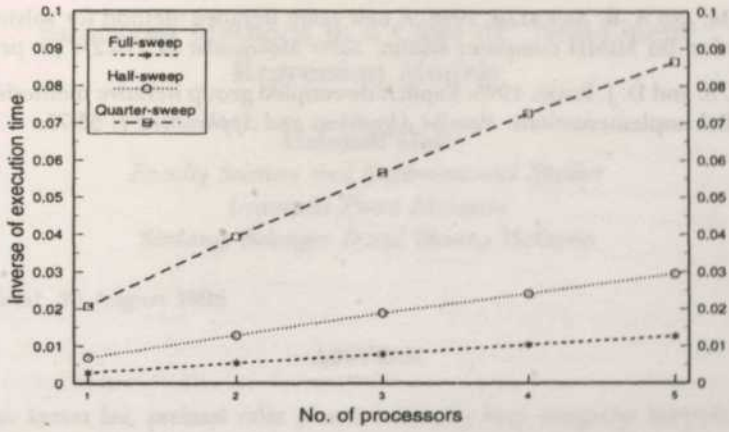

Fig 7. Temporal performance versus number of processors for n=100

sweep point iterative algorithm which uses the CB strategy is superior than the parallel full- and half-sweep point iterative algorithms for any number of processors and as n gets larger. Figure 4 shows the graph of the execution time versus number of processors for case n = 100. This is due to the lower total computational operations in the algorithm since approximately a quarter of the total points are involved in the iteration. The superiority of the algorithm is also indicated by the highest value of the temporal performance and least number of iteration of the algorithm as shown in Figure 7 and Table 1, respectively.

However, the speedup and efficiency of the parallel quarter-sweep algorithm is slightly less than the other two algorithms and it can be improved by increasing the size of points n in the Ω^h, see Figures 5 and 6. In conclusion, the parallel quarter-sweep point iterative algorithm with the CB strategy performs drastic improvement in execution time and it has proved to be an efficient parallel Poisson algorithm among the three algorithms on the SMP parallel computer.

REFERENCES

ALI, N. M. and A. R. ABDULLAH. 1997. New Parallel Point Iterative Solutions for the Diffusion Convection Equation, in *Proc. of the IASTED Intern. Conf. on Parallel and Distributed Computing and Networks*, ed. M. H. Hamza, pp. 136-139, IASTED-Acta Press, Zürich.

ABDULLAH, A. R. 1991. The four points explicit decoupled group (EDG) method: a fast Poisson solver. *Intern. Journal of Computers and Mathematics* **38** : 61-70.

BARLOW, R. H and D. J. EVANS. 1982. Parallel algorithms for the iterative solution to linear system. *Computer Journal* **25** (1): 56-60.

EVANS, D. J. 1984. Parallel S.O.R. iterative methods. *Parallel Computing* **1**: 3-18.

OTHMAN, M. AND A. R. ABDULLAH. 1998. A new point iterative method for solving Poisson equation on MIMD computer system. *Sains Malaysiana* **27** (1&2): (in press).

YOUSIF, W. S. and D. J. EVANS. 1995. Explicit de-coupled group iterative methods and their parallel implementations. *Parallel Algorithms and Applications* **7**: 53-71.

Pertanika J. Sci. & Technol. 8(2): 175-189 (2000)
ISSN: 0128-7680

Bootstrap Methods in a Class of Non-Linear Regression Models

Habshah Midi
Faculty Sciences and Environmental Studies
Universiti Putra Malaysia
Serdang, Selangor Darul Ehsan, Malaysia

Received: 20 August 1998

ABSTRAK

Dalam kertas ini, prestasi ralat piawai bootstrap bagi anggaran berpemberat MM (WMM) dibandingkan dengan ralat piawai Monte Carlo dan ralat piawai Berasimptot. Sifat-sifat selang keyakinan bootstrap bagi anggaran berpemberat WMM seperti 'Percentile' (PB), 'Bias-corrected Percentile' (BCP), 'Bias and Accelerated' (BC_a), 'Studentzed Percentile' (SPB) dan 'Symmetric' (SB) telah diperiksa dan dibandingkan. Keputusan kajian menunjukkan bahawa BSE boleh dianggap hampir kepada ASE dan MCSE sehingga 20% titik terpencil. BC_a mempunyai sifat yang menarik dari segi kebarangkalian liputan, kesamaan hujung dan purata panjang selang yang lebih baik jika dibandingkan dengan kaedah lain.

ABSTRACT

In this paper, the performances of the bootstrap standard errors (BSE) of the Weighted MM (WMM) estimates were compared with the Monte Carlo (MCSE) and Asymptotic (ASE) standard errors. The properties of the Percentile (PB), Bias-Corrected Persentile (BCP), Bias and Accelerated (BC_a), Studentized Percentile (SPB) and the Symmetric (SB) bootstrap confidence intervals of the WMM estimates were examined and compared. The results of the study indicate that the BSE is reasonably close to the ASE and MCSE for up to 20% outliers. The BC_a has attractive properties in terms of better coverage probability, equitailness and average interval length compared to the other methods.

Keywords: Outlier, weighted MM, bootstrap sampling

INTRODUCTION

One of the important aspects in statistical inference is to obtain the standard errors of parameter estimates and to construct confidence intervals for the parameters of a model. There exist abundant procedures to provide approximate confidence intervals. In recent years, an increasingly popular method is bootstrapping method which was introduced by Efron (1979). There are considerable papers related to bootstrap methods (DiCiccio and Romano 1988; DiCiccio and Tibshirani 1987; Efron 1981a, 1981b, 1982, 1985, 1987; Efron and Gong 1983; Efron and Tibshirani 1986, 1993; Hall 1986a, 1986b; Huet *et al.* 1990; Loh 1987, Wu 1986).

In this paper, we want to investigate the bootstrap estimates of the standard errors of the Weighted MM (WMM) estimates and compare them with the asymptotic and Monte Carlo standard errors. Five different bootstrap confidence intervals are used for estimating the WMM estimates, namely, the Percentile (PB), Bias-Corrected Percentile (BCP), Bias-Corrected and Accelerated (BC_a) and the Symmetric bootstrap (SB). A 'good' confidence interval is one which posseses a reasonably accurate coverage probability and 'good' equitailness. By equitailed, we mean that a confidence interval for β of level $(1 - 2\alpha)$ is such that the proportion for β lying outside the interval is divided equally between the lower and upper limits of the intervals. In other words, the proportion of β lower than the lower limit of the interval is reasonably equal to α, as is the proportion of β that exceeds the upper limit. A secondary consideration is the confidence interval length.

THE WEIGHTED MM ESTIMATES (WMM)

The proposed technique for the Weighted MM is computed in four stages:

- Compute the Weighted Nonlinear LMS.
- Calculate an M estimate of weighted scale using rho function ρ_0.
- Compute the weighted M estimate using rho function ρ_1.
- Repeat step 2 dan 3 until convergence.

Hampel redescending psi function (Hampel *et al.* 1986), denoted as ρ_H, is used in the analysis. Yohai (1987) revealed that $\rho_0(r)$ and $\rho_1(r)$ can be taken to be $\rho_H(r/k_0)$ and $\rho_H(r/k_1)$, respectively. Stromberg (1993) demonstrated that selecting $k_0 = 0.212$ and $k_1 = .9014$ will guarantee a high breakdown estimate and will result in 95% efficiency under normal errors, respectively.

Considering the general heteroscedastic nonlinear regression

$$y_i = f(x_i,\beta) + \sigma g\{f(x_i,\beta), z_i, \theta)\varepsilon_i \qquad (1)$$

and the residuals,

$$r_i = \frac{y_i - f(x_i,\beta)}{g\{f(x_i,\beta), z_i, \theta\}} \qquad (2)$$

and assuming that the variance are proportional to the regressor, the residual r_i in (2) becomes

$$r_i = \frac{y_i - f(x_i,\beta)}{x_i} \qquad (3)$$

For model (1), the Weighted Nonlinear LMS, $\hat{\beta}_{WLMS}$ is obtained from

$$\arg\min_{\hat{\beta}_{WLMS}} r^2_{(k)}(\beta_{WLMS}) \tag{4}$$

where

$$r^2_{(i)}(\beta_{WLMS}), i = 1,2,3,...,n \text{ are the ordered } r^2_{(i)}(\beta_{WLMS})$$

and k is given by Stromberg (1993).

The proposed algorithm for the weighted nonlinear LMS and the Weighted MM estimates are similar to Stromberg (1993), except that y_i and $f(x, \beta)$ are replaced by y_i/x_i and $f(x,\beta)/x_i$, respectively.

The steps in the algorithm of the Weighted Nonlinear LMS are as follows:

- Calculate the initial estimate of WLMS denoted by $\hat{\beta}_{WLMS}$, using GNLLS denoted by $\hat{\beta}$.
- Compute the GNLLS estimate to p randomly selected points, denoted by $\hat{\beta}_{WLS}$.
- If the median squared residual at $\hat{\beta}_{WLMS}$ is less than the median squared residual at $\hat{\beta}$, $\hat{\beta}$ is replaced by $\hat{\beta}_{WLS}$ as the current estimate of $\hat{\beta}_{WLMS}$.
- Steps 2 and 3 are repeated k times, where k is specified by Stromberg (1992, 1993).
- $\hat{\beta}$ is used as a starting value for calculating the LS fit $\hat{\beta}^*_{LS}$, for data points such that $r_i^2\left(\hat{\beta}\right) \le \text{med}_{1\le i\le n} r_i^2\left(\hat{\beta}\right)$. If $\text{med}_{1\le i\le n} r_i^2\left(\hat{\beta}^*_{LS}\right) < \text{med}_{1\le i\le n} r_i^2\left(\hat{\beta}\right)$, then $\hat{\beta}$ is replaced by $\hat{\beta}^*_{LS}$ as the current estimate of $\hat{\beta}_{WLMS}$.
- In order to get an even better estimate, the Nelder-Mead Simplex Algorithm (Nelder and Mead 1965) which is implemented in Press *et al.* (1986) with fractional tolerance 10^{-4}, is used to minimize $\text{med}_{1\le i\le n} r_i^2\left(\hat{\beta}\right)$ by using $\hat{\beta}$ as the starting value.

The Weighted M-Estimate for Scale

Let $\hat{\beta}_{WLMS}$ be the parameter estimate of the regression function in (1) with a high breakdown point, and the residuals are defined by

$$r_i\left(\hat{\beta}\right) = \frac{y_i - f\left(x_i, \hat{\beta}_{WLMS}\right)}{x_i}, \qquad 1 \le i \le n$$

The weighted M-scale estimate is defined as the value of s which is the solution of

$$\frac{1}{n}\sum \rho_0(r_i / s_n) = b \tag{5}$$

where
b may be obtained from the equation $E_\phi(\rho(r))=b$.

Let ρ_0 in (5) be a real function which satisfies the following assumptions:

- $\rho(0)=0$
- $\rho(-r)=\rho(r)$
- $0 \le u \le v$ implies $\rho(u) \le \rho(v)$ (6)
- ρ is continuous
- Let $a = \sup \rho(r)$, then $0 < a < \infty$
- If $\rho(u)<a$ and $0 \le u \le v$, then $\rho(u) < \rho(v)$

The constant b is such that

$b/a = 0.5$ where $a = \max \rho_0(r)$ (7)

This implies that this scale estimate has a breakdown point equal to 0.5 as verified by Huber (1981).

The Weighted MM Estimate

The weighted MM estimate is found by minimizing

$$S\left(\beta_{WLMS}\right) = \sum p_1\left(r_i\left(\beta_{WLMS}\right)/S_n\right) \tag{8}$$

where β_{WLMS} and S_n are defined in (4) and (5) respectively. $\rho_1(0/0)$ is interpreted as 0. ρ_1 is another function which satisfies assumption (6) such that

$$p_1(r) \le p_0(r) \tag{9}$$
$$\sup \rho_1(r)=\sup \rho_0(r)=a \tag{10}$$

This implies that $S(\beta_{1WMM}) \le S(\beta_{0WMM})$.

The Standard Error

The covariance matrix of the WMM estimates can be approximated by employing Theorem 4.1 of Yohai (1987). The asymptotic variance of the WMM estimate is the diagonal of the covariance matrix:

$$\left[\frac{\left[\frac{1}{(n-p)}\right]S_n^2 \quad \sum_{i=1}^{n}\left[\psi\left(r_i\left(\beta_{WMM}\right)\right)/\hat{S}_n\right]^2}{\left[\frac{1}{n}\sum_{i=1}^{n}\psi'\left(r_i\left(\beta_{WMM}\right)/\hat{S}_n\right)\right]^2} A^{-1}\right]_{\beta=\hat{\beta}_{WMM}} \tag{11}$$

where
the (jk)-th element of A, j, k $\in$ {1,2...p}, is

$$\sum_{i=1}^{n}\left(\partial\left[h\left(x_i,\beta\right)/x_i\right]/\partial\beta_j\right)\left(\partial\left[\left[h\left(x_i,\beta\right)/x_i\right]/\partial\theta_k\right]\right)$$

and ψ is the derivative of ρ_1 and $\hat{S}_n$ is the scale estimate as defined in (5). However, this estimate possesses several shortcomings when it has a breakdown point equal to 1/n in most regression settings.

THE BOOTSTRAP METHODS

Bootstrap methods can be applied to a nonlinear regression model. Caroll and Ruppert (1988) and Stromberg (1993) used the bootstrap method to compute bootstrap standard errors of the Transform Both Sides (TBS) estimates and the MM estimates, respectively. Huet *et al.* (1990) carried out a simulation study to compare different methods for calculating approximate confidence intervals for parameters in nonlinear regression. The above authors used the resampling method with fixed regressors.

Resampling With Fixed Regressors or Bootstrapping Residuals

- Fit a model to the original sample of observations to get $\hat{\beta}$.
- Construct $\hat{F}$, putting mass 1/n at each observed residuals, $\hat{F}$: masa 1/n at each $\hat{\varepsilon}_i = y_i - f\left(x_i,\hat{\beta}\right), i = 1,2....n.$
- Draw a bootstrap data set, $y_i^* = f\left(x_i,\hat{\beta}\right)+\hat{\varepsilon}$ where $\hat{\varepsilon}$ are i.i.d from $\hat{F}$.
- Compute $\hat{\beta}^*$ for the bootstrap data set.
- Repeat B times the steps 3 and 4, obtaining bootstrap replications $\hat{\beta}^{*1},\hat{\beta}^{*2},...,\hat{\beta}^{*B}$

- Estimate the bootstrap standard errors, by taking square root to the main diagonal of the covariance matrix,

$$\hat{COV} = \frac{1}{B-1}\sum_{b=1}^{B}\left(\hat{\beta}^{*b} - \hat{\beta}^{*\cdot}\right)\left(\hat{\beta}^{*b} - \hat{\beta}^{*\cdot}\right)^{T} \qquad (12)$$

where

$$\hat{\beta}^{*\cdot} = \frac{1}{B}\sum_{b=1}^{B}\hat{\beta}^{*b}$$

Bootstrap Confidence Interval

In practice, the estimated standard errors $\hat{\sigma}$, are usually employed to form approximate confidence intervals to a parameter of interest, β. The usual $(1-2\alpha)100\%$ confidence interval for β is, $\hat{\beta} \pm \hat{\sigma} Z_{\alpha/2}$ where $Z_{\alpha/2}$ is the $100.\alpha/2$ percentile point of a standard normal distribution. The validity of this interval depends on the assumption that $\hat{\beta}$ is normally distributed. Otherwise, this approximate confidence interval will not be very accurate. Bootrstrap confidence intervals do not rely upon the usual assumption of normality.

In this section, we will use the bootstrap to calculate better confidence intervals even if the underlying distribution of the estimate is not normal. Some bootstrap methods make substantial rectifications which significantly improve the inferential accuracy of the interval estimate. There are various methods that can be used to construct bootstrap confidence intervals. Huet *et al.* (1990) carried out simulation studies on a nonlinear regression models by using the Studentized Percentile (SPB), the Ordinary Percentile (OP) and the Symmetric (SB) bootstrap confidence intervals. The bias- corrected percentile (BCP) and the bias- corrected and accelerated (BC_a) confidence intervals could be used in the nonlinear regression models as enumerated by Efron (1984) and Hall et al. (1989). We will review five methods of bootstrap confidence intervals, namely, the Percentile (PB), the bias-corrected percentile (BCP), the bias-corrected and accelerated (BC_a), the studentized percentile (SPB), and the Symmetric bootstrap (SB) for the parameter β.

The Bootstrap Standard Errors

The performance of the Weighted MM (WMM) is found to be better than the MM, NLLS and the GNLLS estimates as shown by Midi (1999). In order to examine its asymptotic, Monte Carlo and bootstrap standard errors, simulations studies were carried out using the Ricker; $\left(y_i = \beta_0 x_i \exp\left(-\beta_1 x_i\right) + \varepsilon_i\right)$ and Micahelis-Menten model; $\left(y_i = \frac{\beta_1 x_i}{\exp\left(\beta_2\right) + x_i} + \varepsilon_i\right)$. 30 'good' data were

generated according to both models, where x_i are uniformly distributed on [0, 10]. For the Michaelis-Menten and the Ricker Models, (β_1,β_2), (β_0,β_1) are set to (10, 0) and (2, 0.04), respectively. The errors ε_i were generated from a normal distribution, $N\left(0,\sigma^2x_i^2\right)$, $\sigma^2=\left(.25\right)^2$. We deleted each observation and replaced with an outlier. The outliers were generated by x_i~U[1,2], ε_i~N(0,1) and y_i=40+ε_i. The performances of the three types of standard errors are presented in Tables 1 and 2 for the Ricker and the Michaelis-Menten models, respectively.

The results in Table 1 for the Ricker model show that the bootstrap standard errors (BSE), the Monte Carlo Standard Errors (MCSE) and the Asymptotic Standard Errors (ASE) are reasonably close to each other for up to 10% outliers. As the percentages of outliers rises, the BSE increases and the increase in BSE of $\hat{\beta}_0$ is remarkably much larger than the ASE and the MCSE. Nevertheless, the BSE of the $\hat{\beta}_1$ increases, but its increment is relatively small. The MCSE and ASE of both $\hat{\beta}_0$ and $\hat{\beta}_1$ increase very little with the increase in outliers and their values are fairly close for up to 40% outliers.

TABLE 1
The Monte Carlo, asymptotic and bootstrap standard errors of the WMM estimates (The Ricker Model)

Outliers %		Monte Carlo Standard Errors	Asymptotic Standard Errors	Bootstrap Standard Errors
0	$\hat{\beta}_0$	.100	.093	.065
	$\hat{\beta}_1$	.009	.010	.008
10	$\hat{\beta}_0$	.104	.091	.294
	$\hat{\beta}_1$	.010	.010	.036
20	$\hat{\beta}_0$	.110	.092	2.460
	$\hat{\beta}_1$	.010	.011	.029
30	$\hat{\beta}_0$	.118	.094	9.910
	$\hat{\beta}_1$	.011	.012	0.113
40	$\hat{\beta}_0$	4.631	.110	24.59
	$\hat{\beta}_1$	.054	.014	.279

TABLE 2
The Monte Carlo, asymptotic and bootstrap standard errors of the WMM estimates (The Michaelis-Menten model)

Outliers %		Monte Carlo Standard Errors	Asymptotic Standard Errors	Bootstrap Standard Errors
0	$\hat{\beta}_0$	.258	.265	.132
	$\hat{\beta}_1$	.066	.052	.027
10	$\hat{\beta}_0$	.268	.277	.150
	$\hat{\beta}_1$	.070	.056	.032
20	$\hat{\beta}_0$	.285	.298	.165
	$\hat{\beta}_1$	.075	.062	.035
30	$\hat{\beta}_0$	.308	.327	2.034
	$\hat{\beta}_1$	.090	.070	3.448
40	$\hat{\beta}_0$	.336	.371	5.457
	$\hat{\beta}_1$	.100	.082	6.419

The results in Table 2 for the Michaelis-Menten model indicate that the BSE is imperceptibly less than the MCSE and ASE for up to 20% outliers. On the other hand, the MCSE is moderately close to the ASE in this situation. It is important to note here that enhancing the proportion of outliers by more than 20% increases the BSE dramatically. This implies that the BSE performs poorly in such a situation. The results of the simulation study also suggest that the reliability of the BSE decreases as the percentages of outliers increases by more than 20%.

A SIMULATION STUDY

In order to investigate the properties of the five types of bootstrap confidence intervals, a series of simulations was conducted, one on a simulated data without outliers and another on a simulated data with 10% outliers. Again, we consider the same simulation procedures as described in section 4 using the Michaelis-Menten and the Ricker models. 200 bootstrap samples were drawn from a sample of size 30 and a bootstrap 95% confidence interval was constructed for each of the five methods. 100 replications of such simulations were executed to determine the percentage of times the true value of the parameter estimates was contained in the interval and the average length was

calculated. The same procedure is repeated for the data with 10% outliers. The results of the simulation studies are illustrated in Tables 3 and 4, respectively.

For the Ricker model (see Table 3), it is quite difficult to decide which confidence interval is better or worse than the others. Judging from the coverage probability, equitailness and average interval length, our results are not in favour of the Percentile (PB), Studentized Percentile (SPB) and Symmetric (SB) intervals for estimating $\hat{\beta}_0$ in the case of 'clean' data. However, they showed an improvement in coverage probability for estimating $\hat{\beta}_1$. The performance of the BC_a is slightly better than the PB, SPB and SB intervals, and in close agreement with the BCP method.

TABLE 3
Coverage probabilities and average width of the five types of bootstrap confidence intervals (The Ricker Model)

No Outlier		Coverage	Lower Coverage	Upper Coverage	Ave. Width
	Method				
$\hat{\beta}_0$	PB	93	2	5	0.436
	BCP	95	2	3	0.434
	BC_a	94	2	4	0.460
	SPB	96	0	4	0.522
	SB	93	1	6	0.435
$\hat{\beta}_1$	PB	92	4	4	0.042
	BCP	91	4	5	0.042
	BC_a	92	4	4	0.041
	SPB	95	3	2	0.048
	SB	94	4	2	0.042
10% Outliers					
$\hat{\beta}_0$	PB	94	1	5	0.445
	BCP	94	1	5	0.445
	BC_a	95	1	4	0.451
	SPB	96	1	3	0.502
	SB	95	0	5	0.672
$\hat{\beta}_1$	PB	91	4	5	0.042
	BCP	91	4	5	0.042
	BC_a	95	3	5	0.042
	SPB	95	3	2	0.047
	SB	93	4	3	0.044

TABLE 4
Coverage probabilities and average width of the five types of bootstrap confidence intervals (The Michaelis-Menten Model)

No Outlier		Coverage	Lower Coverage	Upper Coverage	Ave. Width
Method					
$\hat{\beta}_0$	PB	96	2	2	1.323
	BCP	95	2	3	1.332
	BC_a	95	2	3	1.351
	SPB	95	1	4	1.616
	SB	96	0	4	1.344
$\hat{\beta}_1$	PB	95	2	3	0.782
	BCP	96	2	2	0.737
	BC_a	96	2	2	0.629
	SPB	93	3	4	0.423
	SB	99	0	1	1.848
10% Outliers					
$\hat{\beta}_0$	PB	95	2	3	1.449
	BCP	95	1	4	1.417
	BC_a	96	1	3	1.470
	SPB	93	2	5	1.669
	SB	96	0	4	1.430
$\hat{\beta}_1$	PB	96	3	1	0.925
	BCP	97	2	1	1.118
	BC_a	95	3	2	0.723
	SPB	91	3	6	0.463
	SB	98	0	2	1.570

For the contaminated data, all the confidence intervals have coverage probabilities fairly close to each other. However, the SPB and the SB display wider average interval lengths than the other three methods. Among the PB, BCP and BC_a, the BC_a confidence interval is appreciably the best method, since it possesses a coverage percentage which is equal to the nominal value and reasonably close to the expected value for $\hat{\beta}_0$ and $\hat{\beta}_1$, respectively.

From Table 4 (the Michaelis-Menten model), where the data is 'cleaned' and 'contaminated', it reveals that the SB method gives erroneous results not only from the point of view of equitailness but also from the point of view of coverage probability. In addition, it possesses an average length which is reasonably larger than the other intervals. The performance of the SPB is also not encouraging in both situations. Its coverage probability was lower than the expected value of 0.95 by about 0.04. For the 'clean' data, the coverages of the

BC_a, BCP, and PB confidence intervals were reasonably close to the expected value of 0.95 for both $\hat{\beta}_0$ and $\hat{\beta}_1$. However, the BC_a is considerably the best method because besides displaying a good coverage probability and equitailness, it has relatively shortest intervals than the PB and BCP methods.

A similar conclusion can be made for the case of contaminated data. As before, the BCa confidence interval gives good results in terms of coverage probability, equitailness and confidence interval length. Its coverage probability is almost equal to the nominal value. The average lengths for all bootstrap methods increase and exhibit consistent pattern with the shortest intervals come from the BC_a. This is followed by the PB, BCP, SPB and the longest being the SB confident interval. The results of the study suggest that the BC_a is the best method to estimate the 95% confidence interval for the WMM estimates. The selection of a good bootstrap method is essential.

Since the BC_a confidence interval possesses a 'good' coverage probability, 'good' equitailness and narrowest average interval length, it can be recommended to be incorporated in the NLLS, GNLLS, MM and WMM procedures in an effort to justify the conclusion of Midi (1999) that the WMM is the most robust method among those considered. Again, we use the same simulation procedures as described earlier and apply the BC_a method to the NLLS, GNLLS, MM and WMM techniques. The results of the simulation study are illustrated in Tables 5 – 6. We would expect that a more robust method would be the one with 'good' coverage probability and 'good' equitailness. Another important property is that the method should have the shortest average confidence length. For the Ricker model (see Table 5) and with the 'clean data', the confidence intervals for the NLLS, GNLLS, MM, and WMM have lower coverage percentages than the nominal value of 0.95. Nevertheless, among these intervals the average lengths of the GNLLS and the WMM are fairly close and turn out to be the smallest.

On the other hand, the confidence intervals for the NLLS and GNLLS give the worst results in the presence of outliers in the data set. Their coverage probability was very small and they displayed very bad equitailness. Besides, their average confidence lengths are prominently large. However, the WMM confidence interval for β_0 gives a coverage probability which is in best agreement with the nominal one and signifies the narrowest average interval length. The coverage probability of the WMM confidence interval for β_1 is sligtly less than the nominal value. The performance of the MM confidence intervals estimates are quite good both in terms of coverage probability and average length, but its accomplishment cannot outperform the WMM method.

For the Michaelis-Menten model (see Table 6) and the data with no outliers, it seems that, on the whole, the GNLLS and WMM estimates perform better than the NLLS and MM estimates. Both the methods adequately provide the expected coverage probabilities and the shortest average lengths, though the $\hat{\beta}_0$ of the GNLLS displays a bad equitailness. The results of the study signify

the fact that the NLLS and MM have a lower coverage probability and slightly larger average length than the GNLLS and WMM estimates. The performances of the NLLS and GNLLS are very poor with the presence of outliers. Their coverage probabilities are remarkably much lower than the nominal values and posses average lengths which are much wider than those of the MM and WMM estimates. Nonetheless, the results of the WMM estimates are intuitively appealing. It gives confidence intervals with relatively good coverage probabilities and equitailness. Furthermore, it possesses the smallest average confidence length. On the other hand, the MM estimates yields slightly lower coverage and average lengths than the WMM estimates.

TABLE 5
Coverage probabilities and average width for the BC_a confidence intervals for the NLLS, GNLLS, MM and WMM methods (The Ricker Model)

No Outlier		Coverage	Lower Coverage	Upper Coverage	Ave. Width
	Method				
$\hat{\beta}_0$	NLLS	93	2	5	1.388
	GNLLS	90	0	10	0.434
	MM	91	3	6	0.873
	WMM	94	2	4	0.460
$\hat{\beta}_1$	NLLS	92	6	2	0.268
	GNLLS	91	4	5	0.038
	MM	96	3	1	0.079
	WMM	92	4	4	0.041
10% Outliers					
$\hat{\beta}_0$	NLLS	72	0	28	****
	GNLLS	75	25	0	228.951
	MM	94	3	3	0.876
	WMM	95	1	4	0.451
$\hat{\beta}_1$	NLLS	45	55	0	2.165
	GNLLS	2	98	0	1.653
	MM	95	3	2	0.076
	WMM	92	3	5	0.042

CONCLUSION

The empirical studies suggest that the BSE is fairly close to the ASE and MCSE for up to 20% outliers and its reliability decreases as the percentage of outliers increases by more than 20%. The results also suggest that the BC_a confidence interval stands out to be the best for both situations in which the data are 'clean' and contaminated. The SPB and SB perform poorly in the presence of

TABLE 6
Coverage probabilities and average width for the BC_a confidence intervals for the NLLS, GNLLS, MM and WMM methods (The Michaelis-Menten model)

	No Outlier	Coverage	Lower Coverage	Upper Coverage	Ave. Width
	Method				
$\hat{\beta}_0$	NLLS	87	2	11	1.810
	GNLLS	93	1	6	1.098
	MM	95	2	3	2.003
	WMM	95	2	3	1.351
$\hat{\beta}_1$	NLLS	91	4	5	0.919
	GNLLS	95	3	2	0.262
	MM	95	2	3	0.860
	WMM	96	2	2	0.628
	10% Outliers				
$\hat{\beta}_0$	NLLS	95	0	5	2.110
	GNLLS	46	54	0	14.001
	MM	93	4	3	2.088
	WMM	96	1	3	1.471
$\hat{\beta}_1$	NLLS	3	0	97	56.860
	GNLLS	77	17	6	12.787
	MM	93	4	3	0.996
	WMM	95	3	2	0.723

outliers. The BC_a confidence intervals associated with the WMM and GNLLS are better than those of the NLLS and MM estimates when there is no contamination in the data. Nonetheless, the accomplishment of the GNLLS's interval deteriorates dramatically with the presence of outliers in the data. The results of the NLLS's interval are also in close agreement with the GNLLS's interval in such a situation with remarkably low coverage probability, poor equitailness and wider average interval lengths.

However, the WMM confidence intervals consistently provide adequate coverage probability or to a lesser extent close to the nominal value, good equitailness and shortest average length. The results of the simulation study agree reasonably well with Midi (1999) that the WMM is the most robust method, followed by the MM, the GNLLS and the NLLS methods in the presence of outliers. These results also confirm the conclusions made by Midi (1999) that the WMM and the GNLLS are equally good in a well behaved data.

It is very important to note here that our results are based on limited studies and these could be improved further by increasing the number of resamplings.

REFERENCES

CARROLL, R.J. AND D. RUPPERT. 1982b. Robust estimation in heteroscedastic linear models, *Ann. Stat.* **10** : 429-41.

CAROLL, R.J. AND D. RUPPERT. 1988. *Transformation and Weighting in Regression.* London : Chapman and Hall.

DICICCO, T.J AND J.P. ROMANO. 1988. A review of bootstrap confidence intervals with discussion. *J. Royal Statist. Soc. B.* **50** : 338-370.

DICICCO, T.J. AND R. TIBSHIRANI. 1987. Bootstrap confidence intervals and bootstrap approximations. *J. Amer. Statist. Assoc.* **82**(397) : 163-170.

EFRON, B. 1979 Bootstrap methods: another look at the jackknife. *Ann. Statist.* **7** : 1-26.

EFRON, B. 1981a. Nonparametric standard errors and confidence intervals. (with discussion). *Can. J. Statist.* **9** : 139-172.

EFRON, B. 1981b. Nonparametric estimates of standard errors: the jackknife, the bootstrap, and other methods. *Biometrica* **68** : 589-599.

EFRON, B. 1982. The jackknife, the bootstrap and other resampling plans. *Society for Industrial and Applied Mathematics CBMS.*

EFRON, B. 1984. Better Bootstrap Confidence Intervals. Technical Report. University of Stamford.

EFRON, B. 1985. Bootstrap confidence intervals for a class of parametric problems. *Biometrika* **72** : 45-48.

EFRON, B. 1987. Better bootstrap confidence intervals. (with discussion). *J. Amer. Statist. Assoc.* **82** : 171-200.

EFRON, B AND G. GONG. 1983. A leisurely look at the bootstrap, the jackknife and cross validation. *Amer. Statistician* **37** : 36-48.

EFRON, B. AND R.J. TIBSHIRANI. 1986. Bootstrap measures for standard errors, confidence intervals, and other measures of statistical accuracy. *Statistical Science* **1**: 54-57.

EFRON, B. AND R.J. TIBSHIRANI. 1993. *An Introduction to the Bootstrap.* New York : Chapman and Hall.

HALL, P. 1986a. On the bootstrap and confidence intervals. *Annals of Statistics* **14(4)** : 1431-1452.

HALL, P. 1986b. On the number of bootstrap simulations required to construct a confidence interval. *Ann. Statist.* **14(4)**: 1453-1462.

HALL, P., T.J. DICICCIO and J.P. ROMANO 1989. On smoothing and the bootstrap. *Ann. Statist.* 17. 692-704.

HAMPEL, F. R., E. M. RONCHETTI, P. J. ROUSSEEVW and W. A. STAHEL 1986. *Robust Statistics: The Approach Based on Influence Functions.* New York: John Wiley and Sons.

HUBER, P. J. 1981. *Robust Statistics.* New York: Wiley.

HUET, S., JOLIVET, E AND A. MESSEAN. 1990. Some simulations results about confidence intervals and bootstrap methods in nonlinear regression. *Statistics* **21 (3)**: 369-432.

LOH, W.Y. 1987. Calibrating confidence coefficients. *J. Amer. Statist. Assoc.* **82(397)**: 155-162.

MIDI, H. 1999. Robust non linear regression with heteroscedastic errors. *International Science.* **11** (4).

NELDER, J. and R. MEAD 1965. A simplex method for function minimization. *Computer J.* 7: 308-313.

PRESS, W. H., B. P., FLANNERY, S. A. TEUKOLSKY and W. T. VETTERLING. 1986. *Numerical Recipes: The Art of Scientific Computing.* New York: Cambridge University Press.

STROMBERG, A.J. 1992. High breakdown estimators in nonlinear regression. In *L_1-Statistical Analysis and Related Methods.* ed. Y. Dodge, Amsterdam : North-Holland.

STROMBERG, A.J. 1993. Computational of high breakdown nonlinear regression parameters. *J. Am. Stat. Assoc.* **88 (421)** : 237-244.

STROMBERG, A.J. AND D. RUPPERT. 1992. Breakdown in nonlinear regression. *J. Am. Stat. Assoc.* **87** : 991-997.

WU, C.F.J. 1986. Jackknife, Bootstrap and other resampling plans in regression analysis (with discussion). *Ann. Statist.* **14(4)**: 1261-1350.

YOHAI, V.J. 1987. High breakdown-point and high efficiency robust estimates for regression. *Ann. Statist.* **15.**

Pertanika J. Sci. & Technol. 8(2): 191-204(2000)
ISSN: 0128-7680

Modelling Evaporation and Evapotranspiration under Temperature Change in Malaysia

Md. Hazrat Ali, Lee Teang Shui, Kwok Chee Yan, and Aziz F. Eloubaidy
Faculty of Engineering
Universiti Putra Malaysia
43400 UPM, Serdang
Selangor Darul Ehsan, Malaysia

Received: 15 June 1998

ABSTRAK

Perubahan suhu berkesan terus keatas hidrologi melalui hubungannya dengan sejatpemeluhan. Impak potensi pertukaran iklim terhadap sejatpemeluhan ditaksirkan, dengan menggunakan satu pendekatan model yang berasaskan beberapa ukuran fizikal cuaca. Kaedah- kaedah untuk menganggarkan sejatan permukaan bebas, E_p, dan sejatpemeluhan potensi, ET_p, tanpa menggunakan parameter penentukuran model, untuk masa bersiri bulanan adalah dikemukakan. Keputusan model dikirakan, dengan menggunakan data meteorologi bersejarah purata (1980-97) dan dibandingkan dengan data sejatan panci sejatan kelas A USBR (1971-97) dari Skim Pengairan Muda, Malaysia. Penaksiran harian purata E_p bulanan jangkamasa panjang untuk bulan bulanan dibandingkan dengan sejatan panci terukur. Keputusan simulasi menunjukkan kejituan melebihi 95% dengan data cerapan sejatan panci, dan oleh yang demikian, akan diguna untuk penaksiran ET_p. Kesemua persamaan model yang mengandungi sebutan suhu disetkan bersandar kepada suhu. Sekaitan diantara lembapan nisbi min dan suhu juga dibuat demi untuk menyiasat kepekaan ET_p. ET_p bersiri masa terkesan dengan perubahan suhu bulanan daripada 21°C sehingga 41°C, bertokokan 0.2°C demi untuk menyiasat kepekaan siri itu. Keputusan daripada gangguan menunjuk bahawa suhu memberi kesan bererti terhadap ET_p untuk setiap bulan.

ABSTRACT

Temperature change has a direct effect on hydrology through its link with evapotranspiration. The potential impact of temperature change on the evapotranspiration is assessed; using a modelling approach based on a few physical weather measurements. Methods to estimate free-surface evaporation E_p and potential evapotranspiration ET_p, without any model calibration parameters, for monthly time series are presented. The model results are calculated by using observed average historic (1980-97) meteorological data and compared with USBR Class-A black pan evaporation data (1971-97) from the Muda Agricultural Development Authority, Malaysia. The long-term monthly averaged daily estimates of E_p for different months were compared with measured pan evaporation. Results of this simulation showed an accuracy of more than 95% with the observed pan evaporation data and thus, would be used for ET_p estimation. All the model equations containing temperature terms were set dependent of temperature. The correlation between mean monthly

relative humidity and temperature was also made to investigate the sensitivity of ET_p. The ET_p time series is perturbed by varying monthly temperature from 21°C to 41°C, with 0.2°C increment to investigate the sensitivity of that series. Results from the perturbations showed that the temperature has significant effects on ET_p for each month.

Keywords: temperature change, evaporation, evapotranspiration, simulation, perturbation

INTRODUCTION

In recent years, increased awareness of environmental issues has led to the idea of sustainability, in which a watershed is controlled to maintain a balance between the availability and the use of its resources. To obtain water sustainability, the planners must envisage how climate interacts with various aspects of the water cycle. This means understanding the link between climate and evapotranspiration. Climatic conditions, which determine both the scale and the temporal distribution of watershed hydrology, may attenuate or accentuate evapotranspiration. In the Muda area, Malaysia, it is found from the observed data (1971-1997) that the mean annual actual evaporation can account for 67% of the mean annual precipitation. Thus, a good estimate of evapotranspiration is required if water sustainability is to be achieved. Measurements of evapotranspiration are rarely available and are unlikely to be sufficient to describe the influence on the evapotranspiration regime. In the absence of measurements, an alternative approach is to use mathematical models to predict the variations in evapotranspiration, using meteorological data to describe variations in the temperature.

The present study employs the Penman-Monteith potential evapotranspiration model (Monteith 1965), to estimate ET_p and the Penman equation is used to estimate the free-surface or potential evaporation E_p. The aims of this paper are: (i) to compare model E_p with the observed pan evaporation, (ii) to use the model E_p in ET_p estimation, and (iii) to assess the potential impact of temperature variations on the predicted ET_p.

POTENTIAL EVAPORATION AND EVAPOTRANSPIRATION MODELING

Evapotranspiration involves a highly complex set of processes, which are influenced by many factors dependent on the local conditions. These conditions range from precipitation and meteorology to soil moisture, plant water requirements and the physical nature of the land cover (Dunn and Mackay 1995). The primary reason for differentiating between the free-surface evaporation E_p and potential evapotranspiration ET_p is that the diffusion of water vapor into the atmosphere follows very different pathways in vegetation (transpiration) than it does from free-water-surface water. Gangopadhyaya *et al.* (1966) defined potential evapotranspiration ET as "the maximum quantity of water capable of being lost, as water vapor, in a given climate, by a continuous, extensive stretch of vegetation covering the whole ground when the soil is kept

saturated." Gangopadhyaya's definition of ET therefore recognizes the combined process of transpiration by vegetation and evaporation from saturated bare soil. Estimating ET_p is more difficult than estimating E_p because several vegetation-species-specific model parameters are required. Many simple models to predict the potential evaporation rate exist, such as the Penman formula (Penman 1948) and the Thornthwaite formula (Thornthwaite 1948). These models do not give any indication of how the potential rate may be converted to give an actual evapotranspiration rate as a function of the vegetation type and the soil moisture conditions. However, the only process based model that is widely used, and that accounts for the influence of vegetation on the evapotranspiration regime, is the Penman-Monteith energy formula (Monteith 1965). There are several reasons why the Penman-Monteith energy-balance equation is chosen to estimate the potential evapotranspiration in the present study (Fennessy and Kirshen 1994). Firstly, the Penman-Monteith equation "big leaf" model is presently used by a number of general circulation models (GCMs) to estimate the flux of energy and moisture between the atmosphere and the land surface/water surface boundaries, as described by Milly (1992). Secondly, the model is composed of a number of the GCM prognostic variables, thus lending itself to easy perturbation by climate-change scenarios. Lastly, the model is derived from the energy-conservation equations, and therefore it is generally considered to be universally applicable.

The Penman-Monteith potential evapotranspiration model (Monteith 1965) is

$$ET_p = \frac{\Delta(R_n - G) + \dfrac{\rho_a C_p \left[e^{\circ}(z) - e_d(z)\right]}{r_a}}{\lambda\left(\Delta + \gamma\left[1 + \dfrac{r_s}{r_a}\right]\right)} \qquad (1)$$

where, ET_p is the potential evapotranspiration (mm/day); λ is the latent heat of vaporization of water (MJ kg^{-1}); Δ is the gradient of the saturation-vapour-pressure-temperature function (kPa $^0C^{-1}$); R_n is the net radiation (MJ m^{-2} day^{-1}); G is the soil heat flux (MJ m^{-2} day^{-1}); ρ_a is the air density (kg m^{-3}); C_p is the specific heat of the air at constant pressure = 1.013 kJ kg^{-1} K^{-1}; $e^o(z)$ is the saturated vapour pressure of the air (kPa), a function of air temperature measured at height z; $e_d(z)$ is the mean actual vapor pressure of the air measured at height z (kPa); r_a is the aerodynamic resistance to water-vapor diffusion into the atmospheric boundary layer (s m^{-1}); γ is the psychrometric constant (kPa $^0C^{-1}$); and r_s is the vegetation canopy resistance to water-vapour transfer (s m^{-1}).

One of the limitations of the Penman-Monteith equation is its data requirements. At a minimum, the model requires air temperature, wind speed,

solar radiation, and the saturation-vapour-pressure deficit. Methods employed to determine the solar radiation and vapour pressure deficit are described below.

In Eq. (1), the net radiation R_n is described by

$$R_n = (1 - a)R_s - R_{nl} \quad (2)$$

where R_s (MJ m^{-2} day^{-1}) is the short-wave solar radiation; α is the surface reflectivity or albedo, whose recommended values are 0.08 for open water surfaces and 0.23 for most of the crops; and R_{nl} (MJ m^{-2} day^{-1}) net longwave outgoing radiation.

The quantity of R_s can be computed as

$$R_s\left(0.25 + 0.50\frac{n}{N}\right)R_a \quad (2a)$$

where R_a is the extraterrestrial solar radiation (MJ m^{-2} day^{-1}), n is the actual number of hours of bright sunshine (h/day); N is the possible maximum number of sunshine hours (h/day).

Penman (1948) suggested an expression for R_{nl} as

$$R_{nl} = \sigma T_a^4\left[0.56 - 0.092(e_d)^{0.5}\right]\left(0.1 + 0.9\frac{n}{N}\right) \quad (2b)$$

where α is the Stefan-Boltzmann constant = 4.903 x 10^{-9} MJ m^{-2} K^{-4} day^{-1}; T_a is the mean air temperature in ^{0}C; and e_d is the mean actual vapour pressure of the atmosphere at dew point temperature $= \frac{RH_{mean}}{100} e^0$ (kPa) ; in which RH_{mean} is the mean relative humidity (%) and e^0 is the saturation vapour pressure of the evaporating surface at mean air temperature.

Substituting R_s and R_{nl} from Eqs. (2a), and (2b) into Eq. (2) respectively,

$$R_n = (1-a)\left(0.25 + 0.50\frac{n}{N}\right)R_a - \sigma T_a^4\left[0.56 - 0.092(e_d)^{0.5}\right]\left(0.1 + 0.9\frac{n}{N}\right) \quad (3)$$

The soil heat flux G (MJ m^{-2} day^{-1}) can be computed by using the following equation

$$G = c_s d_s \frac{T_2 - T_1}{\Delta t} \quad (4)$$

where T_2 is the temperature at the end of the period (°C); T_1 is the temperature at the beginning of the period (°C); Δt is the length of period (days); c_s is the soil heat capacity (2.1 MJ m^{-3} $^0C^{-1}$) for average moist soil; and d_s is the estimated effective soil depth (m).

For daily temperature fluctuations (effective soil depth typically 0.18 m) Eq. (4) becomes

$$G=0.38(T_{day2}-T_{day1}) \tag{5}$$

The right-hand term of the numerator of Eq. (1), incorporates the saturation-vapour-pressure deficit (the term enclosed by brackets), which is estimated by

$$e^o(z)-e_d(z)=e^o(z,T_a)\left(1-\frac{RH_{mean}}{100}\right) \tag{6}$$

In Eq. (6), the saturated vapour pressure is estimated by the methods described by Tetens (1930) and Murray (1967), and is described by

$$e^o(T_a)=\exp\left(\frac{16.78T_a-116.9}{T_a+237.3}\right) \tag{7}$$

In Eq. (1), the slope of the saturation vapour pressure-temperature curve Δ is estimated by the methods described by Tetens (1930) and Murray (1967), and is described by

$$\Delta=\frac{4098e^o}{(T_a+237.3)^2} \tag{8}$$

The latent heat of vaporization of water λ is estimated using the method described by Harrison (1963), shown here as

$$\lambda=2501-2.361\times10^{-3}T_a \tag{9}$$

The phychrometric constant γ is estimated by

$$\gamma=\frac{C_pP_a}{0.662\lambda} \tag{10}$$

In Eq. (10), the specific heat of moist air (C_p) is assumed to equal 1.013 $kJ.kg^{-1}.K^{-1}$, as reported by Brutsaert (1982). The atmospheric pressure P_a(kPa) can be computed as

$$P_a = 101.3 - 0.01152z + 0.544 \times 10^{-6} z^2 \quad (11)$$

where z is the elevation above mean sea level (m).

The density of (moist) air ρ_a(kg m^{-3}) can be calculated from the ideal gas laws, but it is adequately estimated from

$$\rho_a = 3.486\frac{P_a}{275+T_a} \quad (12)$$

The rate of water vapor transfer away from the ground by turbulent diffusion is controlled by aerodynamic resistance r_a (s m^{-1}) and can be estimated from

$$r_a = \frac{4.72\left[\ln\left(\frac{z}{z_0}\right)\right]^2}{1+0.536U_2} \quad (13)$$

where z is the height at which meteorological variables are measured (m); z_0 is the aerodynamic roughness of the surface = 0.00137m; and U_2 is the average wind speed at 2m height (m/s). U_2 (km/h) can be computed from observations at any height as $U_2 = U_h\left(\frac{2.0}{h}\right)^{0.143}$ where U_h is the observed wind speed (km/h) at a height of h meters.

The stomata resistance of the whole canopy, referred to as the surface resistance r_s, is less when more leaves are present since there are then more stomata through which transpired water vapor can diffuse. In vapour transport, the measure of potential is the vapor pressure and the vapour flux rate E. Thus the vapour flux rate can be approximately estimated for leaf stomata as

$$E = \frac{k_s\left[e^0(z) - e(z)\right]}{r_s} \quad (14)$$

where k_s is a constant to account for units. One approximation for r_s is

$$r_s = \frac{200}{L} \quad (15)$$

If h_c is the mean height of the crop, then the leaf area index L can be estimated by

$$L=24h_c \quad \text{(clipped grass with } 0.05 < h_c < 0.15 \text{ m)}$$
$$L=5.5 + 1.51\ln(h_c) \quad \text{(alfalfa with } 0.10 < h_c < 0.50 \text{ m)} \qquad (16)$$

The surface resistance of the reference crop of clipped grass r_s^{rc} of 0.12m high is estimated as

$$r_s^{rc} = 69 \text{ s m}^{-1} \qquad (17)$$

Since potential evaporation occurs from an extensive free water surface, it follows that the canopy resistance $r_s = 0$ is the appropriate value of surface resistance for estimating potential evaporation from Eq. (1).

DATA AND CALCULATIONS OF E_p AND ET_p

Long-term monthly averaged daily values of the estimated free-surface evaporation determined in the present study are compared with the USBR class A black pan evaporation measurements (1971-97) by Muda Agricultural Development Authority (MADA). The values quoted here are the average of 30 stations uniformly distributed in Muda area. Similarly, monthly averaged daily values of temperature, wind speed, possible sunshine and relative humidity meteorological data (1980-97), which are all used as input variables to the E_p model, are taken from station 27 (Kepala Batas: Lat. 06°12'N, and Long.100°24'E) of the same Authority. The extra-terrestrial radiation R_a (mm/day) is taken from the literature (Michael 1978) and then multiplied by the latent heat of vaporization of water λ (MJ kg^{-1}) to convert to R_a (MJ m^{-2} day^{-1}) for fulfilling the model requirements. The step-by-step procedures of calculating E_p and ET_p are given in Table 1.

RESULTS AND DISCUSSION

Fig. 1 shows that the long-term monthly averaged daily estimates of E_p for different months simulate more than 95% with the observed pan evaporation. The overall matching, considering the total time series, with the pan evaporation is 99%. The *relative error* = (Pan E_p – Model E_p)/Pan E_p between the observed and model results is shown in *Fig. 2*.

The surface resistance r_s of the crop, assuming seasonal average crop height of 0.2m, is incorporated in ET_p modeling instead of using crop coefficient K_c. Incorporating actual crop height might yield more accurate results than calculated, as the crop height is variable from time to time. In the absence of relevant data, the typical effective soil depth of 0.18m (Wyjk van and de Vries 1963) is considered for daily temperature fluctuations in calculating the soil heat flux G. Since measurements of evapotranspiration are not available at MADA, an alternative approach is to use mathematical models to predict the

TABLE 1
Estimating potential evaporation and evapotranspiration by Penman-Monteith Equation

Parameter	Month											
	Jan	Feb	Mar	Apr	May	June	July	Aug	Sept	Oct	Nov	Dec
*Avg. Temp., T_a (°C)	26.99	27.66	27.96	28.12	27.84	27.63	27.06	26.90	26.71	26.60	26.58	26.47
*Avg. RH_{mean} (%)	72.90	73.00	76.60	81.50	85.20	85.60	86.30	86.30	86.40	87.00	85.00	79.70
*Avg. U_2 (m/s) at 2m altitude	1.39	1.28	1.04	0.90	0.82	0.74	0.80	0.83	0.84	0.78	0.82	1.16
$e_d(z)$ (kPa)	2.60	2.71	2.89	3.10	3.19	3.17	3.09	3.06	3.03	3.03	2.96	2.76
R_a ($MJ.m^{-2}.day^{-1}$)	33.81	35.98	37.47	37.54	36.82	35.88	36.36	37.10	37.30	36.52	34.55	33.31
$e^*(z)$ (kPa)	3.57	3.71	3.77	3.81	3.75	3.70	3.58	3.55	3.51	3.48	3.48	3.46
$e^*(z)-e_d(z)$ (kPa)	0.97	1.00	0.88	0.70	0.55	0.53	0.49	0.49	0.48	0.45	0.52	0.70
λ (MJ kg^{-1})	2.44	2.44	2.43	2.43	2.44	2.44	2.44	2.44	2.44	2.44	2.44	2.44
*Sunshine, n (h/day)	8.70	9.00	8.50	8.70	7.70	7.10	6.60	6.70	5.70	5.70	6.10	7.00
n/N (cloudiness fraction) (N=9h)	0.97	1.00	0.94	0.97	0.86	0.79	0.73	0.74	0.63	0.63	0.68	0.78
R_n ($MJ.m^{-2}.day^{-1}$)	19.09	20.78	20.84	21.20	19.22	17.80	17.27	17.77	16.28	15.94	15.67	16.39
P_a (kPa)	101.16	101.16	101.16	101.16	101.16	101.16	101.16	101.16	101.16	101.16	101.16	101.16
G ($MJ.m^{-2}.day^{-1}$)	0.26	0.11	0.06	-0.11	-0.08	-0.22	-0.06	-0.07	-0.04	-0.01	-0.04	0.20
γ ($kPa°C^{-1}$)	0.06	0.06	0.06	0.06	0.06	0.06	0.06	0.06	0.06	0.06	0.06	0.06
ρ_a ($kg\ m^{-3}$)	1.17	1.17	1.16	1.16	1.16	1.17	1.17	1.17	1.17	1.17	1.17	1.17
Δ ($kPa°C^{-1}$)	0.21	0.22	0.22	0.22	0.22	0.22	0.21	0.21	0.21	0.21	0.20	0.20
r_a ($s.m^{-1}$)	143.50	148.59	160.81	169.16	173.84	179.52	175.05	173.33	172.48	176.81	173.84	154.73
Model E_p (mm/day)	5.94	6.57	6.63	6.81	6.14	5.72	5.46	5.62	5.12	5.00	4.92	5.07
*Pan E_p (mm/day)	6.12	7.07	6.79	6.56	5.65	5.46	5.24	5.49	5.46	5.10	5.25	5.23
r_s ($s.m^{-1}$) at average h_c = 0.2m	64.81	64.81	64.81	64.81	64.81	64.81	64.81	64.81	64.81	64.81	64.81	64.81
ET_p (mm/day)	5.37	5.98	6.08	6.27	5.67	5.29	5.03	5.16	4.71	4.60	4.52	4.61

• Observed Data (Source: Muda Agricultural Development Authority, Alor Setar, Kedah, Malaysia)

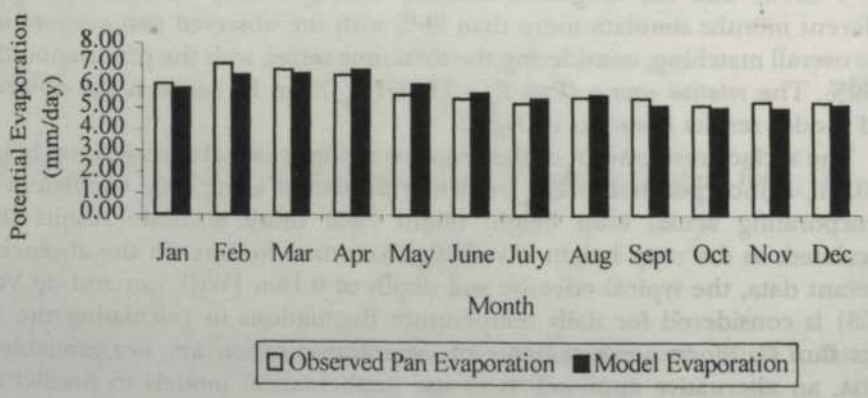

Fig 1. Simulating calculated evaporation with observed pan evaporation

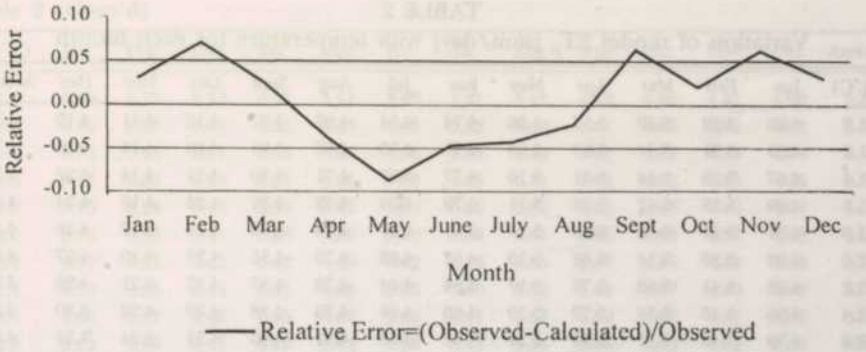

Fig 2. Relative error between observed and calculated evaporation rates

variations in evapotranspiration, with meteorological data describing variations in the climate.

To study the theoretical variations in the evapotranspiration predictions across the Muda area, as influenced by climate, ET_p model parameters are set dependent of temperature. The correlation between mean monthly temperature and relative humidity is also performed using observed values and is shown in *Fig. 3.*

The ET_p time series is perturbed by varying monthly temperature from 21°C to 41°C with +0.2°C increment to investigate the sensitivity of ET_p. The variations of ET_p for each month with temperature change are given in Table 2. The average variation, which corresponds to the same temperature perturbation, is plotted and shown in *Fig. 4.* The results from the perturbations show that the temperature has significant effects on ET_p for each month.

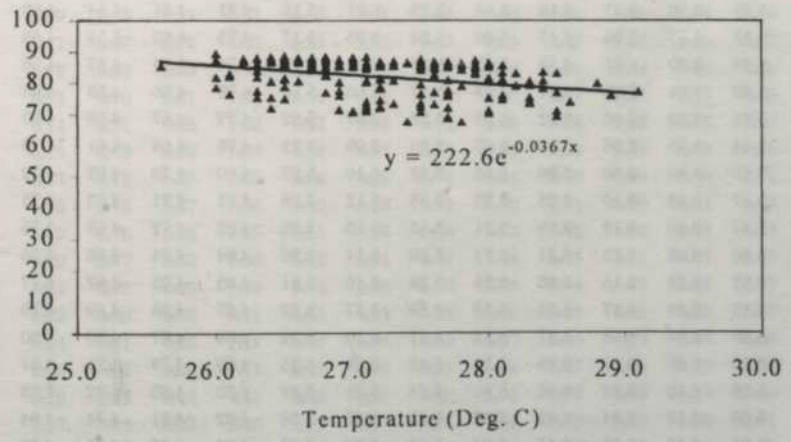

Fig 3. Correlation between mean monthly temperature and relative humidity

TABLE 2
Variation of model ET_p (mm/day) with temperature for each month

T_a(°C)	Jan	Feb	Mar	Apr	May	Jun	Jul	Aug	Sept	Oct	Nov	Dec	Average
21.0	4.83	5.29	5.40	5.57	5.06	4.74	4.54	4.67	4.27	4.18	4.11	4.19	4.74
21.2	4.85	5.31	5.42	5.59	5.08	4.75	4.56	4.69	4.28	4.20	4.13	4.20	4.75
21.4	4.87	5.33	5.44	5.61	5.10	4.77	4.57	4.71	4.30	4.21	4.14	4.22	4.77
21.6	4.89	5.35	5.47	5.63	5.11	4.79	4.59	4.72	4.32	4.23	4.16	4.24	4.79
21.8	4.91	5.37	5.49	5.65	5.13	4.81	4.61	4.74	4.33	4.24	4.17	4.25	4.81
22.0	4.93	5.39	5.51	5.68	5.15	4.82	4.63	4.76	4.35	4.26	4.19	4.27	4.83
22.2	4.95	5.41	5.53	5.70	5.17	4.84	4.64	4.78	4.37	4.27	4.21	4.28	4.85
22.4	4.96	5.43	5.55	5.72	5.19	4.86	4.66	4.79	4.38	4.29	4.22	4.30	4.86
22.6	4.98	5.45	5.57	5.74	5.21	4.88	4.68	4.81	4.40	4.31	4.24	4.32	4.88
22.8	5.00	5.47	5.59	5.76	5.23	4.90	4.69	4.83	4.41	4.32	4.25	4.33	4.90
23.0	5.02	5.49	5.61	5.78	5.25	4.91	4.71	4.85	4.43	4.34	4.27	4.35	4.92
23.2	5.04	5.51	5.63	5.80	5.27	4.93	4.73	4.86	4.44	4.35	4.28	4.36	4.93
23.4	5.06	5.53	5.65	5.82	5.28	4.95	4.74	4.88	4.46	4.37	4.30	4.38	4.95
23.6	5.07	5.55	5.67	5.84	5.30	4.96	4.76	4.90	4.48	4.38	4.31	4.39	4.97
23.8	5.09	5.57	5.69	5.86	5.32	4.98	4.78	4.91	4.49	4.40	4.33	4.41	4.99
24.0	5.11	5.59	5.71	5.88	5.34	5.00	4.79	4.93	4.51	4.41	4.34	4.43	5.00
24.2	5.13	5.61	5.73	5.90	5.36	5.01	4.81	4.95	4.52	4.43	4.36	4.44	5.02
24.4	5.15	5.63	5.75	5.92	5.37	5.03	4.83	4.96	4.54	4.44	4.37	4.46	5.04
24.6	5.16	5.65	5.77	5.94	5.39	5.05	4.84	4.98	4.55	4.46	4.38	4.47	5.05
24.8	5.18	5.67	5.79	5.96	5.41	5.06	4.86	5.00	4.57	4.47	4.40	4.49	5.07
25.0	5.20	5.69	5.80	5.98	5.43	5.08	4.87	5.01	4.58	4.49	4.41	4.50	5.09
25.2	5.22	5.71	5.82	6.00	5.45	5.10	4.89	5.03	4.60	4.50	4.43	4.52	5.10
25.4	5.23	5.73	5.84	6.02	5.46	5.11	4.90	5.05	4.61	4.51	4.44	4.53	5.12
25.6	5.25	5.75	5.86	6.04	5.48	5.13	4.92	5.06	4.63	4.53	4.46	4.55	5.14
25.8	5.27	5.76	5.88	6.06	5.50	5.15	4.94	5.08	4.64	4.54	4.47	4.56	5.15
26.0	5.29	5.78	5.90	6.08	5.51	5.16	4.95	5.09	4.66	4.56	4.48	4.58	5.17
26.2	5.30	5.80	5.92	6.09	5.53	5.18	4.97	5.11	4.67	4.57	4.50	4.59	5.19
26.4	5.32	5.82	5.94	6.11	5.55	5.19	4.98	5.13	4.68	4.59	4.51	4.60	5.20
26.6	5.34	5.84	5.95	6.13	5.57	5.21	5.00	5.14	4.70	4.60	4.53	4.62	5.22
26.8	5.35	5.86	5.97	6.15	5.58	5.23	5.01	5.16	4.71	4.61	4.54	4.63	5.23
27.0	5.37	5.87	5.99	6.17	5.60	5.24	5.03	5.17	4.73	4.63	4.55	4.65	5.25
27.2	5.39	5.89	6.01	6.19	5.62	5.26	5.04	5.19	4.74	4.64	4.57	4.66	5.27
27.4	5.40	5.91	6.03	6.21	5.63	5.27	5.06	5.20	4.76	4.66	4.58	4.68	5.28
27.6	5.42	5.93	6.05	6.22	5.65	5.29	5.07	5.22	4.77	4.67	4.59	4.69	5.30
27.8	5.44	5.95	6.06	6.24	5.67	5.30	5.09	5.23	4.78	4.68	4.61	4.70	5.31
28.0	5.45	5.96	6.08	6.26	5.68	5.32	5.10	5.25	4.80	4.70	4.62	4.72	5.33
28.2	5.47	5.98	6.10	6.28	5.70	5.33	5.12	5.26	4.81	4.71	4.63	4.73	5.34
28.4	5.49	6.00	6.12	6.30	5.71	5.35	5.13	5.28	4.82	4.72	4.65	4.75	5.36
28.6	5.50	6.02	6.13	6.31	5.73	5.36	5.14	5.29	4.84	4.74	4.66	4.76	5.37
28.8	5.52	6.03	6.15	6.33	5.75	5.38	5.16	5.31	4.85	4.75	4.67	4.77	5.39
29.0	5.53	6.05	6.17	6.35	5.76	5.39	5.17	5.32	4.87	4.76	4.69	4.79	5.40
29.2	5.55	6.07	6.18	6.37	5.78	5.41	5.19	5.34	4.88	4.77	4.70	4.80	5.42
29.4	5.56	6.08	6.20	6.38	5.79	5.42	5.20	5.35	4.89	4.79	4.71	4.81	5.43
29.6	5.58	6.10	6.22	6.40	5.81	5.44	5.21	5.37	4.90	4.80	4.72	4.83	5.45
29.8	5.60	6.12	6.24	6.42	5.82	5.45	5.23	5.38	4.92	4.81	4.74	4.84	5.46
30.0	5.61	6.13	6.25	6.44	5.84	5.46	5.24	5.39	4.93	4.83	4.75	4.85	5.48
30.2	5.63	6.15	6.27	6.45	5.85	5.48	5.26	5.41	4.94	4.84	4.76	4.87	5.49
30.4	5.64	6.17	6.28	6.47	5.87	5.49	5.27	5.42	4.96	4.85	4.77	4.88	5.51
30.6	5.66	6.18	6.30	6.49	5.88	5.51	5.28	5.44	4.97	4.86	4.79	4.89	5.52
30.8	5.67	6.20	6.32	6.50	5.90	5.52	5.30	5.45	4.98	4.88	4.80	4.90	5.53

Table 2 (Cont'd)

T_a(°C)	Jan	Feb	Mar	Apr	May	Jun	Jul	Aug	Sept	Oct	Nov	Dec	Average
31.0	5.69	6.22	6.33	6.52	5.91	5.53	5.31	5.46	4.99	4.89	4.81	4.92	5.55
31.2	5.70	6.23	6.35	6.53	5.93	5.55	5.32	5.48	5.01	4.90	4.82	4.93	5.56
31.4	5.72	6.25	6.37	6.55	5.94	5.56	5.34	5.49	5.02	4.91	4.83	4.94	5.58
31.6	5.73	6.26	6.38	6.57	5.96	5.58	5.35	5.51	5.03	4.92	4.85	4.95	5.59
31.8	5.75	6.28	6.40	6.58	5.97	5.59	5.36	5.52	5.04	4.94	4.86	4.97	5.60
32.0	5.76	6.30	6.41	6.60	5.99	5.60	5.38	5.53	5.06	4.95	4.87	4.98	5.62
32.2	5.77	6.31	6.43	6.62	6.00	5.62	5.39	5.55	5.07	4.96	4.88	4.99	5.63
32.4	5.79	6.33	6.44	6.63	6.02	5.63	5.40	5.56	5.08	4.97	4.89	5.00	5.65
32.6	5.80	6.34	6.46	6.65	6.03	5.64	5.41	5.57	5.09	4.98	4.91	5.02	5.66
32.8	5.82	6.36	6.47	6.66	6.04	5.66	5.43	5.58	5.10	5.00	4.92	5.03	5.67
33.0	5.83	6.37	6.49	6.68	6.06	5.67	5.44	5.60	5.12	5.01	4.93	5.04	5.69
33.2	5.85	6.39	6.51	6.69	6.07	5.68	5.45	5.61	5.13	5.02	4.94	5.05	5.70
33.4	5.86	6.40	6.52	6.71	6.09	5.69	5.46	5.62	5.14	5.03	4.95	5.06	5.71
33.6	5.87	6.42	6.54	6.72	6.10	5.71	5.48	5.64	5.15	5.04	4.96	5.07	5.72
33.8	5.89	6.43	6.55	6.74	6.11	5.72	5.49	5.65	5.16	5.05	4.97	5.09	5.74
34.0	5.90	6.45	6.56	6.75	6.13	5.73	5.50	5.66	5.17	5.06	4.98	5.10	5.75
34.2	5.91	6.46	6.58	6.77	6.14	5.74	5.51	5.67	5.19	5.07	5.00	5.11	5.76
34.4	5.93	6.48	6.59	6.78	6.15	5.76	5.52	5.69	5.20	5.09	5.01	5.12	5.78
34.6	5.94	6.49	6.61	6.80	6.17	5.77	5.54	5.70	5.21	5.10	5.02	5.13	5.79
34.8	5.95	6.50	6.62	6.81	6.18	5.78	5.55	5.71	5.22	5.11	5.03	5.14	5.80
35.0	5.97	6.52	6.64	6.83	6.19	5.79	5.56	5.72	5.23	5.12	5.04	5.15	5.81
35.2	5.98	6.53	6.65	6.84	6.21	5.81	5.57	5.73	5.24	5.13	5.05	5.17	5.83
35.4	5.99	6.55	6.67	6.86	6.22	5.82	5.58	5.75	5.25	5.14	5.06	5.18	5.84
35.6	6.01	6.56	6.68	6.87	6.23	5.83	5.60	5.76	5.26	5.15	5.07	5.19	5.85
35.8	6.02	6.58	6.69	6.88	6.24	5.84	5.61	5.77	5.27	5.16	5.08	5.20	5.87
36.0	6.03	6.59	6.71	6.90	6.26	5.85	5.62	5.78	5.29	5.17	5.09	5.21	5.87
36.2	6.04	6.60	6.72	6.91	6.27	5.87	5.63	5.79	5.30	5.18	5.10	5.22	5.89
36.4	6.06	6.62	6.73	6.93	6.28	5.88	5.64	5.80	5.31	5.19	5.11	5.23	5.90
36.6	6.07	6.63	6.75	6.94	6.29	5.89	5.65	5.82	5.32	5.20	5.12	5.24	5.91
36.8	6.08	6.64	6.76	6.95	6.31	5.90	5.66	5.83	5.33	5.21	5.13	5.25	5.92
37.0	6.09	6.66	6.77	6.97	6.32	5.91	5.67	5.84	5.34	5.22	5.14	5.26	5.93
37.2	6.11	6.67	6.79	6.98	6.33	5.92	5.68	5.85	5.35	5.23	5.15	5.27	5.94
37.4	6.12	6.68	6.80	6.99	6.34	5.93	5.70	5.86	5.36	5.24	5.16	5.28	5.96
37.6	6.13	6.70	6.81	7.01	6.36	5.94	5.71	5.87	5.37	5.25	5.17	5.29	5.97
37.8	6.14	6.71	6.83	7.02	6.37	5.96	5.72	5.88	5.38	5.26	5.18	5.30	5.98
38.0	6.15	6.72	6.84	7.03	6.38	5.97	5.73	5.89	5.39	5.27	5.19	5.31	5.99
38.2	6.17	6.73	6.85	7.05	6.39	5.98	5.74	5.91	5.40	5.28	5.20	5.32	6.00
38.4	6.18	6.75	6.87	7.06	6.40	5.99	5.75	5.92	5.41	5.29	5.21	5.33	6.01
38.6	6.19	6.76	6.88	7.07	6.41	6.00	5.76	5.93	5.42	5.30	5.22	5.34	6.02
38.8	6.20	6.77	6.89	7.08	6.43	6.01	5.77	5.94	5.43	5.31	5.23	5.35	6.03
39.0	6.21	6.79	6.90	7.10	6.44	6.02	5.78	5.95	5.44	5.32	5.24	5.36	6.05
39.2	6.22	6.80	6.92	7.11	6.45	6.03	5.79	5.96	5.45	5.33	5.25	5.37	6.06
39.4	6.24	6.81	6.93	7.12	6.46	6.04	5.80	5.97	5.46	5.34	5.26	5.38	6.07
39.6	6.25	6.82	6.94	7.13	6.47	6.05	5.81	5.98	5.47	5.35	5.27	5.39	6.08
39.8	6.26	6.83	6.95	7.15	6.48	6.06	5.82	5.99	5.48	5.36	5.27	5.40	6.09
40.0	6.27	6.85	6.96	7.16	6.49	6.07	5.83	6.00	5.49	5.37	5.28	5.41	6.10
40.2	6.28	6.86	6.98	7.17	6.50	6.08	5.84	6.01	5.49	5.37	5.29	5.42	6.11
40.4	6.29	6.87	6.99	7.18	6.52	6.09	5.85	6.02	5.50	5.38	5.30	5.43	6.12
40.6	6.30	6.88	7.00	7.20	6.53	6.10	5.86	6.03	5.51	5.39	5.31	5.44	6.13
40.8	6.31	6.89	7.01	7.21	6.54	6.11	5.87	6.04	5.52	5.40	5.32	5.45	6.14
41.0	6.32	6.91	7.02	7.22	6.55	6.12	5.88	6.05	5.53	5.41	5.33	5.46	6.15

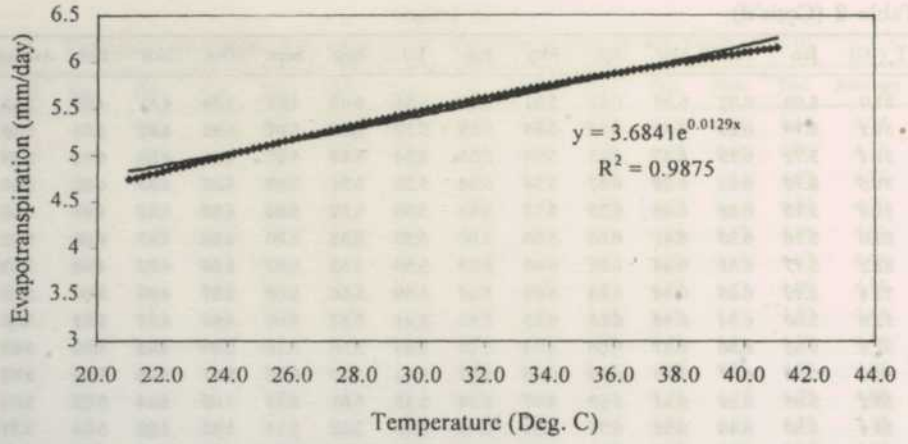

Fig 4. Average variation of potential evapotranspiration with temperature

CONCLUSIONS

This paper describes methods used to calculate daily time series of free-surface or potential evaporation E_p using the Penman equation, and potential evapotranspiration ET_p using the Penman-Monteith equation without keeping any model calibration parameters. The long-term monthly averaged daily estimates of E_p for different months were compared with the observed pan evaporations and more than 95% simulation results were achieved. Thus, these results can be interpreted as a validation of the E_p model and can safely be used in the ET_p model. The calculated ET_p values are less than the calculated E_p values by incorporating the surface resistance of the whole canopy. The surface resistance is less when more leaves are present since there are then more stomata through which transpired water vapor can diffuse. The results suggest that vegetation change resulting in increased canopy resistance decreases ET_p.

In order to investigate the sensitivity of ET_p, all the model equations containing temperature terms are set dependent of temperature and correlation between mean relative humidity and temperature is made. The ET_p time series is perturbed changing monthly temperature from 21°C to 41°C with + 0.2°C increment. The results from the perturbations show that the ET_p values increase towards increasing temperature for each month.

ACKNOWLEDGEMENTS

The research described in this paper was supported by funds provided by the Intensification of Research in Priority Areas Program (IRPA), Ministry of Science, Technology and Environment. The authors gratefully acknowledge the Muda Agricultural Development Authority, Alor Setar, Kedah, Malaysia, for their technical assistance.

REFERENCES

BRUTSAERT, W. 1982. *Evaporation into the Atmosphere.* Dordrecht Holand: D. Reidel Pub. Co

DUNN, S. M., AND R. MAKAY. 1995. Spatial variation in evapotranspiration and the influence of land use on catchment hydrology. *J. Hydrol* **171**: 49-73.

FENNESSY, N. M. AND P. H. KIRSHEN. 1994. Evaporation and evapotranspiration under climate change in New England. *Journal of Water Resources Planning and Management* **120(1)**: 48-69.

GANGOPADHYAYA, M., V. A. URYVAEV, M. H. OMAR, T. J. NORDENSON, AND G. E. HARBECK. 1966. Measurement and estimation of evaporation and evapotranspiration. *Tech. Note No. 83.* Geneva, Switzerland: World Meteorological Oragnization (WMO).

HARRISON, L. P. 1963. Funtamental concepts and definitions relating to humidity, *Humidity and Moisture*, ed, A. Wexler, Vol. 3. New York: Reinhold.

MICHEAL, A.M. 1978. *Irrigation: Theory and Practice.* New Delhi, India: Vikas Publishing House Pvt Ltd

MILLY, P. C. D. 1992. Potential evaporation and soil moisture in general circulation models. *J. Climate* **5(3)**: 209-226.

MONTEITH, J. L. 1965. Evaporation and the environment. *Symp. Soc. Expt. Biol.* **19:** 205-234.

MURRAY, F. W. 1967. On the computation of saturation vapor pressure. *J. Appl. Meteorology* **6:** 203-204.

PENMAN, H. L. 1948. Natural evaporation from open water, bare soil and grass. *Proc. R. Soc. London* **193:** 120-145.

THORNTHWAITE, C. W. 1948. An approach towards a rational classification of climate. *Geogr. Rev.* **38:** 55-94.

WIJK VAN, W. R., and D. A. DE VRIES 1963. Periodic temperature variations in homogeneous soil. In *Physics of the Plant Environment,* ed. p.102-143. W. D. van Wijk, Amsterdam: North-Holland Pub. Co.

APPENDIX I: NOTATION

The following symbols are used in this paper:

C_p = specific heat of air at constant pressure ($kJ.kg^{-1}.K^{-1}$);
c_s = soil heat capacity (2.1 $MJ.m^{-3}.°C^{-1}$);
d_s = estimated effective soil depth (m);
E = vapor flux rate ($kPa.m.s^{-1}$);
E_p = free-surface or potential evaporation (mm/day);
ET_p = potential evapotranspiration (mm/day);
e^* = saturated vapor pressure of the air (kPa);
e_d = mean actual vapor pressure of air at dew point temperature (kPa);
G = soil heat flux ($MJ.m^{-2}day^{-1}$);
h_c = mean height of the crop (m);
k_s = a constant (dimensionless);
n = actual number of hours of bright sunshine (h/day);

N = possible maximum number of sunshine hours (h/day);
P_a = air pressure ($kg.m^{-2}$ or kPa);
RH = relative humidity (%);
R_a = extra-terrestrial radiation ($MJ.m^{-2}day^{-1}$);
R_{nl} = net long-wave outgoing radiation ($MJ.m^{-2}day^{-1}$);
R_s = short-wave solar radiation ($MJ.m^{-2}day^{-1}$);
R_n = net radiation ($MJ.m^{-2}day^{-1}$);
r_a = atmospheric vapor resistance ($s.m^{-1}$);
r_s = vegetation canopy vapor resistance ($s.m^{-1}$);
T_a = air temperature (°C);
U_2 = wind speed at 2m altitude (m/s);
z = measurement height (m);
z_0 = surface roughness height (m);
α = surface albedo (dimensionless);
γ = psychrometric constant ($kPa.°C^{-1}$);
Δ = gradient of saturation vapor pressure-temperature curve ($kPa.°C^{-1}$);
λ = latent heat of vaporization of water ($MJ.kg^{-1}$);
σ = Stefan-Boltzmann constant (4.903×10^{-9} MJm^{-2} K^{-4} day^{-1}); and
ρ_a = air density ($kg.m^{-3}$)

Pertanika J. Sci. & Technol. 8(2): 205-215 (2000)
ISSN: 0128-7680

Effects of Seedling Raising Methods on the Economic Performance of Manually Operated Paddy Transplanter

Md. Syedul Islam[1] and Desa Ahmad[2]
[1]PhD Student and [2]Associate Professor
Faculty of Engineering
University Putra Malaysia
43400 Serdang, Selangor Darul Ehsan, Malaysia

Received: 18 May 1998

ABSTRAK

Satu kajian telah dijalankan untuk mengenalpasti kaedah percambahan benih keatas prestasi ekonomi sebuah jentera penanam padi. Kos percambahan benih padi menerusi kerangka kayu, buluh, plastik, tali nylon dan dulang plastik bagi satu hektar kawasan masing masing adalah US$ 27.21, US$27.77, US$27.20, US$27.04 dan US$44.89. Walaubagaimanapun bagi percambahan jenis semaian basah kosnya hanya US$19.32. Faedah bersih penanaman berjentera dengan menggunakan semaian menerusi kerangka kayu, buluh dan plastik masing masing adalah US$13.48, US$19.46 dan US$16.05 per hektar berbanding penanaman secara manual dengan semaian basah. Diantara kaedah percambahan yang diuji, percambahan menggunakan kerangka plastik didapati lebih sesuai dimana keluasan pulangan setahun adalah 1.9 ha. Dengan teknik ini seorang petani dapat menjimatkan US$16.00 per ha berbanding kaedah penanaman secara manual.

ABSTRACT

A study was conducted to identify the effects of different seedling raising media on the economic performance of a manually operated transplanter. The costs of seedling production in wooden frame, bamboo frame, plastic frame, nylon rope and plastic tray nurseries for transplanting one hectare of land were US$27.21, US$27.77, US$27.20, US$27.04 and US$44.89 respectively. However, for wet bed nursery, it was only US$19.32. The net benefit from machine transplanting with wooden, bamboo and plastic frame seedlings were US$ 13.48, US$ 19.46 and US$ 16.05 per ha respectively compared to hand transplanting with wet bed seedlings. Among the five seedling raising media, plastic frame was considered the most appropriate one, where the break-even area per year is only 1.9 ha. Using this technique, a farmer can save about US$ 16.0 per ha compared to hand transplanting method.

Key words: paddy, seedling, transplanter, Dapog nursery, wet bed nursery, wooden frame, bamboo frame, plastic frame, plastic tray, nylon rope, pre-germinated seed, break-even analysis, partial budget analysis

INTRODUCTION

Rice has been accepted as a staple food for half of the world population and about 90% of them live in Asia. Rice crop may be established by direct seeding or transplanting. Until 1965, people used to produce rice by direct seeding with

traditional varieties. However, with the introduction of high yielding varieties (HYV), the production practice shifted from direct seeding to transplanting. There were some specific studies which confirmed that transplanting rice produced 10 to 20% more yield than broadcasted rice (Ramiah and Hanumontha 1936; Bautista 1938; and Ghose *et al.* 1960). Devasundrarajah (1971) reported that there are two clear advantages in transplanting method of rice production. Transplanted paddy occupies field with lesser time compared to direct seeded paddy and it facilitates the control of weeds. Rice transplanting is a highly labour intensive farming operation which consumes about 30% of the labour needed for rice production. According to Islam (1993), about 400-450 man-hr/ha were necessary for hand transplanting in rows, but in the case of random transplanting, the labour requirement was 300-350 man-hr/ha.

A manually operated rice transplanting machine was developed at International Rice Research Institute (IRRI) in the late seventies and later modified in Bangladesh for adaptation to the farmers. The transplanter needed soil-bearing type seedling and capable of transplanting 5-6 times faster than the hand transplanting method. The field performance and economic feasibility of the transplanter are dependent on the seedling raising methods.

Some studies were conducted at IRRI on the seedling raising media, namely using gunny bag, banana leaves and bracts, concrete floor and plastic sheets (Salazar et al. 1985). But their economic comparisons were not reported. Therefore, this study was undertaken:

(a) to compare the costs of different seedling raising methods for manually operated transplanter with a view to reduce production cost.
(b) to identify an appropriate method which can help promoting machine transplanting among the farmers.

MATERIALS AND METHODS

The costs of seedling production in Dapog and tray nurseries for transplanting one hectare of land by machine were calculated. The cost of seedling production for hand transplanting was calculated based on the wet bed method. The Dapog nurseries were provided with wooden, bamboo and plastic frames; however, the nylon ropes were provided only along the boundaries. The tray nursery was made of plastic material. The size of the tray was 40 cm × 20 cm × 3 cm. The seedlings produced in Dapog nursery with different frames were transplanted by BRRI transplanter. However, seedlings produced in wet bed nursery were transplanted by hand in rows. The transplanting costs by machine and hand were calculated separately. The transplanting costs were added to the seedling production costs. The cost of materials and labour were calculated on the basis of Dhaka market as the study was conducted in Bangladesh which is a typical rice growing country in South East Asia. For Dapog and wed bed nurseries, the seedlings were produced in the beds of 10 m^2 and 20 m^2 areas respectively; however, the seedling production costs were expressed in US$/ha. The sizes of the individual plot for machine and hand transplanting were

2.4 m × 20 m each and the transplanting costs were expressed in US$/ha. The treatments were as follows:

T_1 = Cost of machine transplanting with wooden frame nursery seedling
T_2 = Cost of machine transplanting with bamboo frame nursery seedling
T_3 = Cost of machine transplanting with plastic frame nursery seedling
T_4 = Cost of machine transplanting with nylon rope nursery seedling
T_5 = Cost of machine transplanting with plastic tray nursery seedling
T_6 = Cost of hand transplanting with wet bed nursery seedling

Experimental Design

The experiment was conducted under a Randomized Complete Block (RCB) design and the treatments were replicated thrice in each block.

Data Analysis

The data recorded for the costs of seedling production and transplanting were analyzed by partial budget method. This method of analysis is very effective in making a decision whether to switch over a new system as it take-care of the extra cost and revenue for the new system. Moreover, it takes care of the cost saving from the old system and loss of revenue due to the adoption of the new system. The break even analysis of the data was conducted in order to know the level of use (ha/yr), the transplanting cost for the old and whether it would be the same for the new system.

Dapog Nursery

The seedlings were raised in a modified Dapog bed. Each bed was 1 m wide and 20 m long and raised about 30-40 cm above the general surface of the field by putting mud. Then a plastic sheet was spread on the bed and boundaries were provided with frames. After that, a mud layer of approximately 2 to 2.5 cm thick was put on the plastic sheet. Pre-germinated rice seed (BR-1 variety) at the rate of 0.70 kg/m^2 was uniformly spread on the mud. The bed was mulched with rice straw to protect from bird damage. The straw was removed from the bed after three days. The nursery was cared with sufficient amount of water and proper doses of fertilizer and insecticide. Fourteen to eighteen days old seedlings were cut into 19 cm × 40 cm slices to feed into the machine for transplanting.

Wooden Frame Nursery

A wooden frame accommodated 10 compartments of the size of the transplanter tray. The size of the tray was 40 cm × 20 cm × 3 cm. For transplanting one hectare of land, 1100 seedling trays were necessary. Therefore, 110 frames were necessary. The cross section of the side wall of the frame was 3 cm × 1 cm and that of the inner partition wall was 3 cm × 0.7 cm. The frames were laid on the plastic sheet of the Dapog nursery and the compartments were filled with mud.

Bamboo Frame Nursery

A bamboo frame accommodated 10 compartments of the size of the transplanter tray. The size of the tray was 40 cm × 20 cm × 3 cm. For transplanting one hectare of land 1100 seedling trays were necessary. Therefore, 110 frames were necessary. The cross section of the wall of the frame was 3 cm × 0.5 cm. The frames were put on the Dapog nursery in the field seedling raising. The frames were laid on the plastic sheet of the Dapog nursery and the compartments were filled with mud.

Plastic Frame Nursery

A plastic frame accommodated 6 compartments of the size of the transplanter tray. The size of the tray was 40 cm × 20 cm × 3 cm. For transplanting one hectare of land, 1100 seedling trays were necessary. Therefore, 184 frames were necessary. The cross section of the wall of the frame was 3 cm × 0.2 cm. On both the sides of the frame, rectangular plastic tubes were used to increase the strength of the frame. The frames were put on the Dapog nursery in the field seedling raising. The frames were laid on the plastic sheet of the Dapog nursery and the compartments were filled with mud.

Nylon Rope Nursery

After putting the plastic sheet in the Dapog nursery, the bed was bounded by nylon rope and a 2 to 2.5 cm thick mud layer was applied. The seeds were then sown over the mud. When the seedlings were ready for transplanting, they were cut into 19 cm × 40 cm pieces.

Plastic Tray Nursery

The size of a plastic tray was 40 cm × 20 cm × 3 cm. For transplanting one hectare of land 1100, seedling trays were necessary. Therefore, 184 frames were necessary. The cross section of the wall of the frame was 3 cm × 0.2 cm. The trays were put either in the glass house or in the open field for seedling raising.

Wet Bed Nursery

For hand transplanting, the seedlings were raised in wet bed nursery. Each bed was 1 m wide and 20 m long and raised about 30-40 cm above the general surface of the field by putting mud. The pre-germinated rice seeds at rate of 15 .gm/m^2 were spread uniformly. The seedlings were provided with sufficient amount of water and proper doses of fertilizers and insecticides. Twenty five to 35 days old seedling were ready for transplanting.

RESULTS AND DISCUSSION

Cost of Seedling Production

The method of seedling production is an essential pre-requisite for rice transplanting by machine. The highest cost involvement in seedling production

was US$44.89/ha in plastic tray nursery and the lowest cost was US$19.32/ha in wet bed nursery (Table 1). The seedlings produced in the wet bed nursery were not suitable for machine transplanting, however, they were suitable for hand transplanting. For machine transplanting; the cost of seedling production in wooden frame, bamboo frame, plastic frame, and the nylon rope nurseries were US$ 27.21/ha, US$ 27.77/ha, US$27.20 and US$27.04/ha respectively which were almost identical. However, for the plastic tray nursery the cost was US$ 44.89/ha which was significantly greater than those produced in the above methods. The highest cost involvement in plastic tray method was due to the high initial cost of the plastic trays. Approximately US$ 625.00 was necessary to purchase 1100 trays needed for the production of seedlings for one hectare of land. Considering the longevity, the wooden and bamboo frames were identical, but for the bamboo frame it was difficult to maintain sharp, straight and rectangular strips necessary for partitioning of the seedling compartments.

Plastic frames were light weight and handy but their manufacture would not be as simple as the wooden or bamboo frames. In the manufacture of plastic frame, about 0.8m × 0.6m size moulds were necessary for casting of the frame containing six compartments. When the hot plastic materials were cooled in the mould, there was a possibility of bending of the frame walls due to shrinkage and surface tension. If this type of manufacturing difficulties could be overcome, the plastic frame might be a cheap and appropriate medium in which the seedlings for manually operated transplanter could be produced.

TABLE 1
Cost of seedling production and transplanting by different methods

Method of seedling production	Cost of Seedling production* (US$/ha)	Cost of frame (US$/ha)	Cost of transplanter operation (US$/ha)	Total cost (US$/ha)
Wooden frame nursery	27.21	18.92	14.83	60.96
Bamboo frame nursery	27.77	12.38	14.83	54.98
Plastic frame nursery	27.20	16.36	14.83	58.39
Plastic tray nursery	44.89	50.04	14.83	109.76
Nylon rope nursery	27.04	0.57	20.22	47.26
Wet bed nursery	19.32	0.00	73.86	93.18

* *Seedling production cost to serve one hectare of land*

Cost of Transplanting

Partial Budget Analysis

The net benefit from machine transplanting with wooden, bamboo and plastic frame nursery seedlings were US$13.48, US$19.46 and US$16.05 respectively compared to hand transplanting method with wet bed nursery seedlings (Tables 2, 3 and 4). The highest net benefit i.e. US$ 26.61/ha could be achieved when seedlings were raised in nylon rope nursery technique and transplanted by BRRI manual transplanter (Table 5). On the other hand, when

TABLE 2
Partial budget analysis between machine transplanting with wooden frame nursery seedling and hand transplanting with wet bed nursery seedling

Added return	(US$/ha)	Added cost	(US$/ha)
(A) EXTRA REVENUE:		(B) EXTRA COSTS:	
1. Yield benefit from timely planting	11.93	1. Cost of transplanter (FC + VC)	14.83
2. Benefit from machine renting	9.10	2. Cost of wooden frame (FC + VC)	18.92
		3. Cost of seedling production	27.21
(C) SAVING IN COSTS:		(D) LOSS IN REVENUE:	
1. Labour saved in seedling uprooting and hand transplanting	73.86	1. Yield loss for missing hills	39.77
2. Cost saved in wet bed seedling production	19.32		
Total	114.21	Total	100.73

Net benefit (US$/ha) = Added return - Added cost
= (A + C) - (B + D)
= 114.21 - 100.73
= 13.48

TABLE 3
Partial budget analysis between machine transplanting with bamboo frame nursery seedling and hand transplanting with wet bed nursery seedling

Added return	(US$/ha)	Added cost	(US$/ha)
(A) EXTRA REVENUE:		(B) EXTRA COSTS:	
1. Yield benefit from timely planting	11.93	1. Cost of transplanter (FC + VC)	14.83
2. Benefit from machine renting	9.10	2. Cost of bamboo frame (FC + VC)	12.38
		3. Cost of seedling production	27.77
(C) SAVING IN COSTS:		(D) LOSS IN REVENUE:	
1. Labour saved in seedling uprooting and hand transplanting	73.86	1. Yield loss for missing hills	39.77
2. Cost saved in wet bed seedling production	19.32		
Total	114.21	Total	94.75

Net benefit (US$/ha) = Added return - Added cost
= (A + C) - (B + D)
= 114.21 - 94.75
= 19.46

TABLE 4
Partial budget analysis between machine transplanting with plastic frame nursery seedling and hand transplanting with wet bed nursery seedling

Added return	(US$/ha)	Added cost	(US$/ha)
(A) EXTRA REVENUE:		(B) EXTRA COSTS:	
1. Yield benefit from timely planting	11.93	1. Cost of transplanter (FC + VC)	14.83
2. Benefit from machine renting	9.10	2. Cost of plastic frame (FC + VC)	16.36
		3. Cost of seedling production	27.20
(C) SAVING IN COSTS:		(D) LOSS IN REVENUE:	
1. Labour saved in seedling uprooting and hand transplanting	73.86	1. Yield loss for missing hills	39.77
2. Cost saved in wet bed seedling production	19.32		
Total	114.21	Total	98.16

Net benefit (US$/ha) = Added return - Added cost
= (A + C) - (B + D)
= 114.21 - 98.16
= 16.05

TABLE 5
Partial budget analysis between machine transplanting with nylon rope nursery seedling and hand transplanting with wet bed nursery seedling

Added return	(US$/ha)	Added cost	(US$/ha)
(A) EXTRA REVENUE:		(B) EXTRA COSTS:	
1. Yield benefit from timely planting	11.93	1. Cost of transplanter (FC + VC)	20.22
2. Benefit from machine renting	9.10	2. Cost of nylon rope (FC + VC)	0.57
		3. Cost of seedling production	27.04
(C) SAVING IN COSTS:		(D) LOSS IN REVENUE:	
1. Labour saved in seedling uprooting and hand transplanting	73.86	1. Yield loss for missing hills	39.77
2. Cost saved in wet bed seedling production	19.32		
Total	114.21	Total	87.60

Net benefit (US$/ha) = Added return - Added cost
= (A + C) - (B + D)
= 114.21 - 87.60
= 26.61

TABLE 6
Partial budget analysis between machine transplanting with plastic tray nursery seedling and hand transplanting with wet bed nursery seedling

Added return	(US$/ha)	Added cost	(US$/ha)
(A) EXTRA REVENUE:		(B) EXTRA COSTS:	
1. Yield benefit from timely planting	11.93	1. Cost of transplanter (FC + VC)	14.83
2. Benefit from machine renting	9.10	2. Cost of wooden frame (FC + VC)	50.04
		3. Cost of seedling production	44.89
(C) SAVING IN COSTS:		(D) LOSS IN REVENUE:	
1. Labour saved in seedling uprooting and hand transplanting	73.86	1. Yield loss for missing hills	39.77
2. Cost saved in wet bed seedling production	19.32		
Total	114.21	Total	149.53

Net benefit (US$/ha) = Added return - Added cost
= (A + C) - (B + D)
= 114.21 - 149.53
= (-) 35.20

machine transplanting with plastic tray seedling was compared to hand transplanting, there was a net loss of US$ 35.32 per hectare (Table 6). The reason was that the initial cost for plastic trays and the labour requirement for soil preparation were very high. If the job of soil preparation could be mechanized, the labour requirement would be reduced and then the seedling production in trays would be economically attractive to the farmers.

In the analysis, 0.25 ton/ha yield loss costing about US$40.00/ha was estimated due to missing hills in the machine transplanted field. But in the added return, the summation of the benefit from the timely planting and machine renting was only US$ 20.00/ha. Therefore, the adoption of such a transplanter by a farmer would be a safe and profitable investment.

Break-even Analysis

Using a manually operated transplanter with the seedling raised in a wooden frame nursery, for a farmer who used only one hectare per year, the cost of transplanting was US$142.43 per hectare and the cost of hand transplanting was US$93.18 per hectare. However, with the increase of annual use, the cost of machine transplanting decreased and at the yearly use level of 2.0 ha, the costs of machine transplanting and hand transplanting were the same (*Fig. 1*). Therefore, machine transplanting with wooden frame nursery seedling, when the annual use exceeded 2.0 hectares, would benefit the farmer compared to hand transplanting method. On the other hand, when the annual use level was

less than 2.0 ha, the farmer would be advised not to buy the transplanter and he should continue with the existing hand transplanting method.

Similarly the break even use levels per year of machine transplanting with bamboo frame, plastic frame and nylon rope nursery seedling were 1.6, 1.8 and 0.5 hectares respectively compared to hand transplanting method (*Figures 2, 3* and *4*). For a farmer owning 2 hectares of land and considering the possibility of triple cropping, the annual work load was 6 hectares. Therefore, a farmer having only 2 hectares of land could be advised to buy a transplanter because the yearly break-even use level was less than 2 hectares with seedlings produced by any one of the above methods. The break-even use level of the transplanter with plastic tray nursery seedling was found to be 13.0 ha/year (*Fig. 5*). Therefore, machine transplanting with plastic tray seedling was not recommended for an average size farmer. Considering all the factors, the machine transplanting with plastic frame nursery seedling would be

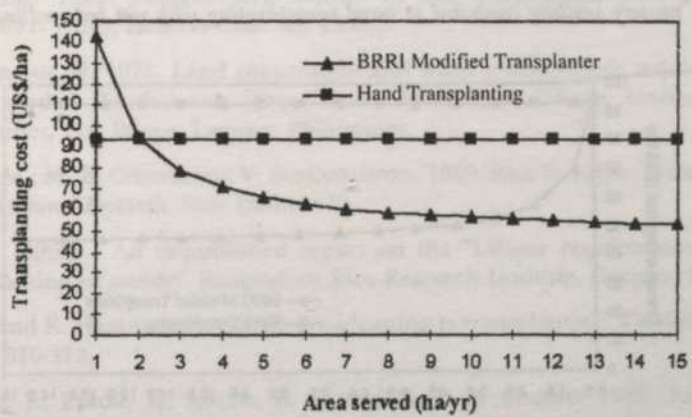

Fig 1. Transplanting cost by BRRI modified transplanter with wooden frame nursery seedling compared to hand transplanting with wet bed seedling in different levels of use.

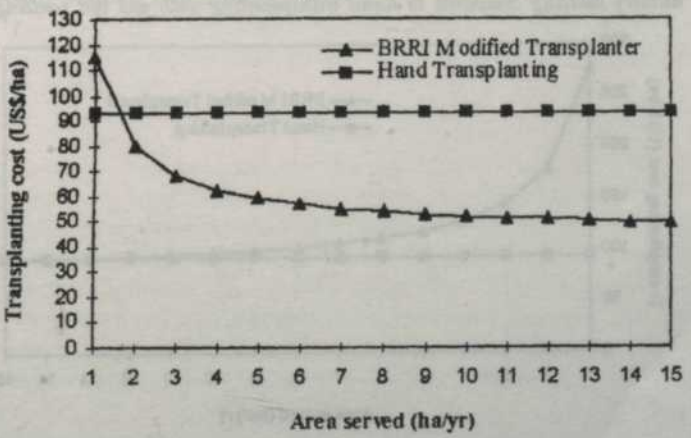

Fig 2. Transplanting cost by BRRI modified transplanter with bamboo frame nursery seedling compared to hand transplanting with wet bed seedling in different levels of use.

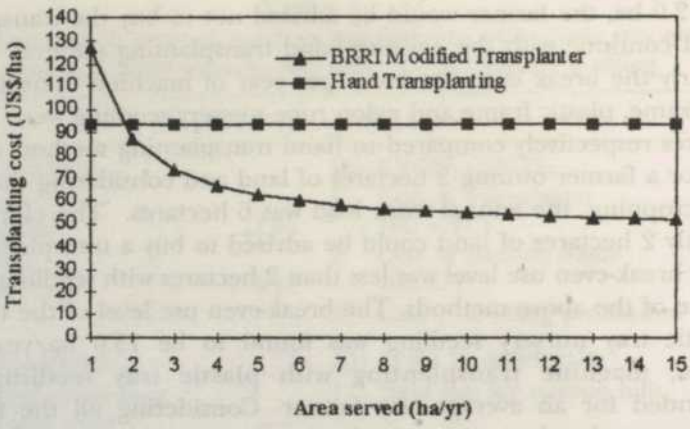

Fig 3. Transplanting cost by BRRI modified transplanter with plastic frame nursery seedling compared to hand transplanting with wet bed seedling.

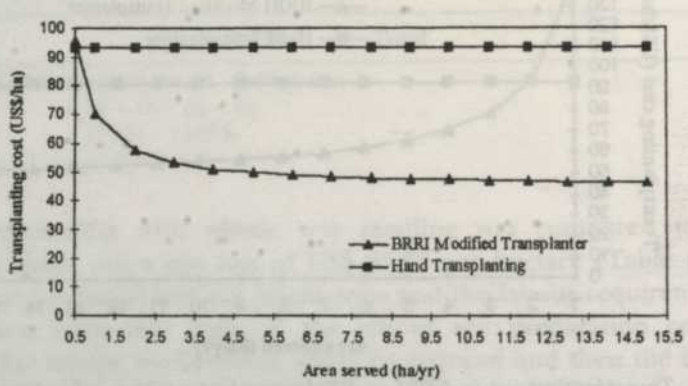

Fig 4. Transplanting cost by BRRI modified transplanter with nylon rope nursery seedling compared to hand transplanting with wet bed seedling.

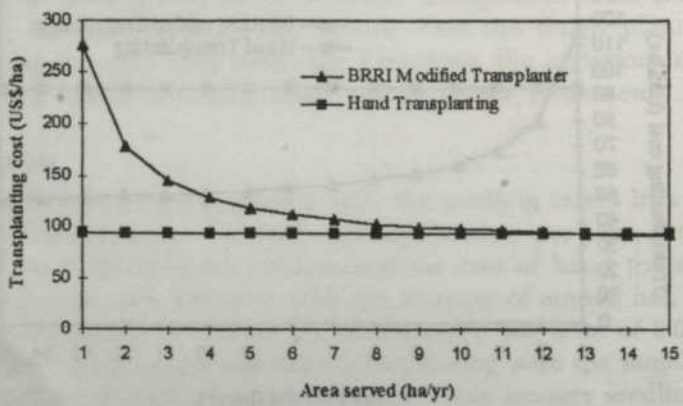

Fig 5. Transplanting cost by BRRI modified transplanter with plastic tray nursery seedling compared to hand transplanting with wet bed seedling.

recommended where the break even use level per year was only 1.8 ha. This process would be workable if the plastic frames are available in the market. Otherwise the farmers are advised to practice machine transplanting with wooden frame nursery seedling where the break even use level is 2.0 ha.

CONCLUSION

Among the five seedling raising methods for machine transplanting, the plastic frame method was the most appropriate, where the break-even area per year was only 1.9 ha. Using this method and transplanting by BRRI transplanter, a farmer could save about US$16.00 per hectare compared to the conventional hand transplanting method.

REFERENCES

BAUTISTA, B.R. 1938. Palagad rice culture in the Philippines. *Phil. Journal Agr.* **2:** 381-391. (Also, farmers Cire. 45, 1938).

DEVASUNDRARAJAH, N. 1971. Land preparation and water management requirements for direct seeded flooded rice *(Oryza Sativa L).* Master's Thesis, University of the Philippines, Los Banos, Laguna, Philippines.

GHOSE, R.L.M., M. B. CHATGE and V. SUBRAHMANYAN. 1960. Rice in India. I*ndian Conference of Agricultural Research*, New Delhi. 470.

ISLAM, M.S. (1993). An unpublished report on the "Labour requirement in manual transplanting of paddy". Bangladesh Rice Research Institute, Gazipur, Bangladesh.

RAMIAH, K. and K. HANUMANTHA (1936) Broadcasting vs transplanting. *Tropical Agriculture.* **26**(5): 310-313.

SALAZER, G., L. EBRON, H. ICALTO, B. DUFF and R. E. STICKNEY 1985. Rice seedling transplanters in the Philippines. *Proceedings of the International Conference on Small Farm Equipment for Developing Countries: Past Experiences and Future Priorities.* 2-6 Sept., 1985, IRRI, Manila, Philippines. 213-229.

ISSN: 0128-7680
Pertanika J. Sci. & Technol. 8(2): 217-227 (2000)

Prediction of Chromatographic Separation of Eugenol by the Fast Fourier Transform Method

Wan Ramli Wan Daud*, San Myint*, Abu Bakar Mohamad* and Abdul Amir Hassan Kadhum*

**Department of Chemical & Process Engineering, Universiti Kebangsaan Malaysia 43600 UKM Bangi, Selangor Darul Ehsan, Malaysia*

***Department of Chemical Engineering, Yangon University of Technology Yangon, Myanmar*

Received: 15 April 1998

ABSTRAK

Masa pensuisan atau penukaran antara jerapan dan nyah-erapan dalam kromatografi cecair, iaitu ketika kepekatan aliran keluar mencapai nilai bulus, amatlah penting dalam pengendalian, peningkatan skala dan pengoptimuman pemisahan secara kromatografi. Masa pensuisan boleh dianggar dengan simulasi komputer turus kromatografi jerapan. Dalam karya ini, simulasi teori turus kromatografi oleh Chen dan Hsu berdasarkan kaedah jelmaan Fourier pantas (JFP) yang dicadangkan pertama kali oleh Hsu untuk sistem kromatografi, yang menggunakan anggaran pekali resapan paksian, pekali pemindahan jisim, dan keresapan liang yang diperolehi daripada pemisahan peringkat analisis, dibandingkan dengan data uji kaji pemisahan kromatografi eugenol. Teknik JFP digunakan untuk menyelesaikan model ini. Penggunaan JFP dan bukan teknik yang lebih anggun seperti kaedah beza terhingga atau penempatan bersama ortogonal adalah beralaskan pengiraan yang lebih mudah dan kedapatan teknik menyongsang yang lebih baik. Model ini disahkan oleh data uji kaji daripada pemisahan kromatografi eugenol pada turus analisis μBondapak C_{18}, fasa bergerak metanol-air (80:20), kadar alir 0.5 ml/min, pada penyuntikan larutan berlainan kepekatan pada keadaan keseimbangan. Data sifat fizik yang diperlukan untuk pengesahan ini seperti data penjerapan keseimbangan sesuhu ditentukan secara uji kaji, dan data pemindahan jisim dihitung dengan korelasi lazim dan daripada pemisahan peringkat analisis. Simulasi ini mengesahkan data uji kaji pada nombor Peclet 6000, parameter panjang lapisan 3.0 dan bilangan sampel 90.

ABSTRACT

The switching time to change from adsorption to desorption in liquid chromatography, which is the time at which the concentration of the effluent reaches the breakthrough value, is important in the operation, scale-up, and optimisation of chromatographic separation. The switching time can be estimated by computer simulation of the chromatographic adsorption column. In this paper, the theoretical simulation of the chromatographic column of Chen and Hsu (1987) based on the Fast Fourier Transform (FFT) method originally proposed for chromatographic systems by Hsu using estimated axial diffusivity, film mass transfer coefficient and pore diffusivity obtained from analytical scale separation, is compared with experimental data of chromatographic separation of eugenol. The use of FFT over more sophisticated techniques such as finite difference or orthogonal collocation methods was dictated by the simpler

computation and the availability of better inverting techniques. The model was validated by experimental data on chromatographic separation of eugenol on μBondapak C_{18} analytical column, mobile phase methanol-water (80:20), and flow rate 0.5 ml/min, at different solution concentration injection at equilibrium condition. Physical property data required for validation such as equilibrium adsorption isotherm data was determined experimentally, and mass transfer data was calculated from normal correlations and from analytical scale separation. The simulation agreed with experimental data at a Peclet number of 6000, a bed length parameter of 3.0 and number of samples 90.

Keywords: separation, high performance liquid chromatography, Fast Fourier Transform

INTRODUCTION

In practice, liquid chromatography is operated in a cyclic manner alternating between adsorption and desorption. During adsorption, the feed containing a solute at certain concentration is introduced into the bed as a band. During desorption or elution, a carrier fluid free of solute is fed into the system until the solute adsorbed on the adsorbent particles is completely recovered. Desorption of the solute is usually initiated when the solute concentration in the effluent stream reaches or passes the breakthrough value; in other words, before the bed is completely saturated. Therefore, the switching time to change from adsorption to desorption, and vice versa, is important in the operation, scale-up, and optimisation of a chromatographic separation. The switching time can be estimated by computer simulation of the chromatographic adsorption column. The simulation model requires equilibrium sorption data which is determined experimentally and mass transfer data including inter-particle mass-transfer coefficients and effective diffusivities for transport within the porous adsorbent particles which are determined from available correlations. In this paper, the theoretical simulation of the chromatographic column of Chen and Hsu (1987) based on the Fast Fourier Transform (FFT) method originally proposed for chromatographic systems by Hsu (1979) using estimated axial diffusivity, film mass transfer coefficient and pore diffusivity obtained from analytical scale separation, is compared with experimental data of chromatographic separation of eugenol.

MATHEMATICAL MODEL

Chen and Hsu (1987) used the fixed bed adsorber model of Rasmuson and Neretnieks (1980) to describe an isothermal adsorption column packed with porous spherical particles of radius a adopted for this simulation work. At time zero, a step change in the concentration of an adsorbable species was introduced into the flowing stream. The adsorption column was subjected to axial dispersion, pore diffusion resistance, and external film diffusion resistance. After introducing dimensionless variables as suggested by Raghavan and Ruthven (1983), the fixed-bed adsorber may be described by the following set of equations. Mass

balance in the mobile phase is given by

$$\frac{\partial U}{\partial \tau} + \psi_1 \delta \frac{\partial U}{\partial x} - \frac{1}{P_e} \psi_1 \delta \frac{\partial^2 U}{\partial x^2} = -3\psi_1 \xi (U - Q|_{\eta=1}) \tag{1}$$

Particle diffusion is given by

$$\frac{\partial Q}{\partial \tau} = \frac{\partial^2 Q}{\partial \eta^2} + \frac{2}{\eta} \frac{\partial Q}{\partial \eta} \tag{2}$$

Initial and boundary conditions are as follows:

$$U(x,\tau = 0) = 0 \tag{3}$$

$$U(x = 0,\tau) = 1 \tag{4}$$

$$U(x = \infty,\tau) = 0 \tag{5}$$

$$Q(\eta,x,\tau = 0) = 0 \tag{6}$$

$$Q(\eta = 0,x,\tau) \neq \infty \tag{7}$$

$$\frac{1}{K_1} \frac{\partial Q}{\partial \eta} \Big|_{\eta=1} = \xi \left(U - \frac{Q|_{\eta=1}}{K_1} \right) \tag{8}$$

where

$$U = C / C_0, Q = \frac{C_P}{C_0}, x = \frac{z}{L}, \tau = \frac{D\theta}{a^2}, \eta = \frac{r}{a}, \psi_1 = \frac{K_1}{m}, \delta = \frac{Va^2 m}{LDK_1}, \xi = \frac{k_f a}{DK_1}$$

and $P_e = \frac{LV}{D_L}$. The Laplace domain solution of U is

$$\overline{U}(x,s) = \frac{1}{s} \exp\left\{ \left[\frac{P_e}{2} - \sqrt{\frac{P_e^2}{4} + \frac{P_e s}{\psi_1 \delta} + \frac{3\xi P_e \phi(s)}{\delta}} \right] x \right\} \tag{9}$$

where $\phi(s) = \dfrac{\sqrt{s}Cosh\sqrt{s} - Sinh\sqrt{s}}{\sqrt{s}Cosh\sqrt{s} - Sinh\sqrt{s} + \xi Sinh\sqrt{s}}$

Multiplying Equation (9) by s gives a transfer function $F(s)$ of the corresponding chromatography system

$$F(s) = \exp\left\{ \left[\frac{P_e}{2} - \sqrt{\frac{P_e^2}{4} + \frac{P_e s}{\psi_1 \delta} + \frac{3\xi P_e \phi(s)}{\delta}} \right] x \right\} \tag{10}$$

where $F(s) = \exp(-\sigma x)$

$$\sigma = \frac{P_e}{2} - \sqrt{\frac{P_e^2}{4} + \frac{P_e s}{\psi_1 \delta} + \frac{3\xi P_e \phi(s)}{\delta}} \tag{11}$$

ADSORPTION ISOTHERM

Adsorption isotherm was generated by pumping solutions of different concentrations of eugenol into a new clean column until it is fully saturated. A standard analytical C_{18} μ Bondapak column 0.39 cm I.D. and 30 cm height, was used in the experiments. The adsorbent particles size is 10 μm. The mobile phase used was a mixture of HPLC grade methanol and doubled distilled water having a ratio of 80:20 by volume. Low pressure column experiments were conducted with a flow rate of 0.5 ml/min. Concentration of eugenol in the fluid leaving the bed was determined from its absorbance at 280 nm. The column was stabilised after each experiment by varying the methanol flow rate for about 5 hours followed by a constant low flow rate of 0.1 ml/min for half a day. When the inlet and outlet concentrations became identical, the amount of eugenol retained on the adsorbent particles could easily be determined from mass balance, knowing the total amount of eugenol which had been fed to the bed. The linearity of the adsorption system was examined by replicate experiments in which the concentration of pumping solution was varied from 0.1 ml to 0.5 ml eugenol/100 ml solvent. The capacity (q_a) is plotted against the equilibrium solution concentrations (C^*) as shown in *Figure 1.* The isotherm is linear in the working range and the expression for the isotherm at room temperature is

$$q_a = 1.8703C^* \qquad (12)$$

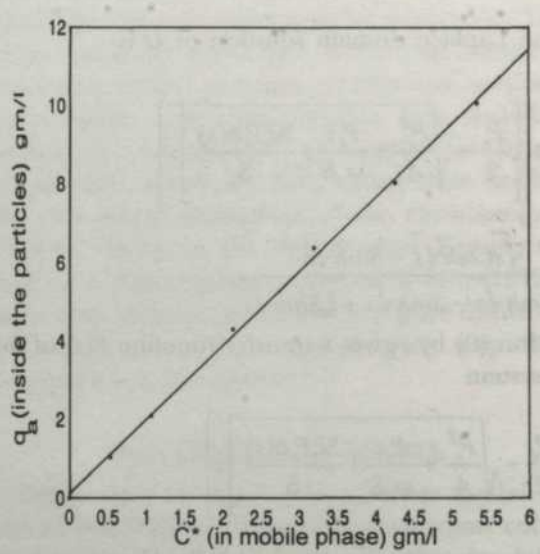

Fig 1. Adsorption isotherm of eugenol at room temperature from packed bed equilibrium adsorption experiments on C_{18} μ Bondapak column (30 cm × 3.9 mm i.d.); mobile phase, methanol/water (80:20); flowrate, 0.5 ml/min.

PARAMETER ESTIMATION

The molecular diffusivity, D_m, of eugenol in methanol-water mixture was estimated by Wilke and Chang (1955) correlation:

$$D_m = \frac{1.173 \times 10^{-16} (\psi_2 M_2)^{0.5} T}{\mu V_1^{0.6}} \quad (13)$$

where M_2 is the molecular weight of the solvent, T is the temperature in ° K, μ is the solvent viscosity (Pa s), ψ_2 is the association factor and V_l is the molal volume (km³/kg mole). The dependence of external film mass-transfer coefficient k_f on flow rate may be obtained from the following Wilson and Geankoplis correlation (Geankoplis, 1983) for Reynolds number between 0.0015 and 55.

$$k_f = \frac{1.09u}{\varepsilon} \left[\mathrm{ReSc}\right]^{-2/3} \quad (14)$$

The axial dispersion coefficient of liquid flowing through fixed beds can be obtained from the correlation equation of Wen and Fan (1975):

$$\frac{1}{\mathrm{Sc}} = \frac{D_L \rho}{\mu} = \frac{\mathrm{Re}}{0.2 + 0.011 \mathrm{Re}^{0.48}} \quad (15)$$

For systems in which the main mechanism of intraparticle diffusion is molecular diffusion within the macropores, intrapore diffusivity Raghavan and Ruthven, 1983) is given as

$$D \approx \varepsilon_P D_m / \chi \quad (16)$$

SIMULATION OF THE PACKED BED SYSTEM

Parameters used in the simulation estimated from the defined data from experimental analytical scale separation are assigned as shown in Table 1.

TABLE 1

Parameter	Value
T	298 K
χ	3.385
ε_P	0.3385
m	0.5117
k_f	4.4076×10^{-2}cm²/sec
D_L	4.89×10^{-4}cm²/sec
D	5.168×10^{-7}cm²/sec
ξ	0.045
P_e	6000

Following the methods of Hsu (1979), Hsu and Dranoff (1987) and Chen and Hsu (1987), the Fast Fourier Transform was applied to solve the fixed-bed

adsorption problem equation (1) to (10). If inversion of $F(s)$ in equation (11), named $f(\tau)$ can be found, then U at bed length x and time τ can be obtained by integrating $f(\tau)$ from zero to τ with respect to τ. The inversion of $F(s)$ by FFT is given by

$$f(t) = f(\tau) = f(j\Delta T') \tag{17}$$

$$= \frac{1}{2T} \sum_{k=0}^{N-1} F\left(ik\frac{\pi}{T'}\right) \exp\left(\frac{2\pi jk}{N_s}\right) \tag{18}$$

where $j = 0,1,2,\ldots\ldots, N_s - 1$

RESULTS AND DISCUSSION

Figure 2 shows effluent concentration profile for injection of different solution concentration to an initially new clean bed versus different length of elution time. It also shows that the effluent concentration first approached the feed concentration and then is reduced to zero at the end of the period. The breakthrough curves at different injection concentration were presented in *Figure 3.*

Figure 4 to *Figure 7* show the theoretical simulation results of the adsorption of a single component eugenol onto a fixed bed of (Bondapak C18 analytical column. The parameters used in the calculation are all estimated from the optimum analytical scale separation. Figure 4 displays the chromatographic elution curves at different bed length parameters calculated from the proposed model. It shows that the elution curves peak height is dependent on the bed length parameter.

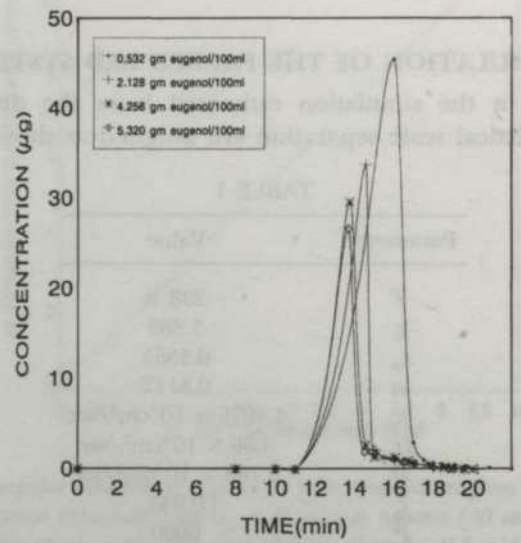

Fig 2. Chromatogtaphic elution curves of eugenol on µ Bondapak C_{18} analytical column, mobile phase methanol-water (80:20), flow rate 0.5 ml/min, at different solution concentration injection at equilibrium condition

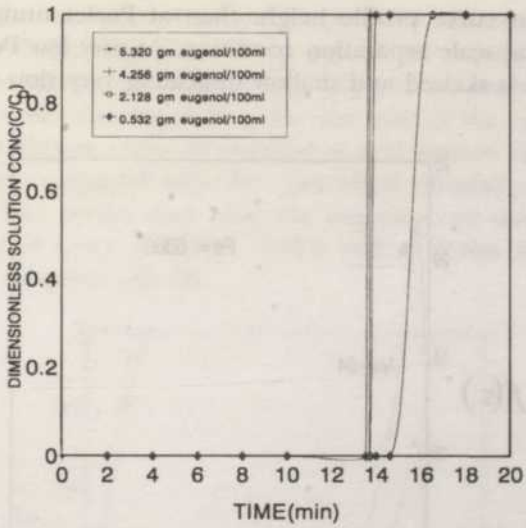

Fig 3. Experimental breakthrough curves at different eugenol injection concentration on μ Bondapak C_{18} analytical column, mobile phase methanol-water (80:20), flow rate 0.5 ml/min

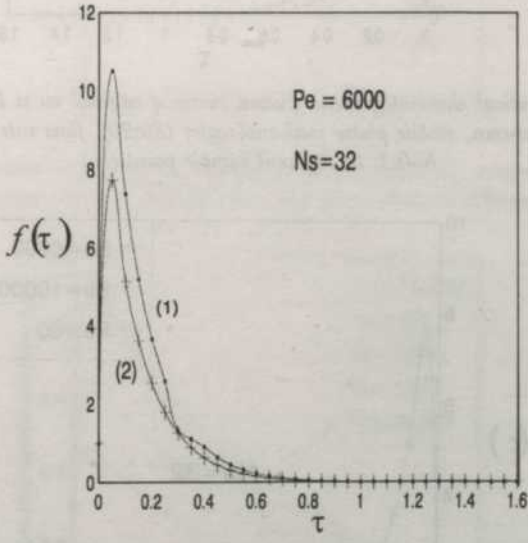

Fig 4. Theoretical chromatographic evution curves of eugenol on μ Bondapak C_{18} analytical column, mobile phase methanol-water (80:20), flow rate 0.7 ml/min, at different bed length parameters, (1) δ=3.0, (2) δ=0.3

Figure 5 shows the effect of number of sampling points on the elution curves at Peclet number 6000 for analytical column. Increasing the sample numbers to 64 gives a higher peak height and vary smoothly than that computed at sample number 32. *Figure 6* shows the theoretical chromatographic curves of eugenol at different Peclet number. Increasing the Peclet number to 10,000 shows a

little difference in curve profile height than at Peclet number 6000 of the optimum analytical scale separation condition. At very low Peclet number 60, the elution curve is skewed and shallow indicating very slow saturation.

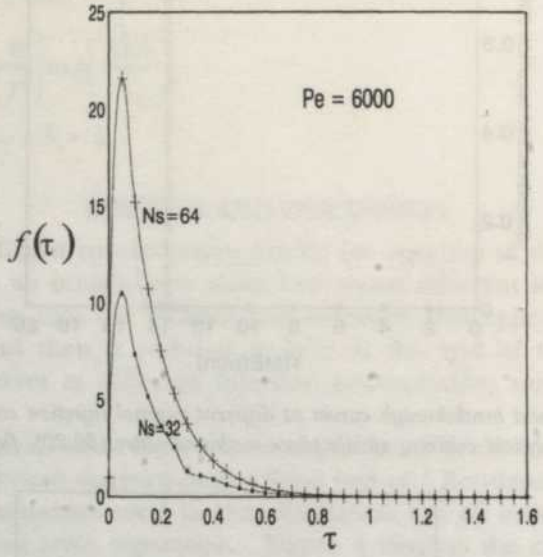

Fig 5. Theoretical chromatographic elution curve of eugenol on μ Bondapak C_{18} analytical column, mobile phase methanol-water (80:20), flow rate 0.7 ml/min, δ=0.3, at different sample points(N_s)

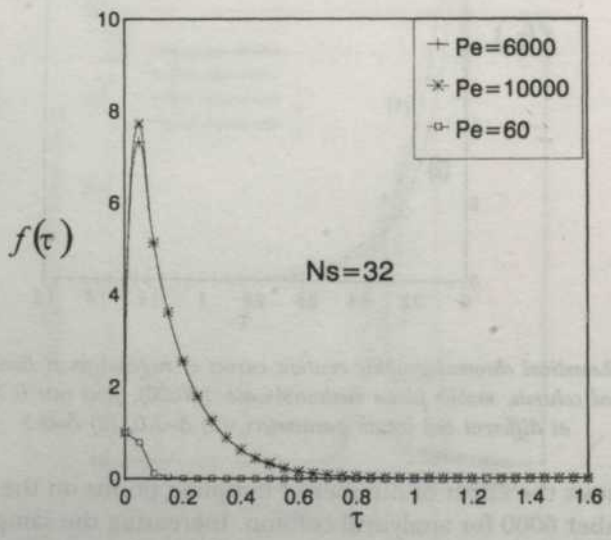

Fig 6. Theoretical chromatographic elution curve of eugenol on μ Bondapak C_{18} analytical column, mobile phase methanol-water (80:20), flow rate 0.7 ml/min, δ=0.3, at different Peclet number

Figure 7 demonstrates the breakthrough curves at different Peclet numbers of 6000 and 10,000 showing initial sharp rise of the curves due to the small particle size of the packing material, followed by a much more gradual increase towards the feed concentration during the later part of the curves. In Figure 8 the experimental elution curve of eugenol at real elution time 0.42 minutes (Figure 5.3.3) was compared with the theoretical simulation data at various Peclet numbers. The results show that the experimental data agree with the theoretical model of Chen and Hsu (1987) well at Peclet number (P_e) near 6000 and sample number (N_s) 90.

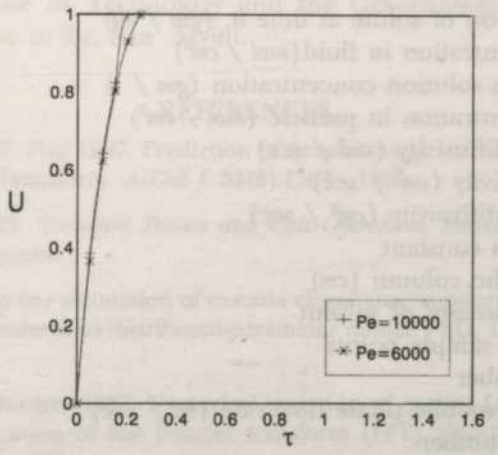

Fig 7. Theoretical breakthrough curve of eugenol on μ Bondapak C_{18} analytical column, mobile phase methanol-water (80:20), flow rate 0.7 ml/min, δ=0.3, at different Peclet number

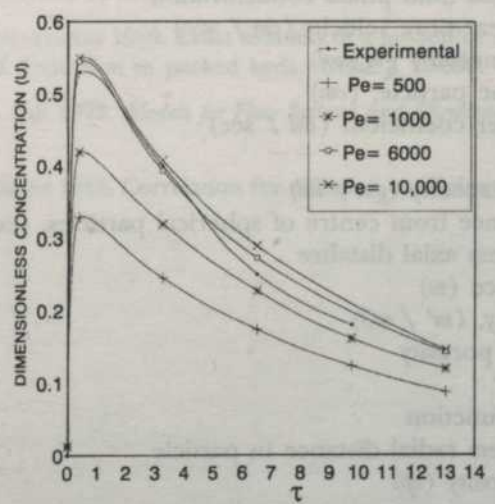

Fig 8. Experimental elution curve of eugenol superimposed on theoretical predictions elution curve at different Peclet numbers. (Experimental conditions μ Bondapak C_{18} analytical column, mobile phase methanol-water [80:20], flow rate 0.7 ml/min. Simulation parameters δ=3.0, N_s=90)

CONCLUSION

The elution profile and the breakthrough curves depend on Peclet number (P_e), bed length parameters (δ) and number of sample points (N_s). The proposed model of Cheng and Hsu (1987) and the accuracy and high computing speed of the FFT technique of Hsu (1979) gives satisfactory agreement between theoretical model and experimental data of chromatographic separation of eugenol.

NOMENCLATURE

C	concentration of solute at time θ, (gm / ml)
C_0	inlet concentration in fluid(mol / cm^3)
C^*	equilibrium solution concentration (gm / l)
C_p	inlet concentration in particle (mol / cm^3)
D	intrapore diffusivity (cm^2 / sec)
D_L	axial diffusivity (cm^2 / sec)
D_M	molecular diffusivity (cm^2 / sec)
K_1	equilibrium constant
L	length of the column (cm)
M_2	molecular weight of solvent
N_s	number of sample points
P_e	Peclet number
Q	volumetric mobile phase flow rate (ml / sec)
Re	Reynolds number
Sc	Schmidt number
T'	half-period of function being considered
U	dimensionless fluid phase concentration
V	average linear pore velocity,(cm / sec)
V_1	molal volume(ml / gm mol)
a	radius of the particle, (cm)
k_f	mass transfer coefficient (cm / sec)
m	$= \varepsilon$ / (1–ε)
q_a	adsorbent capacity (gm / ml)
r	radial distance from centre of spherical particles, (cm)
x	dimensionless axial distance
z	axial distance (m)
ε	bed porosity, (m^3 / $m3$)
ε_p	macropore porosity
θ	time(sec)
ϕ	frequency function
η	dimensionless radial distance in particle
μ	solvent viscosity (cp)
ξ	film resistance parameter
Ψ_1	distribution ratio
Ψ_2	association factor

τ contact time parameter
δ bed length parameter
σ constant
χ tortuosity factor

ACKNOWLEDGEMENTS

The authors would like to thank Universiti Kebangsaan Malaysia for supporting this research, the Government of Malaysia for granting a scholarship under the Malaysian Technical Aid Program to Dr. San Myint to pursue this research and the Yangon Institute of Technology and the Government of Myanmar for granting study leave to Dr. San Myint.

REFERENCES

CHENG, T. L., and J. T. HSU 1987. Prediction of breakthrough curves by the application of Fast Fourier Transform. *AIChE J.* **33(8)**:1387 - 1390.

GEANKOPLIS, C. J. 1983. *Transport Process and Unit Operations.* Massachusetts: Allyn and Bacon, Massachusetts.

HSU, J. T. 1979. Computer simulation of cascade chromatography and the application of Fast Fourier Transform to distributed-parameter model. PhD. Thesis, Northwestern University.

HSU, J. T. and J. S. DRANOFF 1987. Numerical inversion of certain Laplace transform by the direct application of fast Fourier transform (FFT) algorithm. *Comput. Chem. Engng.* **11(2)**:101 - 110.

RAGHAVAN, N. S. and D. M. RUTHVEN 1983. Numerical simulation of a fixed-bed adsorption column by the method of orthogonal collocation. *AIChE J.* **29**:922.

RASMUSON, A. and I. NERETNIEKS 1980. Exact solution of a model for diffusion in particles and longitudinal dispersion in packed beds. *AIChE J.* **26**:686.

WEN, C. Y. and L. T. FAN 1975. *Models for Flow Systems and Chemical Reactors.* New York: Marcel Dekker

WILKE, C. R. and P. CHANG 1955. Correlation for diffusion coefficients in dilute solutions. *AIChE J.* 1:264.

Pertanika J. Sci. & Technol. 8(2): 229-239 (2000)
ISSN: 0128-7680

Effect of Ignition Timing on Fuel Consumption and Emissions of a Dual Chamber Spark Ignition Engine

Ch. Rangkuti
Mechanical Engineering Department
Univ. of North Sumatera
Medan, Indonesia

Received: 12 March 1998

ABSTRAK

Kajian telah dijalankan terhadap penggunaan dan penyebaran bahan api daripada bilik berkembar, cas berstrata, enjin nyalaan pencucuh dengan masa nyalaan yang berbeza. Pembakaran terlambat yang berkait dengan pemasaan MBT, menghasilkan penggunaan bahan bakar kurang baik, terutamanya dengan campuran yang sedikit. Pembakaran lemah yang berkait dengan pembakaran lambat tidak akan meningkatkan penyebaran UHC – sebaliknya penurunan penyebaran CO lebih tinggi (untuk campuran yang sedikit); paras NO_x tidak banyak bezanya apabila terbuka luas dan 65% kecepatan dan kerendahannya signifkan pada 40% kecepatan.

ABSTRACT

Fuel consumption and emissions from a dual chamber, stratified charge, spark ignition engine with different ignition timing were investigated.
Retarded ignition, relative to MBT timing, yielded poorer fuel consumption, especially with lean mixtures. The poorer combustion associated with the late burning did not result in increased UHC emissions - these in fact is reduced. Emissions of CO were higher (for lean mixtures); NO_x levels were much the same at wide-open and 65% throttle settings and significantly lower at the 40% throttle setting.

Keywords : ignition time, combustion speed, emissions, lean mixture

INTRODUCTION

In their earlier investigations using the same engine, British Leyland Technology Ltd. (Weaving 1982) specified a "base-line" test condition which they used as a standard/reference for comparing performance at other test conditions. The base-line conditions were at engine speed of 2000 rpm., pre-chamber air flow at 6 % of total air inlet and pre-chamber air fuel ratio (AFR) of 6 : 1. This condition was reported to give the best compromised emissions for the engine in the previous Leyland experiments.

Tests conducted in this study at the reference running condition revealed some differences in engine performance compared with those conducted previously at British Leyland (Weaving 1982). In particular, unburned hydrocarbon (UHC) emissions were significantly lower in the tests conducted.

The UHC emissions were considered to be the major problem with the engine. Hence further consideration was given to the differences between the two sets of results.

In an attempt to assess the relative contributions of the main combustion event and crevices to UHC emissions the "reference test" was repeated with a fixed ignition advance instead of the maximum best torque (MBT) timing adopted in all other tests. The fixed advance was selected to be 22° Before Top Dead Centre (BTDC), the optimum ignition timing at the wide-open throttle setting for the richest mixture was used in the reference test. This resulted in retarded timing compared with MBT at other AFR's, ignition being particularly "late" for lean mixtures. This was expected to result in poor combustion taking place late in the cycle, with incomplete combustion and increased UHC emissions.

In this paper the experiments are designed to explore this difference and report particularly the effects of ignition timing on fuel consumption and emissions of a dual chamber stratified charge engine.

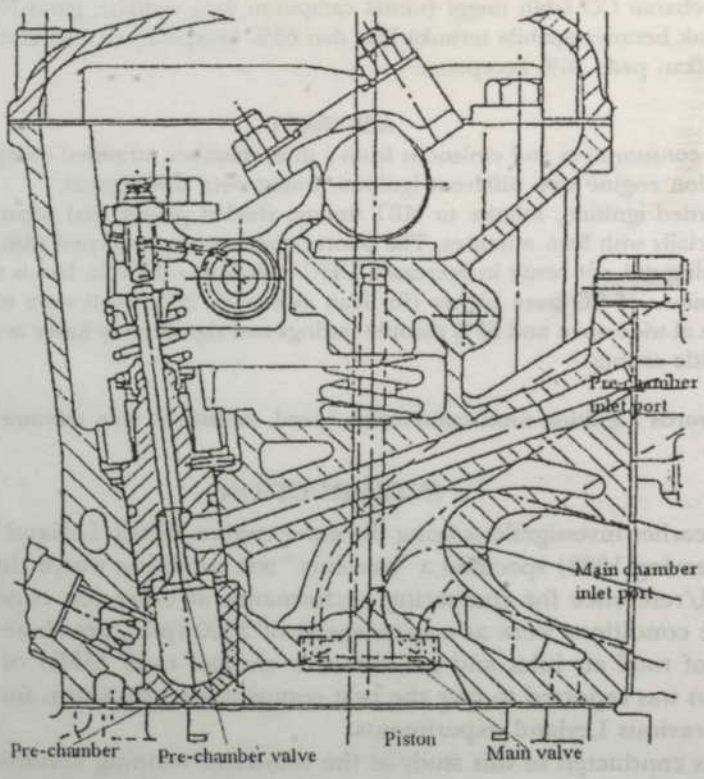

Fig 1. Schematic drawing of engine cylinder head

MATERIALS AND METHODS

Engine

The engine was based on a 4 cylinder Triumph Slant engine with water cooled cylinder block. The cylinder bore was 90.3 mm and stroke of 78.0 mm. A cross section of the cylinder head fitted to the working cylinder is shown in *Fig. 1.* The engine crankshaft was fitted with an extension to drive, via a flexible coupling, a shaft encoder. At the other end, the engine was connected to a D.C. motor type dynamometer by a flexible coupling.

The main chamber carburettor was of SU type AUB9203, and the fuel to the pre-chamber was supplied from the tank via a fine needle control valve, to a rotameter. The pre and main chamber air flows use separate intake systems; the air supply to the main chamber was drawn in via a large surge tank fitted with a 16 mm diameter metering nozzle.

The pre-chamber air flow-rate was measured by an air rotameter and this was fixed at 6 % of the air flow-rate into the engine in all experiments, because this amount proved to be the optimum in the earlier study (Weaving 1982).

The torque developed by the engine was measured using a load cell. A switch at the control panel allowed the polarity of the signal to be changed. This allowed measurement of either firing or motoring torque of the engine.

Engine Instrumentation

The engine instrumentation mainly consists of a dynamometer and the control panel, which includes cycle and timing selector, pressure transducer charge amplifiers, speed dial and torque meter dial.

Pulses created by the commercial shaft encoder were sent to an external clock, incorporated in a VAX-8600 computer, to instruct the analogue to digital converter (ADC) to take samples each time a pulse was generated by the encoder.

The ignition system used comprised a contactless electronic ignition unit, a standard ignition coil, a 12 V battery and a commercial spark plug.

The control system counted the pulses from the shaft encoder and triggered the spark at the required angle. The spark timing could be set to any crank-angle between 99°BTDC and 99° After Top Dead Centre (ATDC). A switch on the panel allowed either 2 or 4 stroke engine operation to be selected. The ignition could be restricted to alternate or every 3rd, 4th or 5th cycle if required. The system provided spark and Top Dead Centre (TDC) signals to be fed to the on-line computer; it also "gated" the shaft encoder pulse which triggered the computer's data acquisition system.

The pressure in each chamber inside the engine cylinder was measured using a piezo electric transducer. They were capable of measuring rapidly varying pressure in the range of 0 to 250 bar, while maintaining good linearity and having a very good frequency response. The signal from each transducer was transmitted, via two balanced leads, to a universal electrostatic charge amplifier; which converted the electrostatic signals into a voltage.

On-line Data Acquisition

A very high speed ADC unit was used to convert the pressure signals (from both chambers), as well as spark and TDC signals to a digital form. The ADC unit was interfaced to the VAX-8600 minicomputer via a direct memory access interface.

Once a signal was sampled, the information could be stored in the computer and immediately processed to yield output such as pressure-crank angle diagram, pressure-volume diagram and indicated mean effective pressure (imep), the data to be used in the figures presented in this paper. The computer programme used for this work was based largely on that developed by Hynes (1986).

Gas Analysers

The system was designed to sample and measure the concentration of total unburned hydrocarbons (UHC), carbon monoxide (CO), carbon dioxide (CO_2), oxygen (O_2) and oxides of nitrogen (NO_x) in the engine exhaust. The system is set out diagrammatically in *Fig. 2.* It includes sample probe, stop valves, heated filter, water traps, drying agents, three way valves and heated line with temperature control. The sample was fed to the hydrocarbon analyser via a continuously heated sampling line which kept the sample temperature at 150°C throughout, in order to prevent any condensation of the higher hydrocarbons. The gas samples fed to the other analysers were led via a water trap and tubes containing drying agents, as it was important to avoid water condensation in the instruments. The oxygen analyser sample was fed from the high range CO analyser, as the former analyser did not have a pump of its own.

Total Hydrocarbon Analyser

The total unburned hydrocarbon concentrations were measured using an Analysis Automation Ltd. Series 520 Hydrocarbon Analyser; this incorporates a flame ionization detector (FID) for total unburned hydrocarbon measurement.

In the current work calibration was effected using a 400 ppm concentration of normal-hexane in nitrogen. The manufacture's claimed accuracy for the unit was ± 1.5% of full scale deflection (FSD); it had ranges 0-10, 0-100, 0-1000 and 0-10,000 ppm by volume.

Infra Red Analysers

Carbon monoxide concentrations were measured using two Grub-Parsons Series 20 infra red gas analysers, one with ranges of 0 - 0.1 % and 0 - 0.5 % the other having ranges of 0 - 3.0 % and 0 - 15.0 % by volume. Carbon dioxide concentrations were measured using a similar type of analyser, with ranges of 0 - 15.0 % by volume. The quoted accuracy of both instruments was ± 1 % FSD.

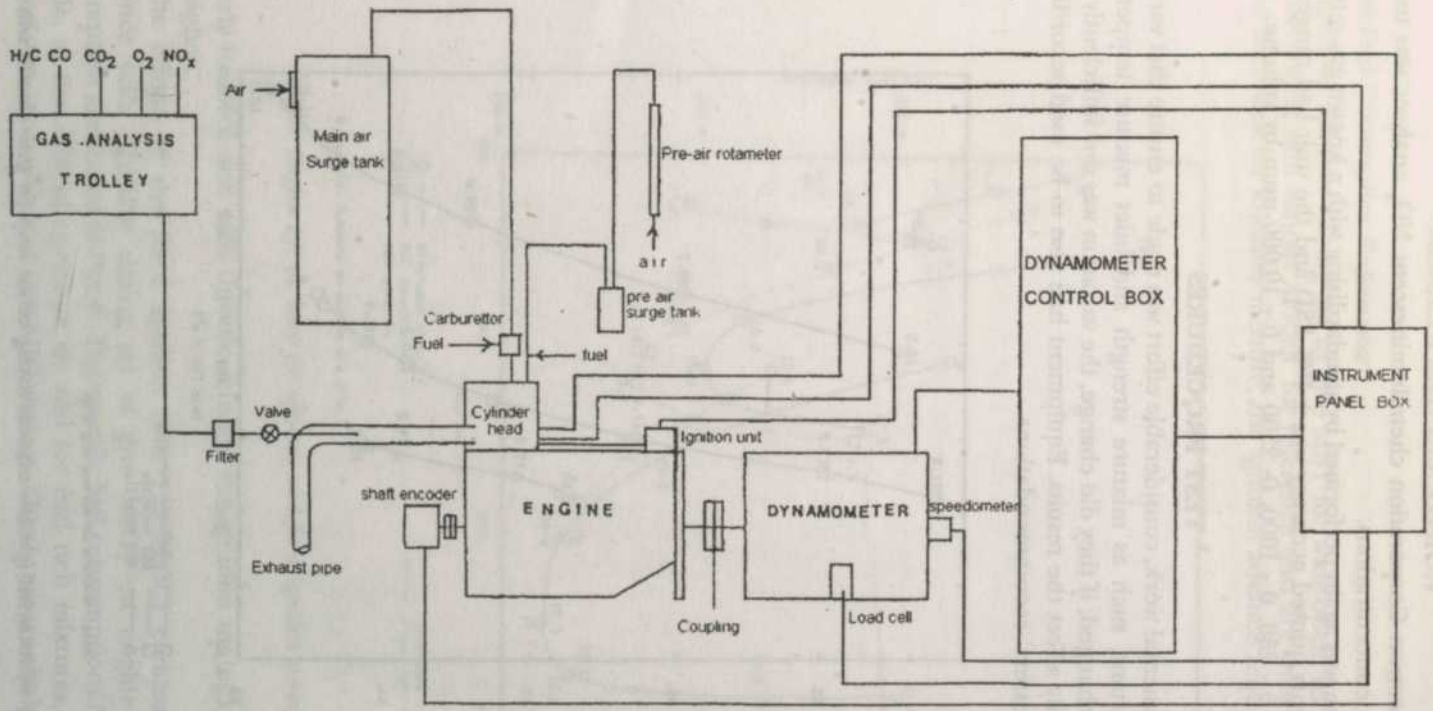

Fig 2. General schematic diagram of equipments system

NO_x Analyser

A Thermo Electron Corporation chemiluminescent NO_x analyser was used to measure NO_x concentrations.

Calibration was again performed by standardising with a known gas mixture. The instruments quoted accuracy was ± 1 % FSD and the unit had ranges of 0 - 25, 0 - 100, 0 - 250, 0 - 1000, 0- 2500 and 0 - 10,000 ppm by volume.

TEST PROCEDURES

In this experimental work, considerable effort was made to ensure that variables assumed constant, such as mixture strength and inlet mixture temperature remained unchanged; if they did change, the variation was not sufficiently great as to materially affect the results. Equipment had also to be used according to the manufacturers' recommendations.

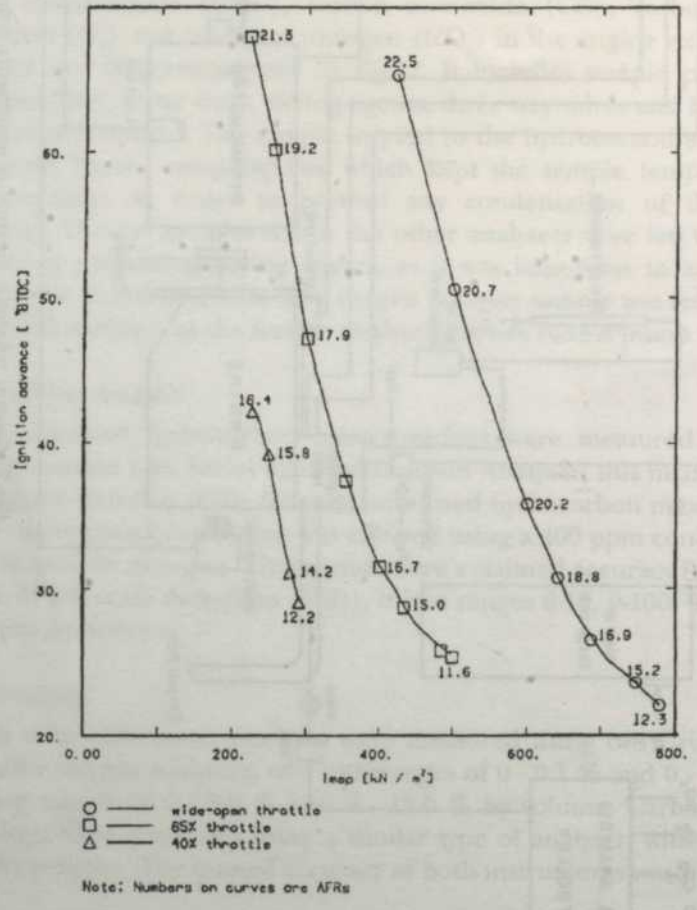

Fig 3. The reference test ignition advance timing versus imep for three throttle settings

RESULTS AND DISCUSSION

Engine Fuel Consumption Performance

The ignition advance timing set to give MBT for wide-open, 65 % and 40 % throttle setting with various AFRÆs for reference tests are shown in *Fig. 3.* It can be seen that for a leaner mixture, the ignition advance required is higher.

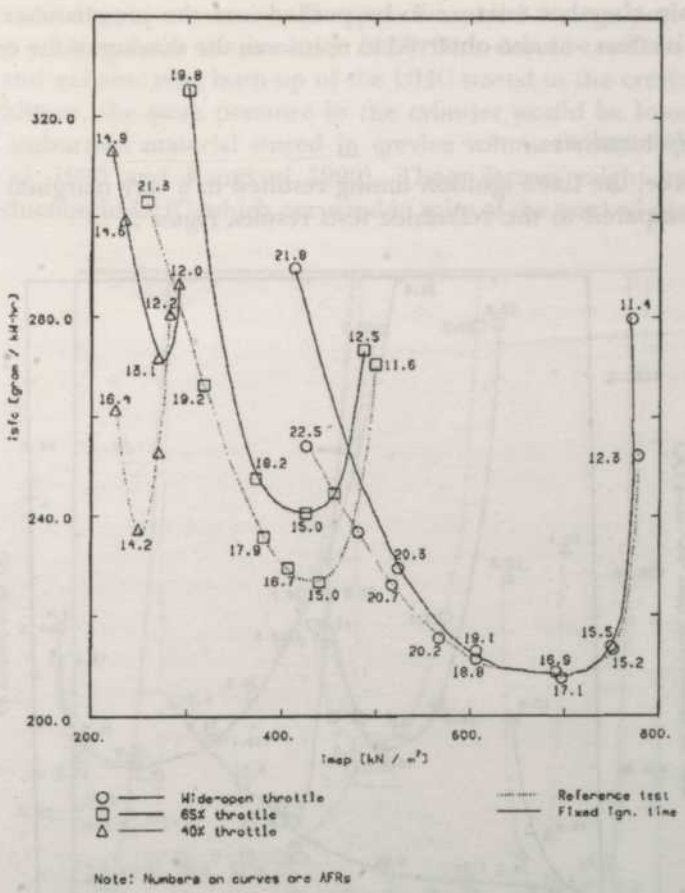

Fig 4. Engine isfc vs. imep for reference and fixed ignition timing

Similarly for 65% and 40% throttle settings, the ignition timings for MBT are also higher.

The effects of the fixed ignition time (22°BTDC) compared with the reference tests (ignition timing set to give MBT) on engine specifc fuel consumption are shown in *Fig. 4.* The specific fuel consumptions for wide-open throttle, at the AFR of optimum sfc and for fuel rich mixtures, were almost identical with those obtained with MBT timing. The sfc progressively deteriorated

with increasingly lean mixtures for the each fixed ignition timing. This was expected, due to the progressively later ignition with respect to MBT timing.

For the 65% and 40% throttle settings these effects were even more obvious because of the relatively greater retardation of the fixed ignition timing as compared with the time ignition giving MBT.

When ignition was retarded, a secondary effect was to produce a weaker mixture in the pre-chamber at ignition since there is time for a greater amount of weak main chamber mixture to be pushed into the pre-chamber by piston motion. This effect was also observed to re-inforce the slowing of the combustion event.

Unburned Hydrocarbons

At full throttle, the fixed ignition timing resulted in a very marginal reduction in UHC, compared to the reference tests results, *Figure 5.*

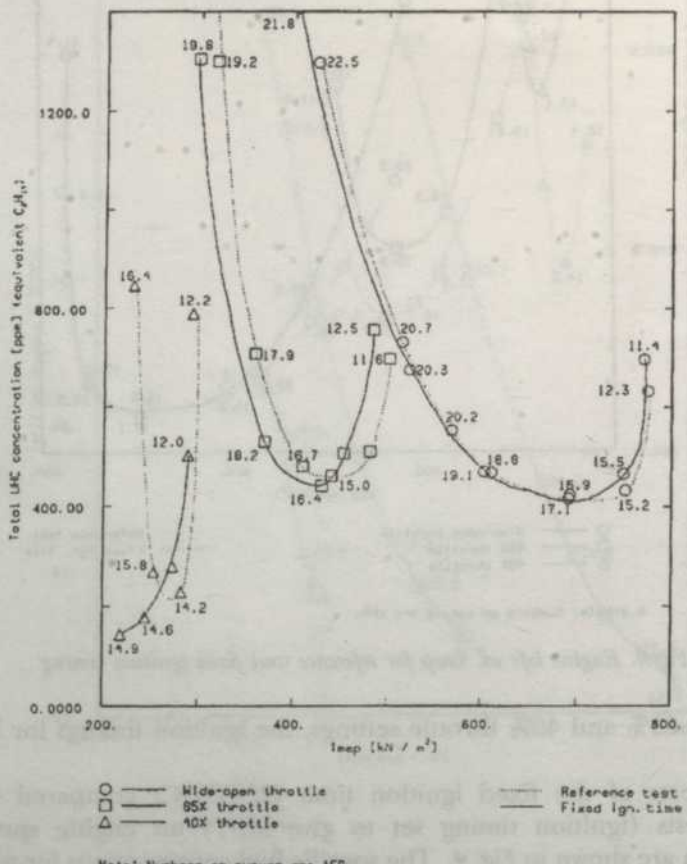

Fig 5. UHC emissions for reference and ignition timing

The UHC concentrations for optimum engine performance at wide-open throttle setting, were almost identical with the reference test, as one would expect, and marginally lower at lean mixtures as in *Fig. 5.* The same trend was even more evident for the 65% and 40% throttle settings. The UHC concentrations were generally lower than for the corresponding MBT timing. The effects were more marked for the heavily throttled lean case, at the time when ignition was most retarded.

With retarded ignition, one would expect increased average post flame and exhaust port temperatures (Kaiser *et al. 1983).* This should result in increased post flame and exhaust port burn-up of the UHC stored in the crevices and oil films. In addition, the peak pressure in the cylinder would be lower and the amount of unburned material stored in crevice volumes should be reduced (Lavoie *et al.* 1980 and Rangkuti 1990). These factors might explain the observed reduction in UHC, which occurred in spite of the marked deterioration in sfc.

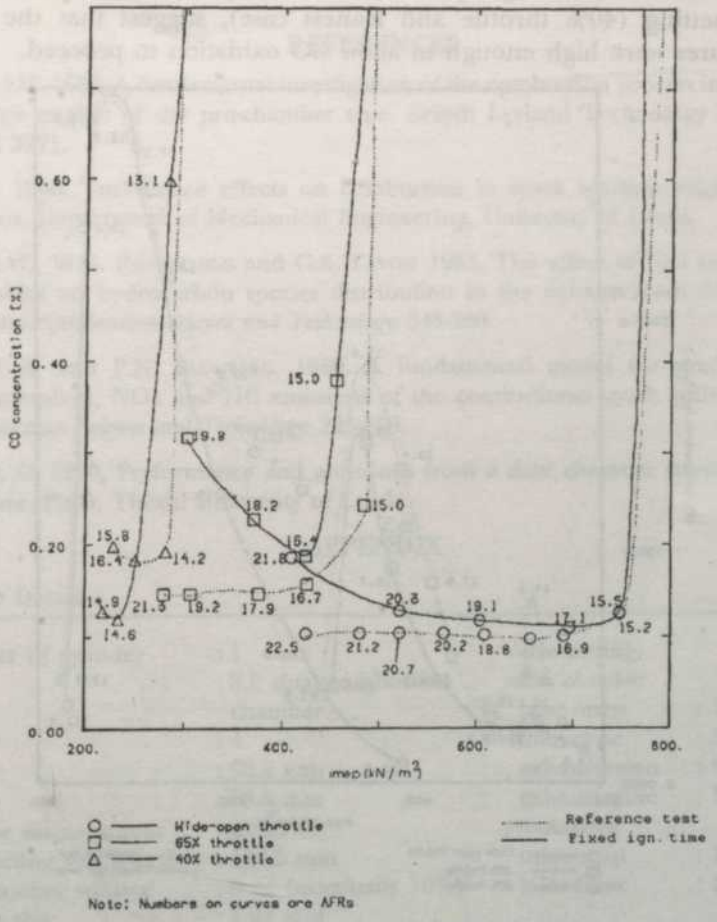

Fig 6. CO emissions for reference and fixed ignition timing

Carbon Monoxide

It can be seen from *Fig. 6* that for rich mixture, CO concentrations at wide-open throttle were essentially the same for fixed and MBT timing. As the mixture became leaner, and the difference in ignition timing more marked, the CO level increased a great deal. At the more retarded ignition conditions at the 65% throttle setting, these effects were even more marked. At the 40% throttle setting, CO levels were similarly higher - except at very lean (late burn and cool) conditions *(Fig. 6)*. With retarded ignition, it was expected that there would be an increase of the average post flame and the exhaust port temperature. This resulted in increased post flame and exhaust port reaction, with some of the UHC (emerging from the crevices late in the cycle) converted to CO. This was particularly so for lean mixtures, with plenty of oxygen available. However, the exhaust temperatures are generally expected to be too low to allow rapid further oxidation of this CO into CO_2 (Lavoie *et al.* 1980). The simultaneously low UHC and CO (with high specific fuel consumption), at the most retarded ignition setting (40% throttle and leanest case), suggest that the exhaust temperatures were high enough to allow CO oxidation to proceed.

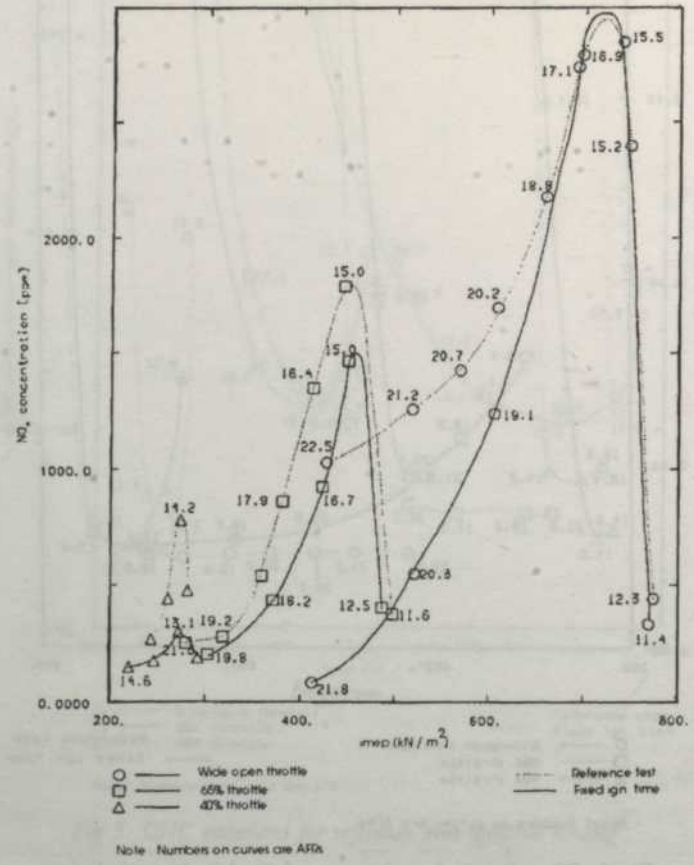

Fig 7. NO_x emissions for reference and fixed ignition timing

Oxides of Nitrogen

The retarded ignition settings resulted in reduction of cylinder pressure and temperature which led to reduced NO_x emissions. Those conditions for most retarded by MBT timing, generally resulted in the most marked fall in NO_x output (see *Fig. 7*).

CONCLUSION

This paper reported the effects of ignition timing on engine fuel consumptions and emissions. The retarded ignition, relative to MBT timing, gave poor fuel consumption, especially with lean mixtures. The poor combustion associated with the late burning did not result in increased UHC emissions - but in fact it reduces. Emissions of CO were high (for lean mixtures), NO_x levels were the same at wide-open and 65% throttle settings but significantly lower at the 40% throttle setting.

REFERENCES

WEAVING, J.H. 1982. A fundamental investigation of the combustion process in a stratified charge engine of the pre-chamber type. British Leyland Technology Report No. ETR 3271.

HYNES, J. 1986. Turbulence effects on combustion in spark ignition engiines. Ph.D. Thesis, Department of Mechanical Engineering, University of Leeds.

KAISER, E.W., W.G. ROTHSCHILD and G.A. LAVOIE 1983. The effect of fuel on operating variables on hydrocarbon species distribution in the exhaust from multicylinder engine. *Combustion Science and Technology*: 245-260.

LAVOIE, G.A. and P.N. BLUMBERG. 1980. A fundamental model for predicting fuel consumption, NOx and HC emissions of the conventional spark ignition engine. *Combustion Science and Technology*: 225-258.

RANGKUTI, C. 1990, Performance and emissions from a dual chamber stratified charge engine. Ph.D. Thesis, University of Leeds.

APPENDIX

Engine Details :

Number of cylinder	: 1	Valve timing,	
Type	: S.I. dual combustion chamber	*main chamber:*	
		inlet-open	: 16°BTDC
Cycle	: 4	inlet-close	: 56°ATDC
Bore	: 90.3 mm	exhaust-open	: 56°BBDC
Stroke	: 78.0 mm	exhaust-close	: 16°ATDC
Volume displacement	: 499.5 cc	*pre-chamber:*	
Connecting rod length	: 129.5 mm	inlet-open	: 20°ATDC
Pre-chamber volume	: 5 cc (nominally 10%)	inlet-close	: 20°ABDC
Throat size	: 7.94 mm		
Compression ratio	: 9.33 : 1		

Pertanika J. Sci. & Technol. 8(2): 241-252 (2000)
ISSN: 0128-7680

Rangkaian Neural Genetik Aplikasi dalam Pengecaman Aksara Jawi

Ramlan Mahmod, Khairuddin Omar and Md. Nasir Sulaiman
Jabatan Sains Komputer
Fakulti Sains dan Pengajian Alam Sekitar
Universiti Putra Malaysia
43400 Serdang Selangor Darul Ehsan, Malaysia.

Received: 27 August 1996

ABSTRACT

The basic objective of Genetic Algorithm (GA) is looking at the original evolution process in the form of software version. It is commonly used for optimization problem. In this process a population can expand, cloned and die within seconds. These changes occur continuously. Now, the concept of GA has been extended to Neural Networks (NN). This paper discusses the concept or the evolution process which was used in the NN.

ABSTRAK

Objektif asas bagi *Algoritma Genetik* (atau ringkasnya AG) ialah melihat proses evolusi asli dalam bentuk satu versi perisian. Ia sering digunakan untuk masalah pengoptimuman. Dalam proses ini suatu populasi boleh berkembang biak, ditot atau diklon, dan mati dalam beberapa saat. Perubahan ini berlaku secara berterusan. Kini, AG telah dikembangkan konsepnya ke dalam *Rangkaian Neural* (atau ringkasnya RN). Kertas ini membicarakan konsep atau proses evolusi yang digunakan didalam RN.

Kata kunci: vektor pemberat, nilai keupayaan, pemberat sinaptik, pincang, matriks pemarkahan, nilai keupayaan ternormalkan, pengeluaran-semula, menyilang, mutasi, generasi

PENGENALAN

Terdapat banyak takrif yang boleh diberikan kepada *Algoritma Genetik* (**AG**). Satu daripada takrif yang sering digunakan ialah satu teknik carian di ruang berdimensi luas, (Rogers, 1991) dan sering digunakan dalam masalah yang melibatkan pengoptimuman. Lihat juga Ramlan dan Azim (1995).

Teknik ini diilhamkan daripada proses pengevolusian DNA. Antara proses yang berlaku ialah ahli satu set rentetan perduaan berlumba-lumba untuk bersaing mendapatkan tempat dalam satu set rentetan yang baru. Penyatuan semula dilakukan dengan memilih dua ahli yang paling berjaya dalam populasi untuk dijadikan generasi datuk-nenek. Rentetan baru dicipta dengan menyambat (splicing) gen datuk-nenek masing-masing. Akhir sekali, satu rentetan baru akan diperoleh untuk menggantikan set rentetan yang lama, dan mana-mana rentetan lama yang tidak terpakai dibuang. Kini **AG** telah dikembangkan

konsepnya di dalam **RN**, (Tsoi 1994). Algoritma bagi **AG** seperti yang diutarakan oleh Tsoi (1994) diberikan oleh Rajah 1.

1. Mengawalkan nilai pemberat VP dengan nilai rawak.
2. Menilai VP sama ada sesuai dengan set latihan atau tidak.
3. Carian – Ulang sebanayak Gc kali.
   (a) Pilih VP yang boleh terus berguna.
   (b) Membentuk generasi baru VP dengan menggunakan operator-operator genetik seperti silang, atau mutasi, atau klon ke atas VP yang dipilih dalam (a).
   (c) Menilai VP yang dipilih itu sama ada sesuai dengan set latihan atau tidak.
4. Pembersihan – ulang sebanyak Gp kali.
   (a) Pilih VP yang boleh terus berguna.
   (b) Membentuk generasi baru VP untuk kegunaan generasi berikut dengan menggunakan klon sahaja ke atas VP yang dipilih dalam (a)
   (c) Menilai VP yang dipilih itu sama ada sesuai dengan set latihan atau tidak.

Akhirnya kita akan peroleh NI kelas VP, yang memberikan bilangan neuron untuk lapisan semasa.

5. Pilih satu perwakilan dari setiap kelas VP.
6. Bentukkan pula satu set latihan untuk lapisan yang berikut.
7. Ulang semula keseluruhan algoritma di atas dengan menggunakan set latihan yang terbentuk daripada langkah 6, jika terdapat lebih daripada satu kelas dalam langkah 5 (iaitu set latihan tidak dapat dikelaskan dengan hanya satu neuron) dan memerlukan satu lapisan lagi.

Rajah 1. Algoritma Genetik

Selain daripada memperoleh pemberat, algoritma yang diutarakan oleh Tsoi ini dikatakan mampu menentukan saiz suatu **RN**. Saiz yang dimaksudkan di sini ialah bilangan neuron yang ada pada lapisan tersembunyi. Lihat Khairuddin dan Ramlan (1996). Bahagian berikut memaparkan beberapa konsep yang digunakan oleh Tsoi untuk menghubungkan **AG** dan **RN**.

Bahagian berikut akan menjelaskan tatacara **AG** secara terperiinci. Ia diikuti dengan struktur seni bina **RN** Genetik. Seterusnya eksperimen bagi seni bina ini dijelaskan di bahagian berikutnya. Akhir sekali kesimpulan hasil eksperimen dipaparkan dan dibincang secara ringkas.

ALGORITMA GENETIK

AG melibatkan operasi ke atas satu set pemberat secara individu yang dinyatakan sebagai *Vektor Pemberat* (**VP**). **VP** akan mengandungi semua maklumat yang diperlukan untuk mendefinisikan satu neuron, iaitu pemberat untuk setiap input kepada neuron dan juga ambangnya. Satu neuron dengan I input dan satu ambang input akan didefinisikan dengan I+1 pemberat. Setiap pemberat disimpan dalam bentuk nombor nyata titik-tetap B bit, atau satu integer B-bit. Oleh itu **VP** didefinisikan sebagai (I+1)B bit. Lihat Tsoi (1994).

VP boleh dinyatakan secara matematik

$$y = f\left(\sum_{i=0}^{I} w_i \quad x_i\right) \qquad (1)$$

di mana y adalah output bagi neuron, w_i, $i = 0, 1, ..., I$ adalah *pemberat sinaptik* input, x_i, $i = 1, 2, ..., I$ adalah I input, dan $x_0 = 1$.

Satu fungsi tak linear $f(\alpha)$ dipilih iaitu

$$f(\alpha) = \begin{cases} 0 \text{ jika } \alpha < 0 \\ 1 \text{ jika } \alpha \geq 0 \end{cases}$$

Secara amnya **AG** melibatkan proses-proses memberikan nilai awal pemberat yang rawak, mengira nilai keupayaan, memilih **VP** untuk terus hidup, dan membentuk generasi baru. Bahagian berikut akan menjelaskan secara terperinci proses-proses tersebut.

AWALAN - MERAWAKKAN VP

Sebanyak (I+1)B bit **VP** disetkan dengan nilai rawak. Ini bermakna nilai pemberat adalah rawak dan disetkan dalam julat tertentu. Julat yang dipilih ialah antara -0.5 dan 0.5 berdasarkan saranan Fausett (1994).

PENGIRAAN NILAI KEUPAYAAN

Operasi ini adalah paling kritikal. Pengiraan *nilai keupayaan* dilakukan untuk setiap set pasangan pemberat dalam **VP** yang telah dipilih secara rawak. *Fungsi keupayaan* adalah seperti berikut:

$$\text{Keupayaan } VP_i = \sum_{i=1}^{T} \alpha_i \qquad (2)$$

$$_i = \begin{cases} 0 \text{ jika VP mengkelaskan vektor latihan i dengan salah,} \\ \text{Pincang } (n_i) \text{ jika VP mengkelaskan vektor latihan i dengan betul} \end{cases}$$

dengan

T = jumlah bilangan vektor dalam set latihan, dan

n_i = jumlah bilangan **VP** yang boleh mengkelaskan vektor latihan secara betul dan *Pincang(x)* adalah *fungsi pengurangan* secara monotonik untuk $x \geq 0$. Secara amnya, ia boleh dipilih secara bebas, sebagai contoh *Pincang(x)* = $\frac{1}{x^{\beta}}$, dan β adalah integer bukan-negatif.

Contoh, *Pincang(x)* = $\frac{1}{x^2}$, *Pincang(x)* = $\frac{1}{x^3}$.

Langkah selanjut boleh dijelaskan secara matematik seperti berikut:

Andaikan terdapat **T** pasangan input output dalam set latihan, dengan output: y_l^d, $l = 1, 2, ..., T$, dan input: x_i^l, $i = 1, 2, ..., I$; $l = 1, 2, ..., T$. Setiap neuron dijelaskan oleh **VP**. Katakan setiap neuron digambarkan oleh persamaan (1) seperti berikut:

$$y_{l,k} = f(\sum_{j=0}^{I} w_j^k x_j^l) k = 1, 2, ..., N; \quad l = 1, 2, ..., T. \tag{3}$$

dengan $y_{l,k}$, $l = 1, 2, ..., T$; $k = 1, 2, ..., N$ adalah output bagi N **VP** yang bertindak balas kepada vektor input ke l, w_j^k, $j = 1, 2, ..., I$; $k = 1, 2, ..., N$ adalah *pemberat sinaptik* yang menghubungkan input ke j kepada neuron ke k, dan $x_j^{(l)}$, $j = 1, 2, ..., I$; $l = 1, 2, ..., T$ adalah vektor input ke l ke lapisan berkenaan. Kesemuanya sejumlah T pasangan input output.

Ralat bagi output neuron ke l adalah

$$e_{l,k} = y_l^d - y_{l,k} = y_l^d - f(\sum_{i=0}^{I} w_j^k x_j^{(l)}). \tag{4}$$

Perlu diingatkan bahawa kita telah mengandaikan output itu perduaan, ralat $e_{l,k}$, $l = 1, 2, ..., T$; $k = 1, 2, ..., N$ kemungkinan bernilai 0 (pengkelasan betul) atau tak-sifar (pengkelasan salah). Untuk tujuan pengiraan markah, andaikan

$$e_{l,k} = \begin{cases} 0 & \textit{jika berada dalam kelas yang salah} \\ 1 & \textit{jika berada dalam kelas yang betul.} \end{cases} \tag{5}$$

Ralat boleh disusun dalam bentuk *matrik pemarkahan* $E = [e_{l,k}, l = 1, 2, ..., T; k = 1, 2, ..., N]$.

Bertolak daripada rumus ini, n_l, $l = 1, 2, ..., T$ boleh dikira sebagai

$$n_l = \sum_{k=1}^{N} e_{l,k}. \tag{6}$$

Maka *fungsi keupayaan* bagi setiap **VP** boleh diperolehi sebagai

$$J(w_j^k, j = 0, 2, ..., I) = \sum_{\substack{l=1 \\ n_l^\beta \neq 0}}^{T} \frac{e_{l,k}}{n_l^\beta}, \tag{7}$$

dengan β adalah integer tak-negatif.

PILIHAN - MEMILIH VP UNTUK TERUS HIDUP

Tugas di sini hanyalah untuk tahap carian dan pembersihan. Saiz populasi semasa boleh dibinakan. Populasi ini boleh digunakan untuk menghasilkan generasi populasi seterusnya. Satu daripada pemberat dalam populasi awal boleh dipilih dengan menggunakan nilai kebarangkalian berikut:

$$\text{Kebarangkalian memilih } VP_i = \frac{r_i}{\sum_{j=1}^{N} j} = \frac{2r_i}{N(N+1)}.$$

dengan

VP_i = pemberat ke i dari populasi semasa,
N = jumlah bilangan **VP**,
dan r_i adalah kedudukan keupayaan pemberat i, yang menyatakan bahawa keupayaan yang tertinggi duduk di tempat tertinggi. Tiada dua pemberat mempunyai kedudukan yang sama.

Jumlahkan *nilai keupayaan* bagi kesemua **VP** menjadi *jumlah keupayaan*

$$J = \sum_{k=1}^{N} J\,(w_j^k, j = 1, 2, ..., I)$$

Kemudian, normalkan setiap keupayaan **VP** dengan *jumlah keupayaan* dan memperoleh

$$j_i = \frac{J\,(w_j^k, j = 1, 2, ..., I)}{J}$$

Akhir sekali magnitud relatif bagi *nilai keupayaan ternormalkan* j_i, $i = 1, 2, ..., N$ diisihkan dalam bentuk menurun supaya boleh memperoleh siri tak-menaik $r_1 \geq r_2 \geq ... \geq r_N$. Di sini kita peroleh *nilai keupayaan ternormalkan* r_i yang terisih. Seterusnya pemberat yang dikatakan terbaik akan disenaraikan untuk membentuk generasi baru dalam langkah yang akan dinyatakan di bahagian berikut.

PENGELUARAN SEMULA - MEMBINA VP BARU DARI VP LAMA

Terdapat tiga pilihan operasi terhadap **VP** lama supaya menghasilkan pemberat baru iaitu *pengeluaran-semula, menyilang, dan mutasi.* Proses-proses ini tidak akan dijelaskan disini. Lihat Rogers (1994); Tsoi (1994); Ramlan dan Azim (1995); dan Khairuddin dan Ramlan (1996).

Pembentukan set populasi pemberat baru atau **VP** baru ini akan membuka ruang semula untuk dinilai keupayaannya. **VP** baru ini akan membentuk generasi baru. Proses di sinilah dikatakan melatih **RN** berdasarkan **AG**. Latihan akan diteruskan sehinggalah terdapat pemberat yang dikatakan berkeupayaan

sebagai pemberat di dalam mana-mana lapisan pemberat. Perkara yang biasa dilihat ialah melihat tindak balas yang betul ke atas satu set atau lebih pemberat ke atas setiap pasangan corak input output yang digunakan.

Dengan menggunakan algoritma seperti yang telah dipaparkan didalam Rajah 1, satu set pemberat yang nilai genetiknya yang dikatakan berkeupayaan akan dipilih untuk mengawalkan pemberat dan pincang pada lapis atau lapis pemberat.

MEMBENTUK SET LATIHAN UNTUK LAPISAN BERIKUTNYA

Set latihan yang dipilih sebelum ini adalah penyelesaian bagi **RN** satu-lapis sahaja. Oleh itu, bagi **RN** multi-lapis penjanaan untuk lapis yang berikut adalah dengan merambat input bagi vektor latihan dalam set latihan semasa melalui lapisan ini dan akan menjadi input kepada neuron-neuron bagi lapisan yang berikutnya. Output yang dikehendaki untuk setiap vektor latihan mestilah sama dengan output yang dikehendaki untuk vektor latihan dalam set latihan semasa.

PARAMETER UTAMA

Berikut diberikan parameter-parameter yang diperlukan dalam **AG**:

- Bilangan bit per pemberat, G_b.
- Julat magnitud pemberat, G_r.
- Saiz Populasi, N - bilangan set pemberat secara individu.
- Kebarangkalian Menyilang, P_c - Kebarangkalian berlakunya proses menyilang.
- Kebarangkalian Mutasi, P_m - Kebarangkalian berlakunya mutasi.
- Bilangan Generasi untuk carian, G_s.
- Bilangan Generasi untuk pembersihan, G_c.

SENIBINA RANGKAIAN NEURAL GENETIK

Dalam kajian ini kita akan melihat penyelesaian pengkelasan aksara jawi dengan menggunakan rangkaian neural multi-aras yang perambatan-balik dipilih

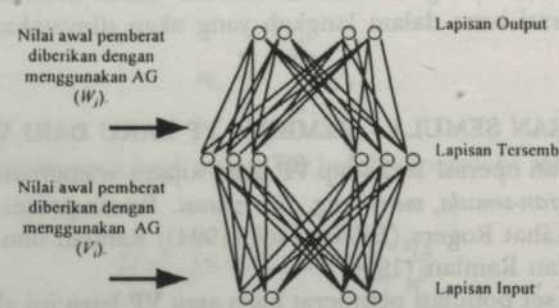

Rajah 2. Struktur genetik rangkaian neural

sebagai pengkelasnya, dan **AG** digunakan untuk mengawalkan nilai pemberat pada lapisan yang menghubungkan lapisan input ke lapisan tersembunyi dan lapisan tersembunyi ke lapisan output. Secara amnya senibina bagi rangkaian ini digambarkan di dalam Rajah 2.

Corak input dan tindak balasnya yang digunakan ketika latihan diwakilkan dalam bentuk perwakilan dwikutub supaya sesuai untuk diproses dalam rangkaian neural. Perwakilan dwikutub dikatakan mempunyai ciri-ciri yang sangat baik jika dibandingkan dengan perwakilan perduaan seperti yang dihuraikan oleh Fausett (1994).

Pertimbangkan huruf-huruf Jawi tunggal seperti yang digambarkan di dalam Rajah 3. Sebanyak tujuh corak input telah digunakan di dalam algoritma latihan. Kita akan menggunakan rangkaian ini untuk mengkelaskan setiap vektor input itu dipunyai atau tidak dipunyai bagi setiap tujuh kelas kategori.

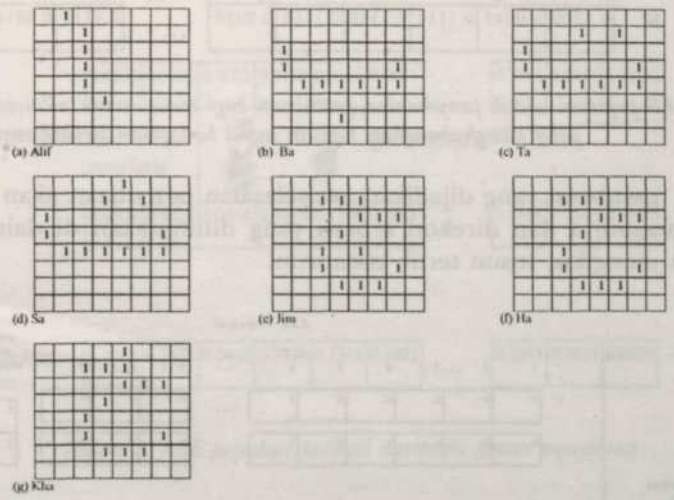

Rajah 3. Contoh Aksara Jawi yang direkabentuk pada Paparan Komputer

Rangkaian akan mempunyai tujuh unit output untuk mengkelaskan setiap unit input. Corak input tersebut boleh diwakil dalam bentuk vektor. Saiz corak piksel yang digunakan ialah 8x8, ini bermakna saiz vektor adalah hasil darab saiz corak tadi iaitu 64-tutupan. Lihat Ramlan dan Khairuddin (1996a).

Rangkaian ini bermula dengan memberikan satu populasi nilai awal pemberat yang rawak atau disebut sebagai *Vektor Pemberat* (**VP**), kemudian diikuti mengira nilai keupayaan **VP** tadi atau setiap ahli didalam populasi tersebut, seterusnya memilih **VP** untuk terus hidup, atau membentuk generasi baru.

VP akan mengandungi semua maklumat yang diperlukan untuk mendefinisikan satu neuron, iaitu pemberat setiap input kepada neuron dan juga ambangnya. Satu neuron dengan I input dan satu ambang input akan didefinisikan dengan n = I+1 pemberat, (Tsoi, 1994). Dalam kajian ini I=64.

Nilai pemberat adalah rawak dan disetkan dalam julat tertentu. Julat yang dipilih ialah antara -0.5 dan 0.5. Lihat Rajah 4 berikut.

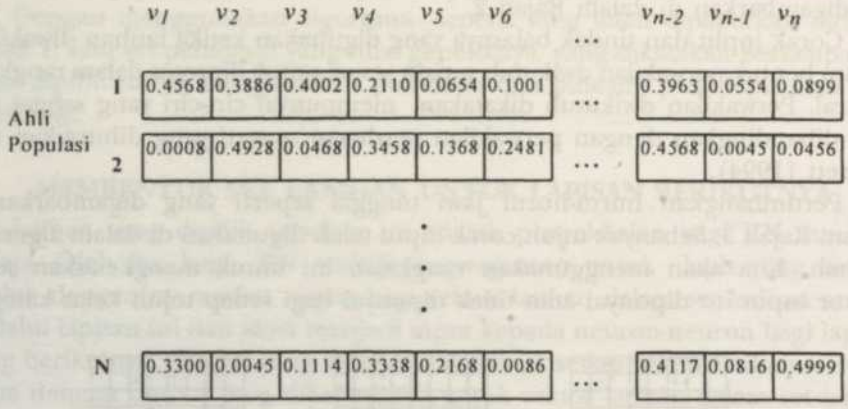

Rajah 4. Ahli populasi untuk penyelesaian percubaan bagi menentukan nilai awal pemberat yang menghubungkan lapisan input ke lapisan tersembunyi

Setiap pemberat yang dijadikan penyelesaian percubaan akan ditentukan nilai kesesuaiannya dan direkod seperti yang ditunjukkan di dalam Rajah 5 serta diisih mengikut susun tertib menurun.

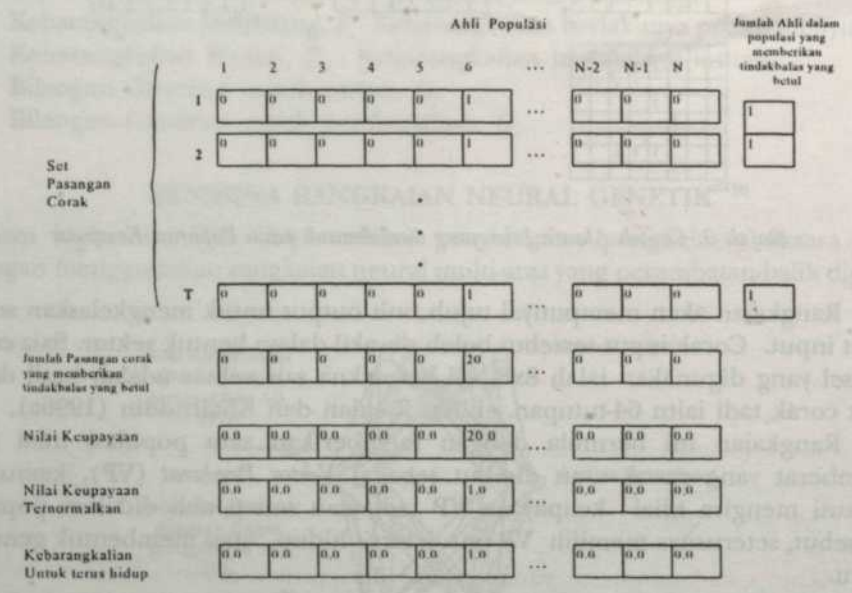

Rajah 5. Ahli populasi untuk penyelesaian percubaan bagi menentukan nilai kesesuaian untuk terus hidup

Pengiraan bermula dengan menentukan pengkelasan vektor sama ada salah atau betul bagi setiap pasangan corak input yang dijadikan sebagai corak latihan. Pengkelasan yang salah akan diberikan nilai 0 manakala pengkelasan yang betul akan diberikan suatu nilai fungsi pincang, lihat Tsoi (1994); Ramlan dan Khairuddin (1996b); Ramlan *et al* (1996). Seterusnya fungsi pincang ini akan digunakan dalam menentukan nilai keupayaan.

Proses yang paling penting di dalam **AG** ialah proses menyilang. Proses menyilang yang dimaksudkan disini ialah menentukan pemberat baru dengan memilih dua ahli di dalam populasi atau **VP** yang terbaik untuk dibiakkan dan dijadikan sebagai ahli baru di dalam populasi. Maksud dibiakkan di sini ialah menemberengkan kedua-dua ahli tadi pada satu atau dua titik menyilang seperti yang digambarkan pada Rajah 6 berikut.

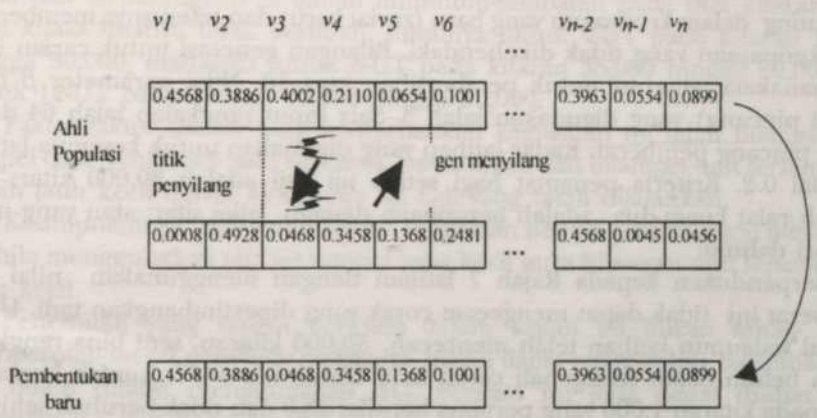

Rajah 6. Ahli populasi terhasil daripada proses menyilang

Dengan menggunakan **AG** seperti yang telah dijelaskan di bahagian 2.0, nilai genetik yang dikatakan berkeupayaan akan dipilih untuk mengawal nilai pemberat dan nilai pincangnya.

Populasi pemberat yang dipilih sebelum ini adalah penyelesaian bagi rangkaian satu lapisan sahaja oleh itu bagi rangkaian neural multi-aras untuk menjanakan satu set lapisan yang berikut, output bagi input vektor latihan dalam set latihan semasa hendaklah dirambatkan melalui lapisan ini dan seterusnya ia akan menjadi input kepada neuron-neuron bagi lapisan yang berikutnya. Output yang dikehendaki untuk setiap vektor latihan dibuat supaya sama dengan output yang dikehendaki untuk vektor latihan dalam set latihan semasa.

Akhir sekali pemberat yang terhasil dari proses genetik (pemberat pada lapisan yang menghubungkan lapisan input ke lapisan tersembunyi dan pemberat pada lapisan yang menghubungkan lapisan tersembunyi ke lapisan output) disimpan dan digunakan pada rangkaian neural multi-aras yang dilatih menggunakan perambatan-balik.

EKSPERIMEN

Seni bina rangkaian ini telah diimplemenkan pada mikrokomputer 486 serasi IBM dan dilarikan menggunakan bahasa C++. Bilangan unit tersembunyi (UT) yang digunakan ialah 4, 8, dan 12 untuk diaplikasikan kepada beberapa huruf jawi seperti yang telah dipaparkan dalam Rajah 3. Dalam hal ini sebanyak tiga ujikaji telah dijalankan iaitu ujian ke atas (i) 4-UT; (ii) 8-UT; dan (iii) 12-UT. Saiz populasi yang dipilih ialah 10 dan daripada sepuluh populasi tersebut, kami telah bahagikan kepada empat subpopulasi supaya senang diproses. Daripada empat subpopulasi tersebut 25% diperuntukkan untuk populasi terbaik, 25% populasi baru dan 50% diperuntukkan untuk populasi menyilang. Proses mutasi tidak dipertimbangkan. Menurut De et al (1996) mutasi boleh memberi kesan kepada penumpuan yang dikehendaki iaitu memperlahankan proses penumpuan dalam keadaan mana ia boleh menukarkan nilai bit terpenting dalam kromosom yang baru (zuriat baru) dan seterusnya memberikan nilai keupayaan yang tidak dikehendaki. Bilangan generasi untuk carian ialah 10, manakala generasi untuk pembersihan juga 10. Nilai parameter β (bagi fungsi pincang) yang digunakan ialah 3. Saiz input rangkaian ialah 64 dan 1 input pincang pemberat. Kadar latihan yang digunakan untuk kesemua latihan bernilai 0.2. Kriteria penamat bagi setiap uji kaji adalah 50,000 kitar; atau jumlah ralat kuasa-dua adalah bersamaan denagn nilai sifar; atau yang mana dicapai dahulu.

Berpandukan kepada Rajah 7 latihan dengan menggunakan nilai awal pemberat ini tidak dapat mengecam corak yang dipertimbangkan tadi. Untuk kes ini walaupun latihan telah mencecah 50,000 kitaran, seni bina rangkaian masih belum dapat mengenali corak tadi. Untuk kes 4-UT, jumlah kuasa-dua ralat pada kitaran 1,000 yang pertama bernilai 18.0 dan tidak berubah sehingga ke kitaran 5,000 dan beransur menyusut ke nilai 8.0 pada kitaran ke 13,000 dan meningkat sebanyak 1.0 pada kitaran berikutnya menjadikan 9.0 sehingga ke kitaran 50,000. Bagi 8-UT pula mempunyai ralat kuasa dua permulaan yang

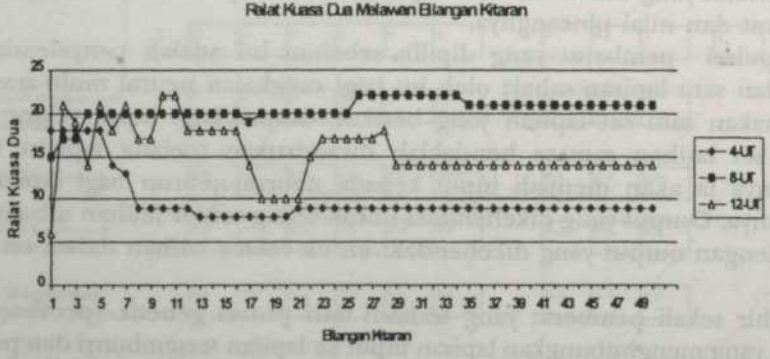

Rajah 7. Latihan menggunakan pengawalan pemberat genetik untuk seni bina 4-UT, 8-UT, dan 12-UT
(Catatan: *Bilangan kitaran adalah dalam '0000)*

sedikit rendah berbanding dengan 4-UT (iaitu bernilai 15.0 dan meningkat ke nilai 22.0 pada kitaran 26,000 dan terus tidak banyak perubahan sehingga ke kitaran 50,000) tetapi masih gagal mengecam corak tadi. Bagi 12-UT pula penumpuan bertambah baik dan nilai kuasa dua ralat menjadi 6.0 pada kitaran ke 1,000 yang pertama dan bertambah secara mendadak pada 1,000 kitaran yang berikutnya dan terus meningkat pada kitaran berikutnya. Jumlah ralat tersebut berkurangan pada kitaran 18,000 hingga 21,000 kepada 10.0, dan kembali meningkat pada kitaran berikutnya dengan nilai konsisten iaitu 14.0.

KESIMPULAN

Daripada corak yang diberikan itu, seni bina ini masih gagal untuk mengecam aksara jawi. Nilai pemberat yang diperoleh daripada proses genetik itu masih gagal dan terperangkap di dalam minimum-tempatan pada titik kitaran yang ralat kuasa duanya tidak berubah, misalnya untuk 4-UT pada kitaran 20,000 hingga 50,000, manakala untuk 8-UT pada kitaran 35,000 hingga 50,000 dan untuk 12-UT pada kitaran 29,000 hingga 50,000.

Faktor-faktor utama yang menyebabkan kegagalan ini ialah bilangan saiz sampel data yang kecil iaitu sebanyak 1set sempel; dan bilangan unit tersembunyi masih jauh kecil dalam ketiga-tiga uji kaji yang telah dijalankan.

Kesimpulannya ialah penumpuan rangkaian neural genetik gagal menumpu apabila menggunakan saiz set sampel yang kecil serta bilangan unit tersembunyi yang kecil.

Penemuan yang sangat berguna dalam kajian ini bukan sahaja boleh memperoleh sat set pemberat rangkaian malah dapat mengetahui bagaimanakah **RN** boleh dilatih menggunakan **AG**. Perkara ini jelas dapat dilihat pada Bahagian 2.4 dan Bahagian 2.5.

BIBLIOGRAFI

De, S., Gosh, A., dan Pal, S. K. 1996. Fitness Evaluation in Genetic Algorithms with Ancestors' Influence. Dalam *Genetic Algorithms for Pattern Recognition*, ed. S. K. Pal dan Wang, P. P. Boca Raton Florida: CRC Press.

Khairuddin bin Omar dan Ramlan bin Mahmod. 1996. Genetik-Rangkaian Neural Untuk Pengkelasan Aksara Jawi. Dalam *Pascasidang National Conference on Research and Development in Computer Science and Its Applications (REDECS '96)* pada 26-27 Jun 1996. Anjuran Jabatan Sains Komputer, Universiti Pertanian Malaysia.

Ramlan bin Mahmod, dan Khairuddin bin Omar. 1996a. Analisis Pengawalan Pemberat Rangkaian Neural Perambatan-Balik untuk Pengecaman Aksara. Pracetak.

Ramlan bin Mahmod, dan Khairuddin bin Omar. 1996b. Genetik-Rangkaian Neural. Laporan Teknik SAK/TR-007/96.

Ramlan bin Mahmod, Khairuddin bin Omar dan Md. Nasir bin Sulaiman. 1996. Genetik-Rangkaian Neural. Dalam *Pascasidang National Conference on Research and Development in Computer Science and Its Applications (REDECS '96)* pada 26-27 Jun 1996. Anjuran Jabatan Sains Komputer, Universiti Pertanian Malaysia.

RAMLAN BIN MAHMOD dan ABDUL AZIM BIN ABDUL GHANI. 1995. Pengoptimuman Menggunakan Algoritma Genetik. Jabatan Sains Kumputer, Universiti Pertanian Malaysia, Serdang. Laporan Teknik SAK/TR-012/95.

ROGERS, D. 1994. Whether Prediction Using A Genetic Memory. Dalam *Neural Networks: Concepts, Applications, and Implmentations.* Vol. IV, 1994, ms. 275-289. New Jersey: Prentice-Hall.

TSOI, AH CHUNG 1994. Constructive Algorithms. A Course on Artificial Neural Networks. Jointly Organised by MIMOS & Computer Centre, University of Malaya on 4-8 July 1994.

Pertanika Journal of Science and Technology

Subject Index for Vol. 8, Nos. 1 and 2, 2000

Pertanika Journal of Science & Technology

Author Index for Volume 8, Nos. 1 & 2, 2000

ACKNOWLEDGEMENTS

The Editorial Board acknowledges the assistance of the following reviewers in the preparation of Volume 8, Numbers 1 & 2 of this journal

Prof. Madya Dr. Amin Mohd. Soom
Dr. Baharum Sanugi
Prof. Madya Dr. Bujang Kim Huat
Dr. D.J. Evans
Prof. Dr. Faizal Hj. Ali
Prof. Dardo Guaraglia
Dr. Hishamudin Jamaludin
Prof. Coskan Ilicali
Dr. Ithnin Abd. Jalil
Dr. Ramfiel Janius
Prof. Kwok Chee Yan
Prof. S.N Maiti
Prof. Dr. Mashitah Hassan
Prof. Madya Dr. Md. Rahim Sahar
Prof. Dr. Mohd. Ghazali Mohayidin
Prof. Madya Dr. Muhammad Idress
Dr. Muhammad Salleh
Dr. Muhammad Yahya
Ir. Dr. Norman Mariun
Prof. Madya Dr. Pooi Ah Hui
Dr. Rosmi Abdullah
Dr. Salim Said
Dr. Sameer Abd. Kareem
Dr. S. Sankarayanan
Dr. Anond Snidvongs
Dr. Sinin Hamdan
Dr. Yusof Ali
Dr. Zarita Zainuddin

Preparation of Manuscript

General
The manuscript, including footnotes, tables, and captions for illustrations, should be typewritten double spaced on paper 210 x 297 mm in size, with margins of 40 mm on all sides. Three clear copies are required. Typing should be on one side of the paper only. Each page of the manuscript should be numbered, beginning with the title page.

Title page
The title of the paper, name of author and full address of the institution where the work was carried out should appear on this page. A short title not exceeding 60 characters should be provided for the running headline.

Abstract
Abstracts in Bahasa Melayu and English of not more than 200 words each are required for full articles and communications. No abbreviation should appear in the abstract. Manuscripts from outside of Malaysian may be submitted with an English abstract only.

Keywords
Up to a maximum of ten keywords are required and they should be placed directly below the abstract.

Footnotes
Footnotes to material in the text should not be used unless they are unavoidable. Where used in the text, footnotes should be designated by superscript Arabic numerals in serial order throughout the manuscript. Each footnote should be placed at the bottom of the manuscript page where reference to it is made.

Equations
These must be clearly typed, triple-spaced and should be identified by numbers in square brackets placed flush with the right margin. In numbering, no distinction is made between mathematical and chemical equations. routine structural formulae can be typeset and need not be submitted as figures for direct reproduction but they must be clearly depicted.

Tables
Tables should be numbered with Arabic numerals, have a brief title, and be referred to in the text. Columns headings and descriptive matter in tables should be brief. Vertical rules should not be used. Footnotes in tables should be designated by symbols or superscripts small italic letters. Descriptive materials not designated by a footnote may be placed under a table as a *note.*

Illustrations & Photographs
Illustration including diagrams and graphs are to be referred to in the text as 'figures' and photographs as 'plates' and numbered consecutively in Arabic numerals. All photographs (gloosy black and white prints) should be supplied with appropriate scales.

Illustrations should be of print quality; outputs from dotmatrix printers are not acceptable, Illustrations should be on separate sheets, about twice the size of the finished size in print. All letters, numbers and legends must be included on the illustration with the author's name, short title of the paper, and figure number written on the vereso. A list of captions should be provided on a separate sheet.

Unit of Measure
Metric units must be used for all measurements.

Citations and References
Items in the reference list should be referred to in the text by inserting, within parentheses, the year of publication after the author's name. If there are more than two authors, the first author should be cited followed by '*et al*'. The names of all authors, however, will appear in the reference list.

In the case of citing an author who has published more than one paper in the same year, the papers should be distinguished by addition of a small letter, e.g. Choa (1979a); Choa (1979b); Choa (1979c).

In the reference list, the names should be arranged alphabetically according to the name of the first author. Serials are to be abbreviated as in the *World List of Scientific Periodicals.*

The abbreviation for Pertanika Journal of Science and Technology is *Pertanika J. Sci. Technol.*

The following reference style is to be observed:

Monograph
Alefed, G. and J. Herzberger. 1983. *Introduction to Interval Computations.* New York: Academic Press.

Chapter in Edited Book
Muzzarell, R.A.A. 1980. Chitin. In *Polymers in Nature,* ed. E.A. MacGregor and C.T. Greenwood, p. 417-449. New York: John Wiley.

Serials
Kamaruzaman Ampon. 1991. The effect of attachment of hydrophobic imidoesters on the catalytic activity of trypsin. *Pertanika* **14(2)**: 18-185.

Proceedings
Mokhtaruddin, A.M. and L.M. Maene. 1981. Soil erosion under different crops and management practices. In *Agricultural Engineering in National Development,* ed. S.L. Choa, Mohd Zohdie Bardaie, N.C. Saxena and Van Vi Tran, p. 245-249. Serdang, Malaysia: Universiti Pertanian Malaysia Press.

Unpublished Materials (e.g. theses, reports & documents)

Sakri, 1. 1990. Proper construction set-up of Malaysian Fish Aggregating Devices (Unjam). Ph.D. Thesis, Universiti Pertanian Malaysia, Serdang, Selangor.

Pertanika Journal of Science & Technology

Volume 8 No. 2, 2000

Contents

ISSN 0128-7680

07

9 770128 768083